AN INVESTIGATION INTO THE PARTIAL OXIDATION OF C-4 ALKANES OVER VANADYL PYROPHOSPHATE AND HETEROPOLY ACIDS

6

A thesis submitted to the
UNIVERSITY OF CAPE TOWN
in fulfilment of the requirements for the degree of
MASTER OF SCIENCE IN ENGINEERING

by
Stéfan Walters Robertson
BSc (Chemical Engineering)

Catalysis Research Unit
Department of Chemical Engineering
University of Cape Town
Rondebosch
7700
South Africa

November 1997

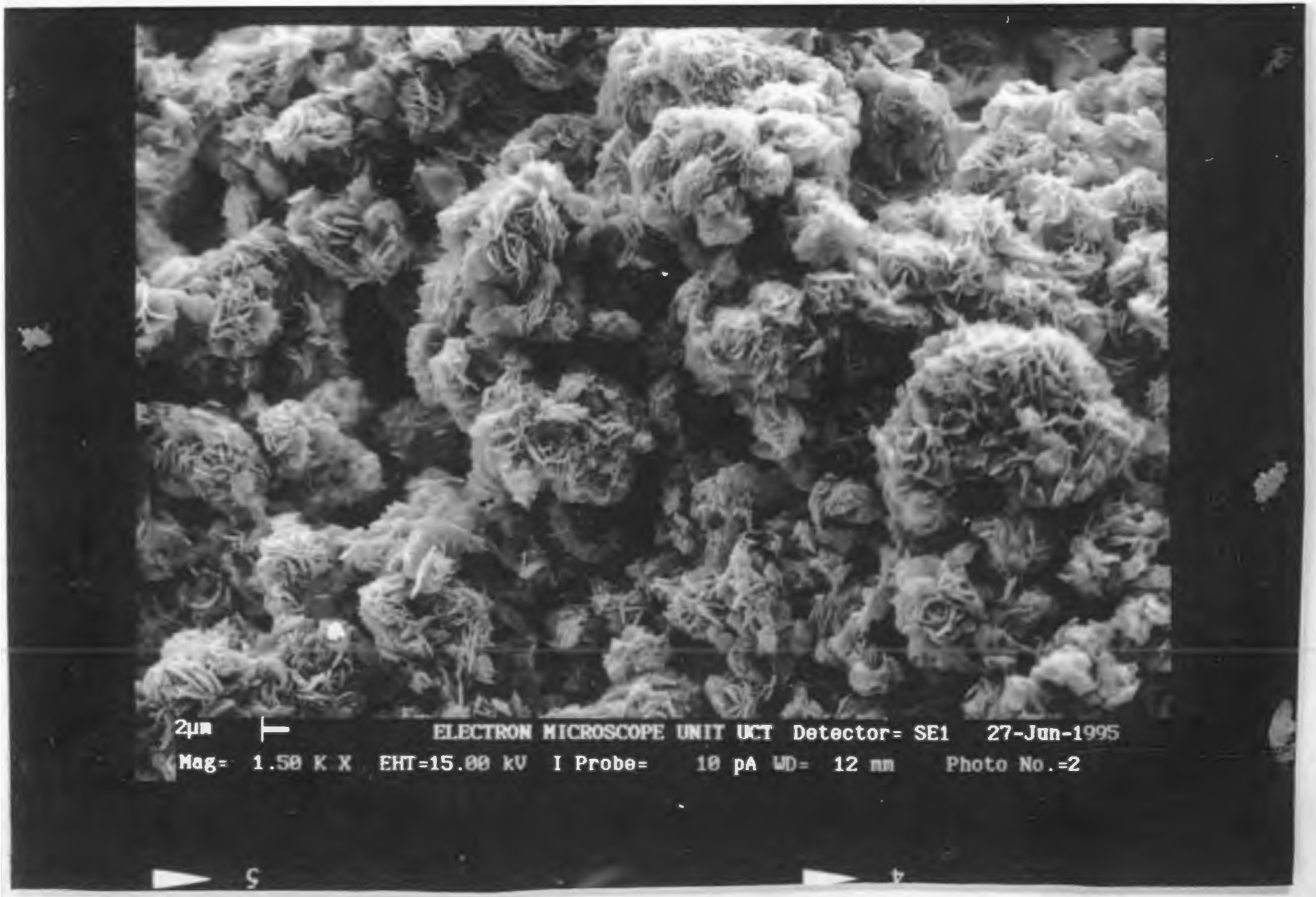
2µm
ELECTRON MICROSCOPE UNIT UCT Detector= SE1 27-Jun-1995
Mag= 1.50 K X EHT=15.00 kV I Probe= 10 pA WD= 12 mm Photo No.=2

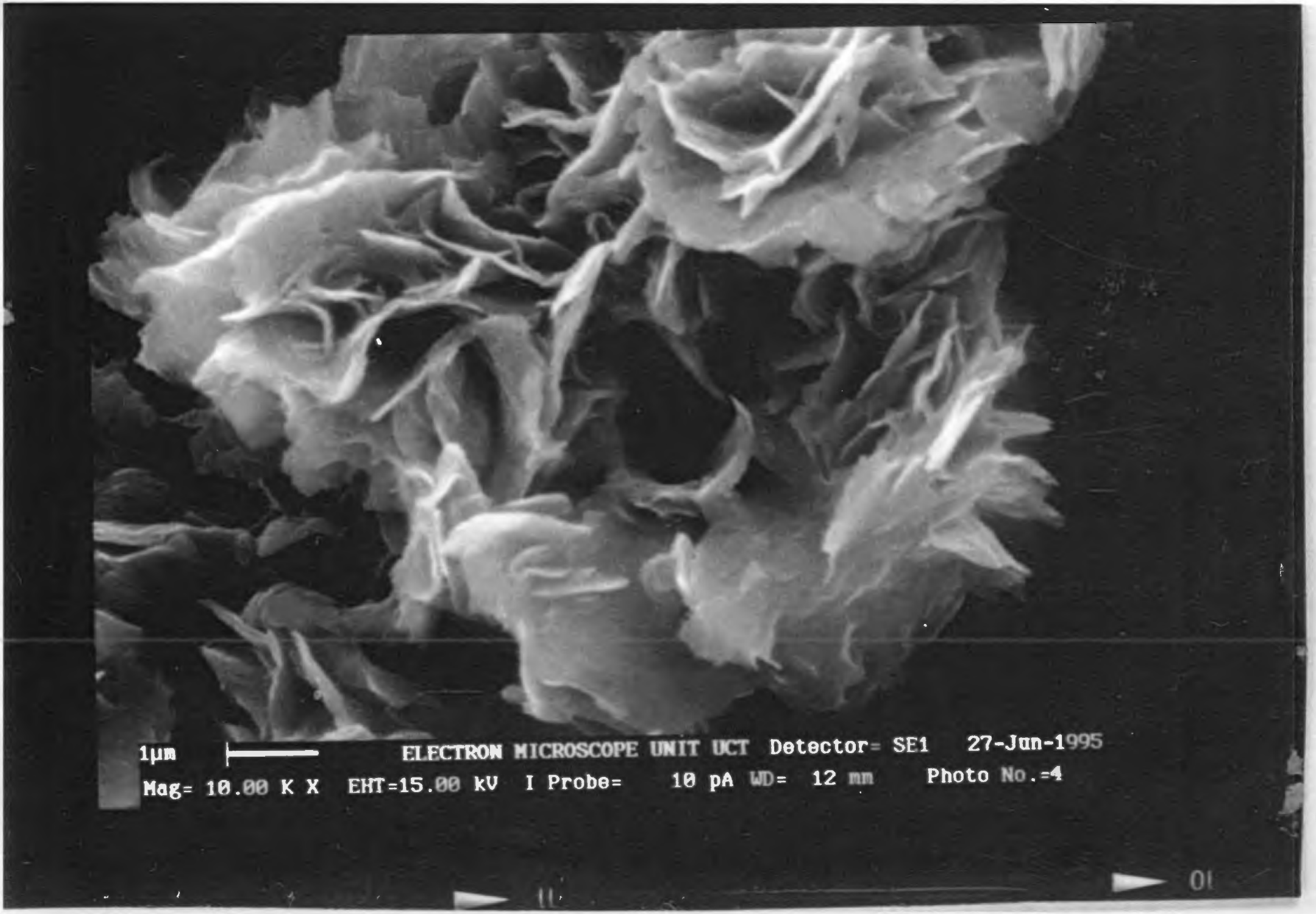
1µm
ELECTRON MICROSCOPE UNIT UCT Detector= SE1 27-Jun-1995
Mag= 10.00 K X EHT=15.00 kV I Probe= 10 pA WD= 12 mm Photo No.=4

ACKNOWLEDGEMENTS

I would like to thank Dr Eric van Steen and Professor Cyril O'Connor for their input and advice in directing the research.

I also wish to express my appreciation to the following people for their technical assistance: Tony Barker, Michael Schnobel, Dr Klaus Möller, Granville de la Cruz, Peter Dobias, Joachim Mäcke, Rein Weber, Peter Röger, Bill Randall and Craig Balfour.

I thank Leslie Petrik, Suzanna Vasic and Linda Harrower for their assistance with catalyst characterisation, likewise Pam Linck, Pauline Bettison, Meg Winter and Jill Stevenson for their help with purchasing and administrative issues.

I would also like to thank Dr Johan de Villiers and Daleen van Eeden at the Council for Mineral Technology (MINTEK) for their assistance.

Lastly, I would like to thank MINTEK for their financial support.

SYNOPSIS

Two different partial oxidation catalysts for paraffin functionalisation were studied: the vanadyl pyrophosphate catalyst for the conversion of n-butane to maleic anhydride and the heteropoly acid catalyst for the conversion of isobutane to methacrylic acid.

PARTIAL OXIDATION OVER VPO CATALYST

The vanadyl pyrophosphate catalyst for the manufacture of maleic anhydride is important because it is the only example of an industrially practised selective oxidation catalyst involving alkane activation. The ternary VPO system is complex, with 15 different phases. Only the phase $(VO)_2P_2O_7$ with V^{4+} produces maleic anhydride from n-butane. However, the active VPO catalyst has an average oxidation state of between 4.04 and 4.1. Active catalysts are thought to possess micro-domains of V^{5+}, present as defect sites in the $(VO)_2P_2O_7$ crystal. VPO catalyst samples were prepared with P/V ratios during preparation of 1, 1.1, 1.15, 1.2 and 1.5 by reduction in aqueous and organic reducing agents. These catalyst samples were calcined in air, N_2 and in a feed atmosphere of n-$C_4/O_2/N_2$ = 1.44/20/78.56 respectively, at temperatures of between 350°C and 450°C.

X-ray diffraction spectra were obtained for the VPO catalyst for the range of P/V ratios given above. Catalyst samples prepared for X-ray diffraction were calcined in air or nitrogen at 380°C for 3 hours, or in reaction feed for 5 hours at T = 400°C. Infrared spectra were obtained for VPO species calcined for 5 hours at 400°C in the reaction feed mixture. Both XRD and IR spectra agree with literature and indicate the presence of a single crystalline $(VO)_2P_2O_7$ phase, as well as an amorphous precursor phase. XRD peak broadening is indicative either of defect sites associated with V^{5+} micro-domains in the crystal structure, or of low crystallinity associated with short equilibration times. The XRD spectrum of a deactivated commercial catalyst was also obtained and shows greater crystallinity corresponding to longer equilibration times.

The partial oxidation of n-butane in a feed of n-$C_4/O_2/N_2$ = 1.44/20/78.56 was carried out at temperatures of between 350°C and 450°C and at space velocities of between 3 and 24 g/g.h in a fixed-bed glass reactor. Over the range of reaction conditions, only total oxidation products (CO and CO_2) were however observed for the prepared VPO catalysts. A run was also carried out over a 190 hour period to test for increased selectivity with time on stream, but no maleic anhydride was observed. The deactivated commercial catalyst, on the other hand, gave yields of up to 6% of maleic anhydride under these conditions, showing that maleic anhydride, if formed, can be detected. Good carbon balances and outlet line temperatures of above 180°C preclude the condensation of product in the outlet lines. n-Butane was found not to combust over sand at the reaction conditions studied, but when maleic anhydride was fed with a saturator in air over a reactor filled with sand at 400°C, up to 2 ml/min of maleic anhydride was combusted. The presence of impurities in the catalyst was ruled out by carrying out an elemental analysis. Although the correct VPO catalyst phase for the oxidation of n-butane to maleic anhydride appears to have been synthesised, XRD and IR do not show the exact nature of the species on the surface of the catalyst and the reaction is known to be surface specific. Due to the simplicity and consistency of the preparation method and activation procedure discussed in literature, it is suggested that the correct preparation method had been followed.

On account of the low concentrations and flowrates of n-butane, maleic anhydride, if formed, will be present in concentrations of less than 1.44% and flowrates of less than 1.44 ml/min. It is thought that these small quantities may undergo further oxidation in the lower part of the reactor. It is therefore suggested that higher n-butane feed partial pressures be studied (although this will be difficult on account of explosion limits) and that a less parabolic temperature profile be developed for the reactor.

PARTIAL OXIDATION OVER THE HETEROPOLY ACID CATALYST

Heteropoly acid catalysts are commercially used for the partial oxidation of isobutyric acid to methacrylic acid. Another route to methacrylic acid is the direct oxidation of isobutane to methacrylic acid. Methacrylic acid selectivities of more than 50% and yields of up to 9% have been reported for the Keggin-type heteropoly acid salts of the type $M_3Mo_{12-x}V_xPO_{40}$ where M = Cs^+ or a mixture of K^+ and NH_4^+. The heteropoly acid, 12-molybdophosphoric acid, was prepared with K^+ and NH_4^+ substitution and doped with iron on the surface. The catalyst was tested for the oxidative conversion of isobutane (i-C_4/O_2/N_2 = 17/30/53) between 300 and 450°C. Space velocities of between 0.82 and 18.2 $g_{ISOBUTANE}$ /$g_{CATALYST}$h were studied.

The yields of products as a function of time on stream make possible the drawing of conclusions on the nature of catalyst activation. With time on stream, the yields of total oxidation products decrease by about 50%. The yield of methacrylic acid increases by about 50%, until a steady state is reached. Yields of organic by-products propanal and methacrolein remain constant, while yields of ethyl methyl ether and dimethyl benzene decrease to zero with time on stream. Infrared spectra of $K(NH_4)_2PMo_{12}O_{40}$, calcined for 1 hour at T = 300°C in oxygen, and reacted for 1 hour, 1.5 hours, 3 hours and 5 hours on stream at T = 380°C, were obtained. IR shows the presence of the Keggin structure. The absorbances of all bonds relating to the Keggin structure increase with time on stream. Relative absorbances of different peaks remain constant, indicating that the whole Keggin structure evolves with time on stream out of an amorphous phase.

Changes in contact time were studied at 380°C and 400°C on an equilibrated catalyst which has been on stream for more than 8 hours. Selectivities of methacrylic acid, methacrolein and propanal tend to finite values as contact time tends to zero, indicating primary products. Selectivities of total oxidation products tend to zero as contact time tends to zero, indicating serial formation. Intermediates for the formation of methacrylic acid do not desorb. Isobutane adsorbs on the catalyst, is transformed to organic products and once reaction is complete, methacrylic acid desorbs. Methacrylic acid and other organic byproducts can over-oxidise while adsorbed on the catalyst to form total oxidation products.

The model which is favoured is that of parallel formation of primary organic products with serial formation of total oxidation products. It is proposed that differing degrees of electronic interaction of the heteropoly acid cation with the Mo-O active sites, located at different positions in the anion complex, result in active sites with differing Mo-O bond strengths and therefore different degrees of oxidation strength. Due to the high unsteady state yields of CO and CO_2, it is suggested that total oxidation also takes place on the amorphous precursor phase during equilibration. During equilibration, changing electronic interaction of crystalline and non-crystalline species results in the observed changes in the yields of products.

TABLE OF CONTENTS

LIST OF FIGURES

LIST OF TABLES

1. INTRODUCTION

Partial oxidation offers a route for the functionalisation of paraffins which has potential for industrial applications. Two partial oxidation catalysts for paraffin functionalisation were studied: the vanadyl pyrophosphate (VPO) catalyst for the conversion of n-butane to maleic anhydride (MA) and the heteropoly acid (HPA) catalyst for the conversion of isobutane to methacrylic acid (MAA). Both end-products are important industrial intermediates.

Functionalisation of a lower cost alkane feed has obvious financial advantage over traditional feedstocks in industrial applications. At present, the partial oxidation of n-butane over a vanadyl pyrophosphate catalyst is the only industrially practised selective oxidation reaction involving alkane activation. The development of a selective catalyst for this reaction has provided maleic anhydride manufacturers with a cheaper and more environmentally-friendly feed material than the traditional feedstock benzene and other feeds such as butenes. A better understanding of these alkane partial oxidation systems will contribute to advances in alkane activation in general and may lead to the development of viable industrial processes.

1.1. n-BUTANE CONVERSION TO MALEIC ANHYDRIDE OVER THE VPO CATALYST

Maleic anhydride is an important industrial chemical which is synthesized from n-butane-containing feed over a vanadyl pyrophosphate catalyst. The object of the research is to synthesize the correct VPO phase to produce maleic anhydride from n-butane with industrial yields (60 to 70%).

1.1.1. ECONOMICS: THE GROWING WORLD MARKET FOR MALEIC ANHYDRIDE

Maleic anhydride is largely used as a monomer for the production of unsaturated polymer resins (54% of US demand in 1988) but other applications are also growing [Irving-Monshaw et al, 1989]. Its use in paper making is increasing at an estimated 10% per year (1989 estimate). Other uses include lubricating oil additives (12% of the market in 1989), acidulants and flavouring agents (11%) and agricultural chemicals (4%). Maleic anhydride is also used as a building block for L-aspartic acid, used in the artificial sweetener Nutrasweet [Irving-Monshaw et al, 1989].

The maleic anhydride market expanded at about 4.5% per year for several years prior to 1989, when the worldwide recession dampened demand. However, the demand for maleic anhydride continued to grow at about 3% per year from 1992 to 1997 according to SRI international [Shelley et al, 1993]. Whereas Western Europe has a maleic anhydride capacity of around 200 000 tons/annum, demand is around 240 000 to 250 000 tons/annum and is increasing by about 3 to 5% per annum. The current shortfall in local supply is provided for by imports, especially from the 620-million-pound United States market. In 1995, the United States exported about 100 million pounds of maleic anhydride globally.

The European shortfall, as well as the planned increases in the production of downstream chemicals by producers such as Sisas and Lonza, is thought to be the cause of the planned increase in capacity announced recently by several European producers [Milmo, 1996]. Plans for capacity expansion have been announced by the Sisas group (Milan) and Lonza (Basel). Sisas announced it will triple capacity to 220 000 m.t./year and will enter production of downstream specialty chemicals at a total investment of $140 million. The downstream applications will include the production of 1,4 butanediol (BDO), gamma-butyrolactone (GBL), tetrahydrofuran (THF) and N-methylpyrrolidone (NMP). Lonza, meanwhile, plans to build a 50 000 m.t./year plant in Piesteritz, Germany, representing a DM120-million ($79 million) investment. Lonza is involved with the manufacture of polyester resins and fumaric acid and is building a maleic acid plant (10 000 m.t./year) based on maleic anhydride to come on stream in 1996 [Alperowicz, 1996]. Huntsman Corporation and Condea of Hamburg, Germany, have also announced plans to build a 40 000 m.t./year joint venture plant in Meerbeck Germany. Startup is planned for late 1998. Huntsman recently closed down a benzene-based plant in the United Kingdom because of outdated technology and is supplying the European market from its 105 000 tons/annum plant in Florida. Huntsman and Condea believe their expansion will be well positioned as their competitors, Sisas and Lonza, will need much of the maleic anhydride they produce for their own planned expansion in downstream chemicals [Milmo, 1996].

European companies producing maleic anhydride and their capacities are given in Table 1.1:

TABLE 1.1 : EUROPEAN MALEIC ANHYDRIDE PRODUCTION [Cornitus, 1996]

COMPANY	CURRENT CAPACITY	EXPANSION (metric tons / year)
Sisas	80 000	140 000
Lonza	90 000	50 000
Pantochim	65 000	-
Condea-Huntsman	12 000	50 000
Hüls	38 000	-
Polioli	25 000	-
Chemie Linz	24 000	-
Cray Valley	12 000	-
Bayer	12 000	-
UCB-Ftal	3 000	-
BASF	6 000	-

The development of new uses for maleic anhydride therefore augurs favourably for that market and this is confirmed by worldwide expansion in maleic anhydride production and an increase in the demand for the VPO catalyst. As South Africa is a major vanadium producer, the manufacture of vanadium-containing compounds, such as the VPO catalyst for the manufacture of maleic anhydride, adds to the value to our raw materials.

1.1.2. INDUSTRIAL PROCESSES FOR MALEIC ANHYDRIDE PRODUCTION

Whereas previously benzene was the most widely used feedstock for maleic anhydride production, n-butane is cheaper and more environmentally-friendly. By the end of the 1980s, most American plants had converted to butane. With all feedstocks, the VPO catalyst is used, since it produces maleic anhydride from both saturated and unsaturated feeds such as benzene, butene or butane. Annually, 630 000 tons of maleic anhydride is produced from butane and 248 000 tons from benzene [Cavani et al, 1994]. With n-butane feeds, however, selectivities to maleic anhydride at higher conversions are lower than with benzene. Because the yields from n-butane are lower, worldwide increases in capacity were required when conversion to this feedstock started.

Various processes are used for the production of maleic anhydride (See Table 1.2). Traditional fixed-bed technologies give molar selectivities to maleic anhydride of around 67-75% under typical operating conditions of less than 2 molar % butane, conversions of between 70 and 85%, temperatures of between 400 and 450°C and space velocities of around 1100-2600h^{-1} [Centi et al, 1988].

TABLE 1.2: INDUSTRIAL TECHNOLOGIES FOR MALEIC ANHYDRIDE MANUFACTURE [Cavani et al, 1994]

PROCESS, LICENSOR CO.	TYPE OF REACTOR	PRODUCT RECOVERY
ALMA (Alusuisse-Lummus)	Fluidised bed	Anhydrous
Alusuisse Italia	Fixed bed	Anhydrous or aqueous
Mitsubishi Chem.	Fluidised bed	Aqueous
Monsanto	Fixed bed	Anhydrous
Scientific Design	Fixed bed	Aqueous
DuPont	Circulating fluidised bed - riser reactor	Aqueous
Sohio-UCB	Fluidised bed	Aqueous

The processes in Table 1.2 differ with regard to the type of reactor, the method of recovering the maleic anhydride from the reactor effluent (water versus organic quench) and the final purification step. Several companies have developed the use of fluidised bed technology. Fluidised bed reactors have improved heat removal and technologies that allow for the use of higher n-butane feed concentrations, which would be explosive in the less advanced fixed-bed reactors.

Scale-up of fluidised bed reactors is more complicated. Furthermore, the catalyst experiences attrition, and the use of a promoter such as silica is required to strengthen the catalyst. Little information is available on the promoters used for the fluidised bed catalysts. All companies using fluidised bed processes for maleic anhydride production claim low catalyst losses. The approaches taken to reduce catalyst losses are not disclosed. The process of DuPont, using a circulating fluidised bed-riser reactor, is considered to be the most economical. This process operates at lower conversions per pass and with higher selectivities than either fixed-bed or fluidised bed technologies [Centi et al, 1988].

A diagram of the ALMA fluidised bed process is given in figure 1.1 [Hydrocarbon processing, 1985]. The process consists of three main areas: reaction, maleic anhydride recovery and purification. n-Butane and air are fed to a fluid-bed catalytic reactor. Cooling coils are included in the fluid bed to generate high-pressure steam from the heat of reaction. The use of a fluid-bed reactor eliminates hot spots and permits operation with a close to stoichiometric reaction mixture. This results in a greatly reduced air rate relative to fixed-bed processes, which in turn results in lower investment and utility costs.

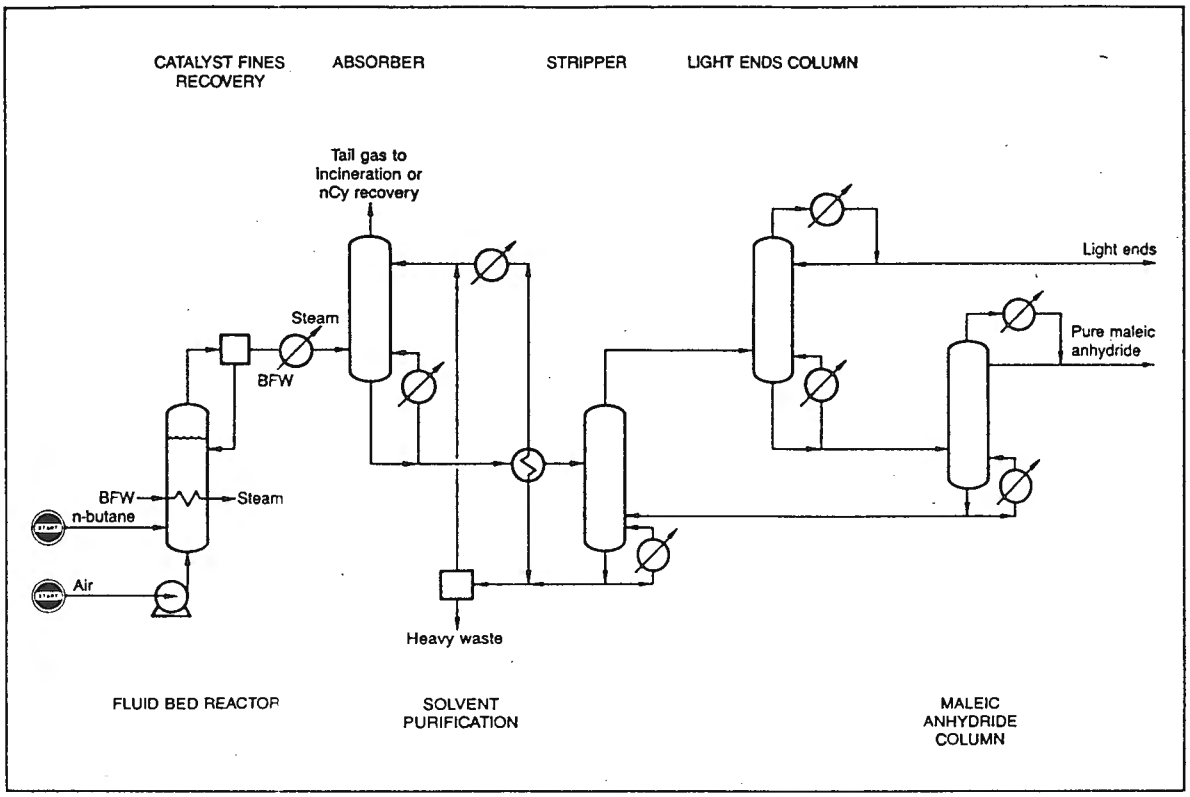

FIGURE 1.1: THE ALMA MALEIC ANHYDRIDE PROCESS [Hydrocarbon Processing, 1985]

1.1.3. STRUCTURE OF THE VPO CATALYST

The ternary VPO system is complex. Fifteen different $V_xP_yO_z$ crystal structures have been identified near the P/V ratio of 1 which have vanadium in the 4+ and 5+ oxidation states (among them five different forms of $VOPO_4$). Table 1.3. lists the different vanadium-phosphorus compounds, and their colours are given for reference in section 2.1.1, which describes the catalyst preparation:

TABLE 1.3: DESCRIPTION OF THE DIFFERENT VPO PHASES [Bordes, 1987]

PHASE	SYMMETRY	DESCRIPTION
$VOPO_4.2H_2O$	tetragonal	bright yellow platelets
α_I-$VOPO_4$	tetragonal	bright yellow hygroscopic platelets
α_{II}-$VOPO_4$	tetragonal	yellow plates
β-$VOPO_4$	orthorhombic	yellow powder
δ-$VOPO_4$	orthorhombic	dark-yellow hygroscopic platelets
γ-$VOPO_4$	monoclinic (?)	lemon-yellow platelets
$VOHPO_4.4H_2O$	triclinic	blue powder
$VOPO_4.0.5H_2O$	orthorhombic	blue platelets
$(VO)_2P_2O_7$	orthorhombic	grey to brown according to preparation
$VO(H_2PO_4)_2$	tetragonal	greenish-blue powder
$VO(PO_3)_2$	tetragonal	blue rods
$VPO_{4.75}$	monoclinic (?)	greenish-brown powder

Catalysts which are active and selective for the partial oxidation of n-butane to maleic anhydride indicate the presence of the vanadyl pyrophosphate phase $(VO)_2P_2O_7$ (V^{4+}) when characterised with XRD. Most investigators agree [e.g. Centi et al, 1988] that this phase is active for the reaction.

Based on a comparison of reactivity, XRD patterns and UV spectra, Bordes [1987] proposes that the catalyst which is selective for the partial oxidation of n-butane to maleic anhydride consists of the $(VO)_2P_2O_7$ phase (V^{4+}), with micro domains of γ-$VOPO_4$ (V^{5+}) formed by surface topotactic reoxidation. This effect, and the dynamic effect due to the set of oxidation-reduction reactions which occur in catalysis, is said to account for the observed amorphous surface. The structural disorder found with XRD analysis in the (100) plane (the plane which forms the reaction surface) was related to greater activity [Bordes, 1993].

The average valence state of vanadium in an equilibrated catalyst is given as between 4 and 4.03 [Trifiro, 1993]. The average oxidation state, as measured on the best working catalysts, is given by Zhang et al [1993] as 4.1. Nguyen et al [1996] claim that the 5+ species are present as defect sites in the $(VO)_2P_2O_7$ bulk structure. This explains the broadening in XRD peaks normally observed in the XRD structure of working catalysts, where only peaks due to the $(VO)_2P_2O_7$ species are observed. No peaks due to the $VOPO_4$ structures are observed. However, although only the 4+ phase is observed in the XRD of an equilibrated catalyst, a vanadium valence state slightly in excess of 4 is normally observed.

Nguyen et al [1996] found that the quantity of V^{5+} species, obtained by titration and P NMR spin echo mapping, correlate with the defect concentration. NMR confirmed that 5+ species are associated with $(VO)_2P_2O_7$ and not a second phase. These defects were the most prominent in samples which turned out to be optimum catalysts. Furthermore, Contractor et al [1988] have shown that a VPO catalyst, which has been reacted with pure butane until reaction ceases, still shows a vanadium oxidation state of higher than 4.00. After equilibration, the vanadium oxidation state of a given VPO catalyst does not change significantly, even if the oxygen fugacities differ by several orders of magnitude [Nguyen et al, 1996]. Since reaction only takes place on the surface, changes which affect surface oxidation state do not change the overall oxidation state of the catalyst. Nguyen et al [1996] therefore suggest that the 5+ species in an equilibrated catalyst are primarily in the bulk.

It is also claimed that typical VPO catalysts are inhomogeneous. In other words, there are different vanadium oxidation states in different positions in a typical fixed-bed, plug-flow reactor bed, due to temperature gradients and feed composition changes during calcination and reaction. This inhomogeneity could cause further peak broadening features on XRD spectra. Inhomogeneity is also introduced during standard methods of activation. In air, $(VO)_2P_2O_7$ can eventually be converted completely to $VOPO_4$. The calcination time must therefore be limited to produce a valence state of close to 4. Due to the presence of organic residue in the VPO structure of catalysts prepared with an organic reducing agent, the centre of a sample may also be reduced by interaction with the organic species at the same time that the exterior is being oxidised. NMR studies have shown that different regions of a converted precursor have different vanadium oxidation states. Calcination in inert gas or vacuum yields reductive conditions and some 3+ species are formed [Nguyen et al, 1996].

Figure 1.2. shows the theoretical XRD of pure VPO phases according to Abdelouahab et al [1992] and Table 1.4 indicates the positions of the different VPO peaks and the planes they represent. This can be compared with figure 1.3a, which shows the XRD of a catalyst prepared by Zhang et al [1993]. Three main peaks due to the $(VO)_2P_2O_7$ phase can be seen at $2\theta = 23.61°$, 28.45° and 30°. Unlike the theoretical pure phases, some peak broadening is shown for the XRD of Zhang et al (Figure 1.3a, catalyst 2) for a catalyst which, according to the authors, gave 60% selectivity to maleic anhydride with a feed of 1.2% n-butane, 16.4% O_2 and 82.4% He at T = 380°C. Figure 1.3b shows the development of the XRD spectrum of catalyst 2 of figure 1.3a with time on stream. The peak broadening, as mentioned by Nguyen et al [1996], is shown, and the spectra indicate only one phase.

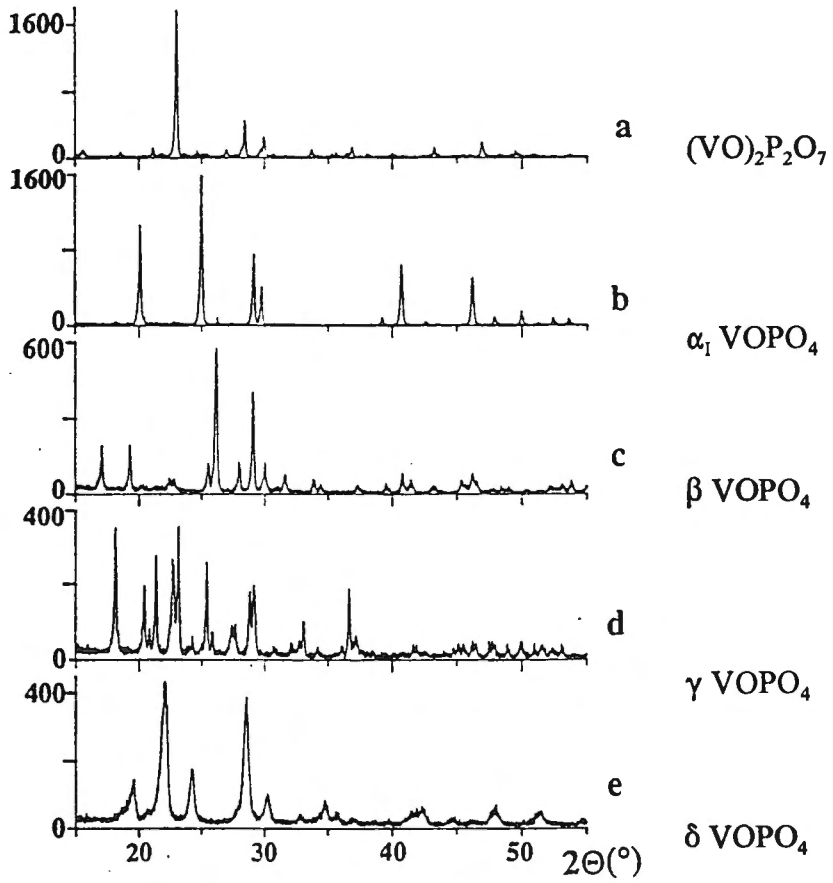

FIGURE 1.2: X-RAY DIFFRACTION PATTERNS OF THE PURE VPO PHASES [Abdelouahab et al, 1992]

TABLE 1.4: VPO XRD PEAK POSITIONS [Zhang et al, 1993]

$(VO)_2P_2O_7$	23.00°(200), 23.61°(201), 25.43°(211), 26.99°(212), 28.45°(024), 29.64°(213), 29.94°(032), 30.70°(115)
α_{II} $VOPO_4$	25°(101), 29.14°(111), 29.75°(200)
β $VOPO_4$	22.40°(111), 22.80°(200), 25.54°(002), 26.17°(201), 28.07°(102), 29.09°(020), 20.02°(211)
γ $VOPO_4$	21.37°(004), 22.65°(221), 23.16°(040), 25.40°(230), 25.89°(213), 27.69°(223), 28.80°(105), 29.16°(311), 30.74°(312)
δ $VOPO_4$	22.08°(111), 24.16°(012), 28.55°(020), 30.26°(021)

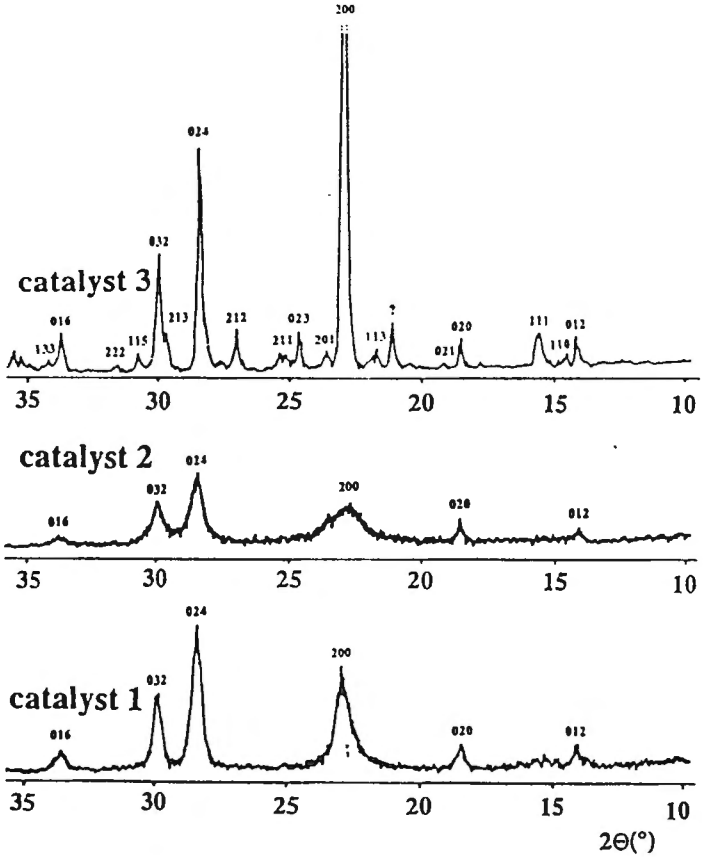

FIGURE 1.3. [Zhang et al, 1993]

a) EFFECT OF CALCINATION ON CATALYST STRUCTURE

Catalyst 1: Calcined at T = 440°C in $C_4H_{10}/O_2/N_2$ = 1.2/16.4/82.4 for 25 h

Catalyst 2: Calcined in Argon at T = 440°C for 25 h

Catalyst 3: Calcined in Argon at T = 880°C for 10 h

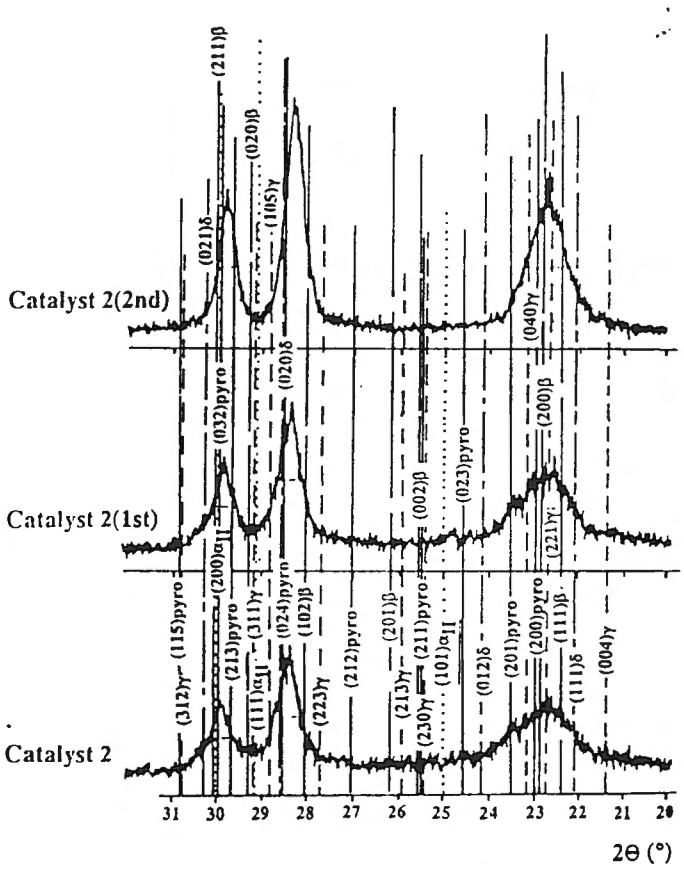

b) EFFECT OF TIME ON STREAM ON CATALYST STRUCTURE

Catalyst 2 (1st):
Catalyst 2 after set of reaction runs at T = 300-450°C

Catalyst 2 (2nd):
Catalyst 2(1st) after set of reaction runs at T = 300-450°C

Figure 1.3a shows the catalysts of Zhang et al [1993]. Catalyst 1 was calcined in $C_4H_{10}/O_2/N_2$ = 1.2/16.4/82.4 at T = 440°C for 25 hours, catalyst 2 in Argon at T = 440°C for 25 hours and catalyst 3 in Argon at T = 880°C for 10 hours. As may be seen, catalyst 3 shows a decrease in peak broadening compared to catalysts 1 and 2. Zhang et al also state that the peak intensity of the (200) plane more than doubles from catalysts 2 to 3. Peak intensities due to the (032) and (024) planes, on the other hand, decrease. Catalyst 3 gives low yields of maleic anhydride and its XRD spectrum shows little change during reaction. Zhang et al conclude that the XRD spectrum of catalyst 3 indicates a particular $(VO)_2P_2O_7$ catalyst, of which the presence of only V^{4+} sites and no V^{5+} shows a comparatively lower development of the basal (100) face and a higher development of the side faces in the d direction.

Catalyst 2 of Zhang et al (Figure 1.3a) shows greater specific activity for n-butane oxidation ($200x10^{-9}$mol/g.s at T = 400°C) than catalyst 3 ($10x10^{-9}$mol/g.s at T =400°C). Maleic anhydride selectivity increases with time on stream. This correlates to the development of the X-ray spectrum of catalyst 2 of Zhang et al shown in figure 1.3b. It is suggested that figure 1.3b shows the same trend as figure 1.10 of Cavani et al [1994], which indicates the transformation of the amorphous and oxidised phases to crystalline pyrophosphate.

The structure of vanadyl pyrophosphate, $(VO)_2P_2O_7$, was first solved by Gorbunova et al [1979]. It consists of sheets made of pairs of edge-sharing VO_6, with trans V=O bonds, equatorially linked to PO_4 tetrahedra. These sheets are stacked on each other, so as to form double columns of distorted VO_6 (chains O=V..O=V), parallel to bent pyrophosphate groups. The structure of $(VO)_2P_2O_7$ is given in Figure 1.4 below.

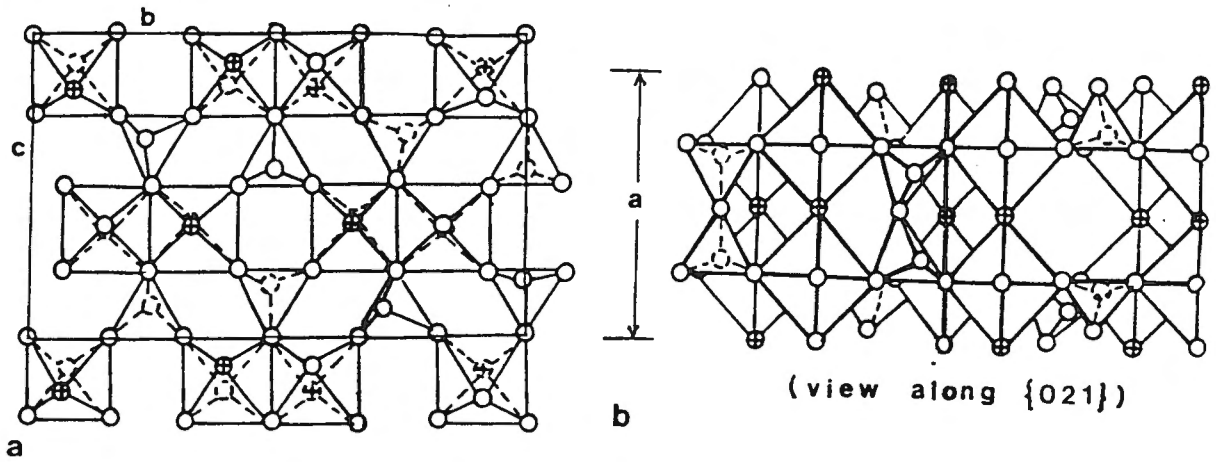

FIGURE 1.4: CRYSTAL STRUCTURE OF $(VO)_2P_2O_7$ SHOWING THE POSITIONS OF THE LATTICE OXYGENS [Bordes, 1987]
KEY: ○ = SINGLE BONDED OXYGEN
KEY: ⊕ = DOUBLE BONDED OXYGEN

The $(VO)_2P_2O_7$ lattice has an orthorhombic unit cell. Authors such as Bordes [1987] and Ebner et al [1993] agree that reaction only takes place on the (100) crystal plane. The reaction is thus not only structure sensitive but also crystal-face sensitive. If the orthorhombic crystals are grown in equilibrium conditions, the (100) plane contributes 32% to the external area of the orthorhombic crystal, the (021) plane 45% and the (001) plane 23%. The extent to which the (100) crystal face is exposed in the crystal macro-structure will influence reactivity. This exposure will depend on the solvent used, the promoter added and the temperature of calcination [Bordes, 1993]. For example, organic reducing agents expose greater surface area than aqueous reducing agents. A projection of the (100) plane of the hexagonal crystal is shown in Figure 1.5 [Ebner et al, 1993].

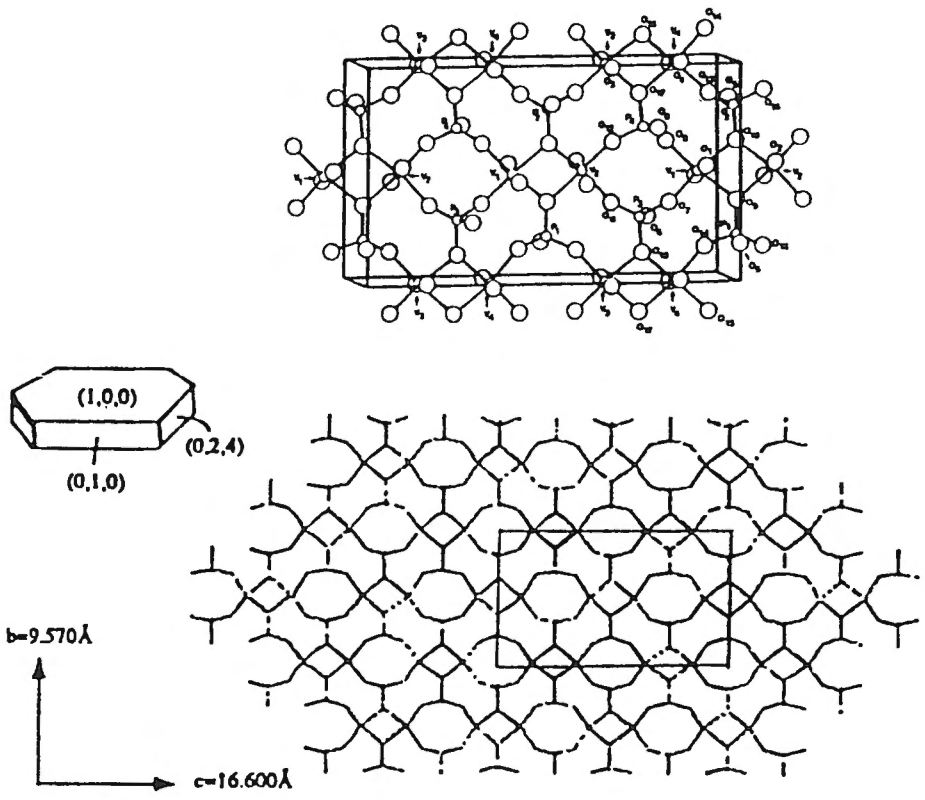

FIGURE 1.5: PROJECTION OF THE (100) PLANE OF THE $(VO)_2P_2O_7$ HEXAGONAL PLATELET CRYSTAL [Ebner et al, 1993]

1.1.3.1. ACTIVE SITES ON THE VPO CATALYST

Hodnett [1985] reports that when calcination is carried out below 380°C, excess phosphorus remains on the surface as PO_4^{3-}. Above this temperature, phosphorus enters the solid to stabilise the 4+ state by solid-state reaction. This is confirmed by Cavani et al [1994], who state that the surface P/V ratio on an equilibrated industrial catalyst was found to be between 1.5 and 3.

As shown in Figure 1.6, two hypothetical surface atomic arrangements are proposed [Ebner et al, 1993]. In the model of a phosphorus poor surface, columns of vanadium are exposed, producing a surface consisting of vanadium equatorial sites terminating with hydroxide and bridging oxide species. Exposing a vanadium rich surface results in a selectivity penalty as observed with catalysts having P/V ratios which are not much in excess of 1. Ratios of much lower than one will, on the other hand, result in the formation of $VOPO_4$ phases. Alternatively, a surface of pyrophosphate anions, which shield the vanadium columns and expose P-OH groups, is proposed for a phosphorus rich surface. A phosphorus rich surface will again result in good selectivity, but with an activity penalty.

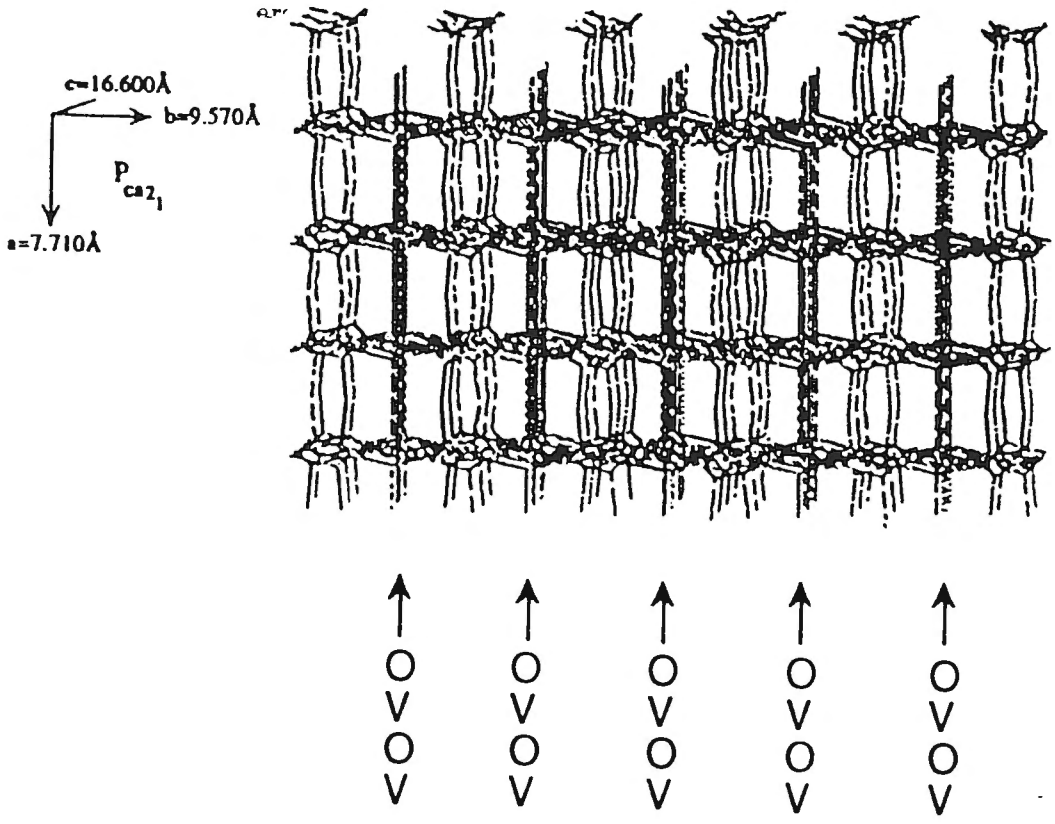

FIGURE 1.6: PROJECTION OF (010) OF $(VO)_2P_2O_7$ ILLUSTRATING PYROPHOSPHATE TERMINATION AT TOP OF STICK FIGURE VERSUS ORTHOPHOSPHATE TERMINATION AT BOTTOM OF STICK FIGURE [Ebner et al, 1993]

As shown in Figure 1.7 [Ebner et al, 1993], six pendent pyrophosphate groups overhang the ensemble of vanadium sites in the surface cleft, creating a total of twelve hydrogen binding sites as surface -P-O- in the unprotonated form, as well as a facile transport mechanism for movement of abstracted hydrogen atoms from the surface cleft region to sites of water formation and desorption. This model illustrates the role of the oxygen species surrounding the vanadium Lewis site.

Many different reactive species are present on the $(VO)_2P_2O_7$ surface. The trans-disposition of the V=O in the pairs of octahedra results in one vanadium with an oxygen vacancy - a Lewis acid site - on the surface. The Lewis acid site of the V^{4+} is suggested by Bordes [1987], Matsuura [1993] and Busca et al [1986] to be the site on which n-butane could first adsorb. "In order to be activated, butane needs strong acid sites such as $V^{+3.7}$ to $V^{+4.4}$ in $(VO)_2P_2O_7$, situated near suitably bonded oxygen atoms able to catch the hydrogen of CH_2 groups." [Bordes, 1987]. Upon dehydrogenation the V^{4+} is reduced to V^{3+}, which is regenerated with O_2.

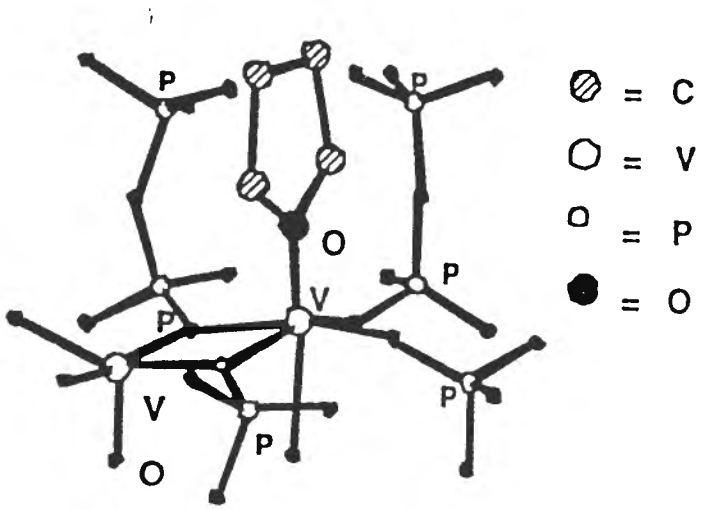

FIGURE 1.7: PROPOSED SURFACE FURAN INTERMEDIATE INVOLVING LATTICE OXYGEN ORIENTED WITH SURFACE PENDENT PYROPHOSPHATE GROUPS [Ebner et al, 1993]

Zhang-Lin et al [1994] propose that activation takes place on the $(V=O)^{2+}$, with the $(V=O)^{3+}$ species abstracting the H^-. This could be valid since "much of the surface vanadium in $(VO)_2P_2O_7$ is available for oxygen chemisorption" [Centi et al, 1988]. However, it is more generally accepted that the chemisorption takes place on a V^{4+} Lewis acid site, with the various oxygen species involved in dehydrogenation and oxygen insertion reactions [Ebner et al, 1993]. Although the exact role of oxygen surface species is disputed, Cavani et al [1994] propose the following oxygen species on the surface:

(1) $O^{\delta-}$ of surface $V^{5+}=O$ and $V^{4+}=O$
(2) Triply bridged $O^{\delta-}$ associated with two adjacent vanadiums of a dimer unit and a phosphorus of the pyrophosphate moiety VO(P)V
(3) Numerous doubly bridging $O^{\delta-}$ e.g. V-O-V, V-O-P
(4) The $O^{\delta-}$ from P=O and -(PO-) groups associated with terminating phosphate tetrahedra
(5) Surface activated $(O_2)^{\delta-}$ species associated with vanadium or adsorbed oxygen as η^2-superoxo and η^1-peroxo species

Figure 1.8 gives a model of the (100) $(VO)_2P_2O_7$ surface showing the various oxygen sites [Bordes, 1987]. The model accounts for the presence of V^{5+} species on the surface.

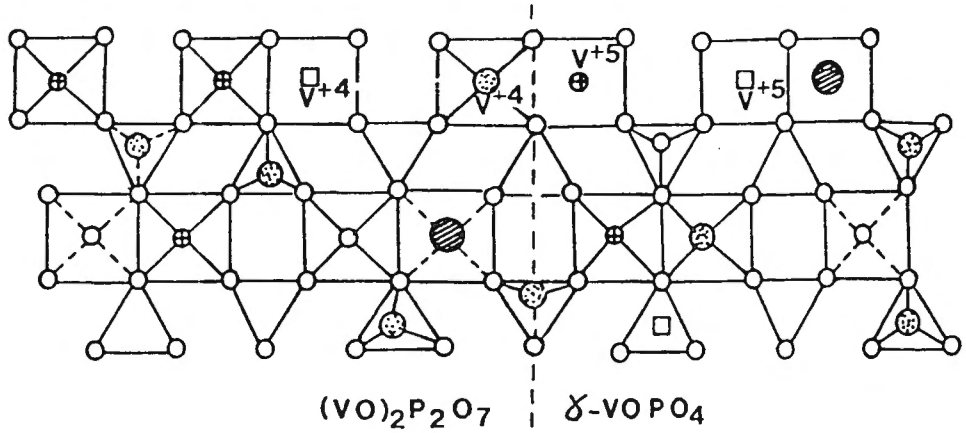

FIGURE 1.8: MODEL OF THE (100) PLANE OF $(VO)_2P_2O_7$, TRUNCATED TO FORM THE REACTION PLANE [Bordes, 1987]

○ = oxygen
⊕ = vanadyl oxygen
⊘ = OH_2, free or co-ordinated to V
◎ = OH co-ordinated to P

Abon et al [1997] used isotopic labelling to investigate the respective roles of lattice and adsorbed oxygen in the n-butane oxidation. It was concluded from the isotopic labelling that only lattice oxygen is active in the formation of maleic anhydride, CO, CO_2 and water, and the participation of any chemisorbed oxygen was precluded.

Based on the finding that only a few subsurface layers are affected by reoxidation, Bordes [1987] proposed that oxygen atoms extracted from the catalyst surface during n-butane oxidation can be replenished by gliding of the layer below the surface, producing a micro-domain of γ-$VOPO_4$. Since the $(VO)_2P_2O_7$ and the γ-$VOPO_4$ frameworks are made up of the same elementary units (pairs of octahedra), only small displacements of the atoms lying in the planes (010) are needed. The transformation is therefore facile.

The presence of 5+ species associated with prominent defect sites in the bulk of the $(VO)_2P_2O_7$ structure (See section 1.1.3) of the best VPO catalysts, has led Nguyen et al [1996] to suggest that the active sites for selective n-butane oxidation may be associated with regions where the extended defect sites meet the surface. Schuurman et al [1997] also confirm the need for V^{5+} species in the catalyst and state that an increase in 5+ species in the catalyst improves activity and selectivity. Oxygens linked to V^{5+} are required for the oxygenation step and the redox reaction proceeds between V^{5+} and V^{4+}.

1.1.4. PREPARATION OF THE VPO CATALYST

A wide variety of preparation parameters such as P/V ratio, solvent and calcination conditions has been studied. The following is an attempt to give the parameters that are the most generally used and should give the best results. Investigators who give the same general preparation method often obtain yields of maleic anhydride which vary considerably: 5% [Bosch et al, 1987], 50% [Abon et al, 1995] or 80% [Nguyen et al, 1996]. It is therefore not certain whether all the controlling variables are given. However, these and other authors are consistent in their description of the preparation method.

Preparation generally involves three steps:

I Reduction of V_2O_5
II Reaction with o-H_3PO_4
III Calcination and activation

The starting compound for the formation of the pyrophosphate is a 5+ species such as V_2O_5 [US Patent 330354 (1975), US Patent 4315864 (1982)] or NH_4VO_3 [US Patent 3856824 (1974)]. This species is reduced to a 4+ species in either aqueous or organic medium. In aqueous medium, this is achieved by dissolution and boiling of V_2O_5 in HCl(aq) or if the precursor is NH_4VO_3, oxalic or lactic acid. In organic medium, this is achieved by suspending the V_2O_5 in an alcohol or a mixture of alcohols and refluxing. o-H_3PO_4 is then added to either mixture once reduction has taken place. The use of precursors other than V_2O_5 is uncommon in the patent literature and in recent academic literature.

In the aqueous case, precipitation does not occur until the solution is concentrated and hot water is added, which results in the precipitation of blue vanadyl orthophosphate. The precipitate is then filtered, washed and dried. The aqueous method is quoted in earlier papers [e.g. Morselli et al, 1982] and in a range of patents: US Patent 330354 (1975), US Patent 4016105 (1977), German Offenlegungsschrift 2636800 (1977), Japanese Kokai 7843687 (1978), US Patent 4219484 (1980) and US Patent 4209423 (1986).

The organic reducing agent is more effective and is extensively used in recent literature. US Patents 4317778 (1982) and 4244879 (1981) report the use of isobutanol as reducing agent. Other organic reducing agents reported are allyl alcohol [US Patent 4315864 (1982)], crotyl alcohol [US Patent 4315864 (1982)] and a mixture of allyl alcohol and tert-butyl alcohol [US Patent 4315864 (1982)]. A mixture of strong reducing agents such as benzyl and allyl alcohol has been reported to give a very active catalyst with high surface areas [US Patent 4132670 (1979)]. Most recent investigators therefore use the method described in US Patent 4132670 by Katsumoto and Marquis [1979]. This method employs a V_2O_5 precursor and a strong organic reducing agent or mixture of strong organic reducing agents. Vanadium in the 5+ oxidation state forms soluble alcoholates, which can be reduced in the liquid phase to 4+, which does not form soluble alcoholates. To this black suspension, o-H_3PO_4 is added and the V_2O_4 solid reacts with the H_3PO_4 in the liquid phase to form the precursor $VOHPO_4.0.5H_2O$ (4+) [Okuhara et al, 1993], also written by some investigators as $(VO)_2P_2O_7.0.5H_2O$ (4+) [Poli et al, 1981, Nguyen et al, 1996].

For aqueous or organic preparation, the calcination of the precursor $(VOHPO_4).0.5H_2O$ takes place at around 400°C in either N_2 [Japanese Kokai 8145815 (1981)] or air [US Patent 330354 (1975), US Patent 4219484 (1980), US Patent 4244879 (1981), US Patent 4317778 (1982), US Patent 4315864 (1982)]. Alternatively, the calcination can take place in the reaction mixture [US Patent 4652543 (1987)]. During calcination, the alcohol is released and water is driven off. A topotactic dehydration leads to a layered compound which presents its cleavage plane at the surface. Cavani et al [1994] propose the following scheme during activation:

$$VOHPO_4.0.5H_2O \rightarrow \text{amorphous phase} \rightarrow (VO)_2P_2O_7 \rightarrow \beta\text{-}VOPO_4$$

$$\searrow$$

$$V^{5+} \text{ phases}$$

The amorphous intermediate shown above is formed when organic residue is not washed from the catalyst after reduction in organic medium [Nguyen et al, 1996]. The transformation from $(VO)_2P_2O_7$ to β-$VOPO_4$ and the reverse occur via the crystallographic shear plane (CS) mechanism shown in Figure 1.9.

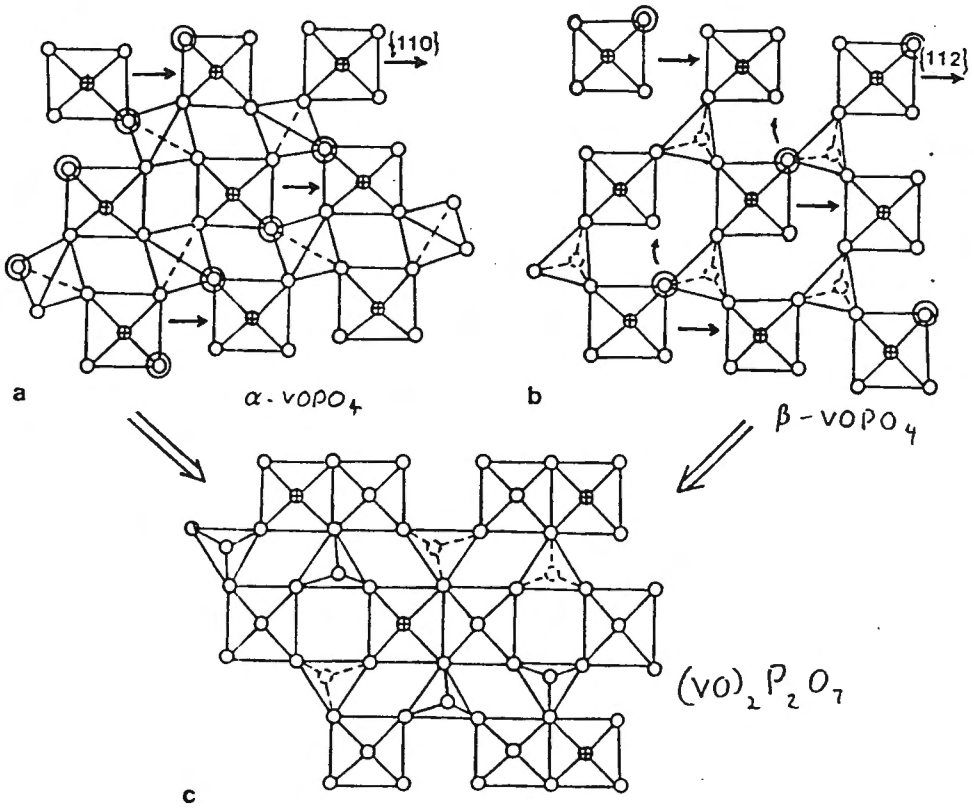

FIGURE 1.9: REDUCTION OF $VOPO_4$ TO (100) $(VO)_2P_2O_7$ BY THE CS MECHANISM. DOUBLE CIRCLES CORRESPOND TO V-O-P BONDS TO BE BROKEN [Bordes, 1987]

This mechanism is chosen by Bordes [1987] because it accounts for the similar behaviour of α-$VOPO_4$ and β-$VOPO_4$ and for the formation of pairs of edge-sharing and corner-sharing octahedra (P_2O_7) from single VO_6 and PO_4 groups respectively. On the other hand, pseudomorphism is shown between the (010) planes of $VOHPO_4.0.5H_2O$, $(VO)_2P_2O_7$ and γ-$VOPO_4$ as a consequence of topotaxy. The dehydration of $VOHPO_4.0.5H_2O$ and the reduction of γ-$VOPO_4$ to $(VO)_2P_2O_7$ have low activation energies. Whereas the β-$VOPO_4$ phase has been observed as a separate crystalline phase in XRD spectra, the γ-$VOPO_4$ phase is simply a structural model proposed by Bordes [1987] to explain the presence of V^{5+} sites in the $(VO)_2P_2O_7$ structure. Bordes [1987, 1993] suggests that γ-$VOPO_4$ "micro domains" occur in the $(VO)_2P_2O_7$ structure whereas Nguyen et al [1996] show the presence of defect sites correlated to 5+ species.

Bordes [1993] proposes that during air calcination the redox pair $(VO)_2P_2O_7$ and β-$VOPO_4$ forms. With nitrogen calcination or in-situ calcination in reaction feed, the redox pair $(VO)_2P_2O_7$ and γ-$VOPO_4$ forms. The $(VO)_2P_2O_7$ phase, whose vanadium forms a redox pair with the vanadium of β-$VOPO_4$, is also called the β^* -phase by some investigators [Bosch et al, 1987, Poli et al, 1981]. A mixture of β-$VOPO_4$ and the so-called 4+ β^*-phase (described in section 1.1.4.1.2) has been shown by Bosch et al [1987] to form when calcining in air but not nitrogen (only $(VO)_2P_2O_7$ forms) at P/V ratio = 1. The mixture of the β-$VOPO_4$ and $(VO)_2P_2O_7$ phases has been shown to produce maleic anhydride with lower yields than when the single $(VO)_2P_2O_7$ phase is present. Pure β-$VOPO_4$ has been shown to produce only CO and CO_2 [Bosch et al, 1987], but is active for the oxidation of butene to maleic anhydride [Bordes, 1987]. Limiting the calcination time in air leads to an oxidation state of close to 4 [Nguyen et al, 1996]. A catalyst which has been kept in a flow of reactants for at least 200 hours on stream is called an equilibrated catalyst. Such a catalyst is more crystalline, does not reoxidise in air at 673K and is less reactive than a fresh catalyst, but has a higher selectivity towards maleic anhydride. Figure 1.10 [Cavani et al, 1994] shows the difference in X-ray diffraction patterns between a fresh catalyst and an equilibrated catalyst.

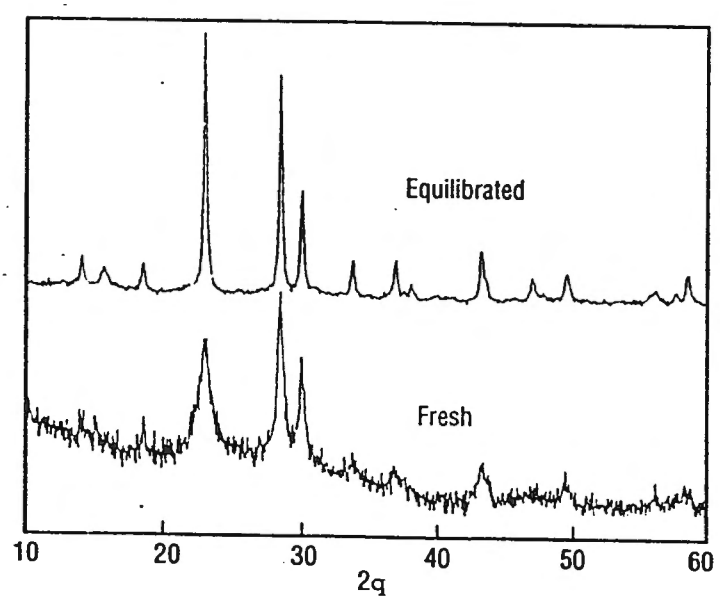

FIGURE 1.10: X-RAY DIFFRACTION PATTERNS OF FRESH (100 HOURS ON STREAM) AND EQUILIBRATED (1 MONTH ON STREAM) CATALYSTS. THE PATTERN OF THE FRESH CATALYST IS INDICATIVE OF LESS CRYSTALLINE MORPHOLOGY [Cavani et al, 1994]

Figure 1.11 [Abon et al, 1995] shows the change in selectivities and conversion with time on stream. The average vanadium valence state of an equilibrated catalyst is slightly above 4 although it is always a single phase [Nguyen et al, 1996], even when calcined in air. This is explained by the presence of 5+ species associated with defect sites originating from the dehydration step [Nguyen et al, 1996]. The V^{5+} orthophosphate crystalline compounds (β-$VOPO_4$), formed during the initial activation period, are reduced to $(VO)_2P_2O_7$ over several hundred hours on stream in the butane oxidation reaction [Kubias et al, 1992].

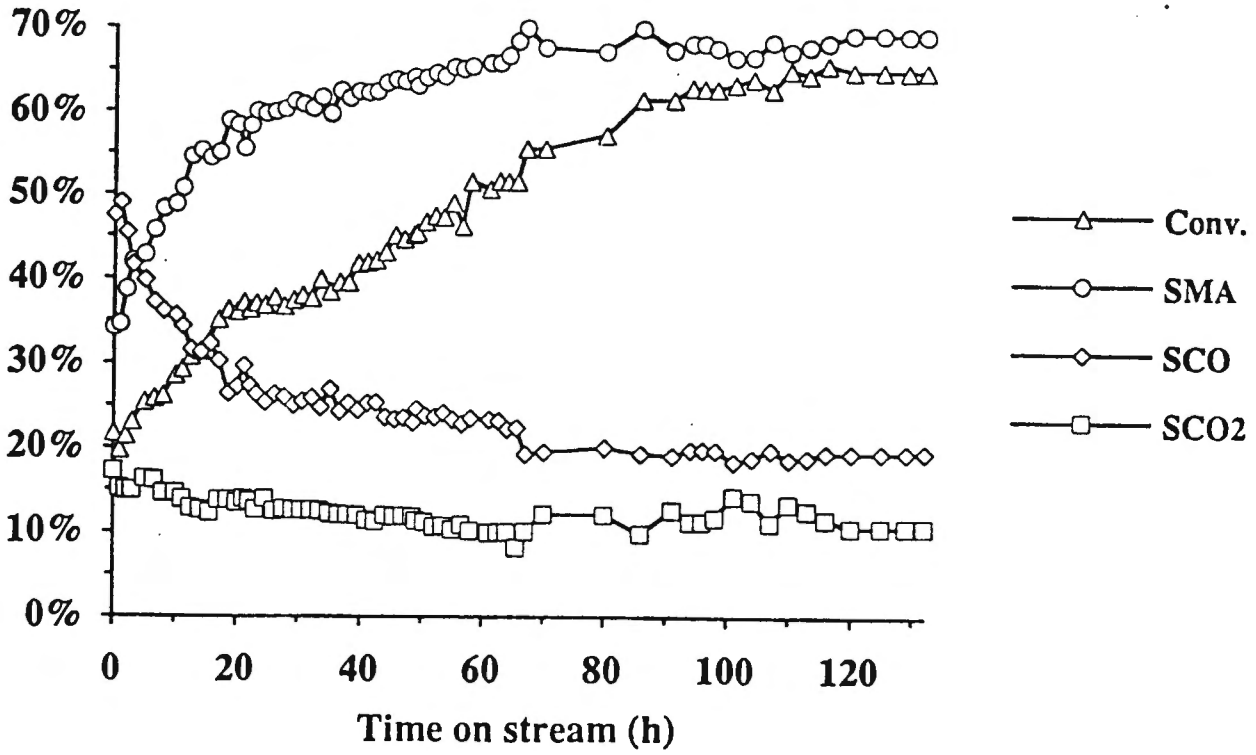

FIGURE 1.11: EVOLUTION OF CATALYTIC PERFORMANCE WITH TIME ON STREAM [Abon et al, 1995]

Temperature:	**400 °C**
Feed Comp:	**n-C_4H_{10}/O_2/He: 1.6/18/80.4**
Total Flow:	**2.4 litre/hour**
VHSV:	**1500 h^{-1}**
P/V Ratio:	**1.1**
Reducing agent:	**isobutanol**
Calcination:	**no prior calcination**

1.1.4.1. EFFECT OF PREPARATION VARIABLES ON ACTIVITY AND SELECTIVITY

The catalytic properties, which depend on the phase present, are influenced by several preparation factors: the reducing agent (either aqueous or organic), the P/V atomic ratio and the calcination and/or activation conditions. It is therefore important to observe the right synthesis variables in order to obtain the right phase. For instance, when calcining the $VOPO_4.0.5H_2O$ hemihydrate precursor, the use of air can cause the formation of V^{5+} species at temperatures of as low as 450°C whereas the use of nitrogen will still form only V^{4+} species at temperatures of up to 750°C. Calcination in air for too long periods or at too high temperatures will convert the precursor completely to $VOPO_4$. Whereas aqueous and organic reducing agents both produce the $VOPO_4.0.5H_2O$ hemihydrate precursor, the organic reducing agent produces a less crystalline form with greater surface area, leading to better reactivity. Lower P/V ratios can result in over-oxidation to the V^{5+} species, whereas higher P/V ratios stabilise the V^{4+} form. The V^{5+} phase has been shown to produce only CO and CO_2 in n-butane oxidation.

Figure 1.12 gives the infrared spectra of VPO catalyst samples prepared by different investigators. Figure 1.12a shows the spectra of catalyst samples prepared by Igarashi et al [1993]. Catalyst c of Figure 1.12a was prepared by the reduction of V_2O_5 in organic medium and spectrum d by the reduction of V_2O_5 in aqueous medium. Both c and d were calcined in N_2 at 550°C for 2 hours.

Figure 1.12b shows VPO catalyst samples prepared by Cavani et al [1984] by the reduction of V_2O_5 in aqueous or organic medium. Sample a of Cavani et al (Figure 1.12b) shows the infrared of the catalyst precursor $VOHPO_4.0.5H_2O$ prepared in organic medium. Sample b shows the infrared spectrum of a catalyst prepared in aqueous medium and calcined in N_2. Sample c is reduced in organic medium and calcined in air at 380°C for 3 hours. Samples d and e are calcined in air at 430°C and 500°C respectively. Sample c has an optimal surface area on account of its temperature of calcination (See Figure 1.15). The more severe the calcination conditions in air, the lower the percentage of V^{4+} species in the catalyst as determined by titration (See Figure 1.16). The infrared spectra show an increase in intensity of the peak at $960cm^{-1}$ (V=O) with increase in calcination temperature. The three peaks at 1085, 1130 and 1240 cm^{-1} become indistinguishable at more severe calcination conditions.

Based on the increase in the percentage of V^{5+} species with increase in temperature of calcination (Figure 1.16) and the work of other investigators [Nguyen et al, 1996, Bordes, 1987, Bosch et al, 1987], which show the formation of the $VOPO_4$ phase during calcination in air at high temperatures and long calcination times, it can be concluded that spectra c, d and e of Cavani et al (Figure 1.12b) show the presence of both the 4+ and 5+ phases, with the 5+ phase increasing as calcination conditions in air become more severe for samples c to d.

FIGURE 1.12: INFRARED SPECTRA OF VPO CATALYST

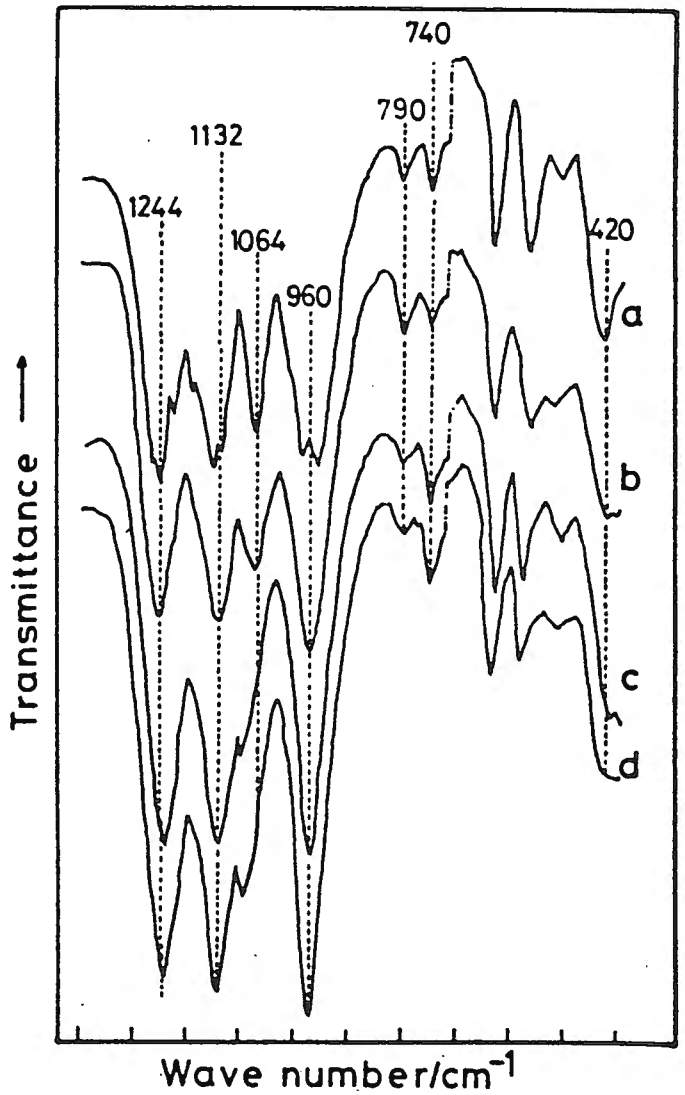

a) IGARASHI ET AL. [1993]

a: prepared by reduction with $NH_2OH.HCl$
b: prepared by reduction of V_2O_4 with organic solvent
c: prepared by reduction of V_2O_5 with organic solvent
d: prepared by reduction of V_2O_5 in aqueous medium

a,b,c,d calcined for 2hours at 823K in N_2

b) CAVANI ET AL. [1984]

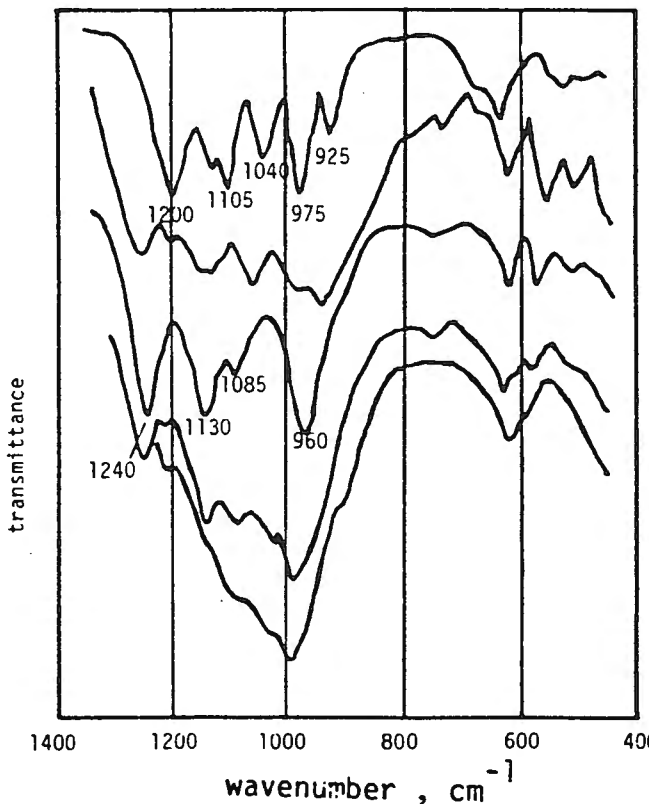

a catalysts dried at 150 °C for 10 hours

b catalysts prepared in aqueous medium after calcination in nitrogen

c catalysts prepared in organic medium after calcination in air at 380 °C for 3 hours

d P:V 0.95 calcined in air at 430 °C for 3 hours

e P:V 0.95,1.08,1.16 calcined in air at 500 °C for 10 hours

1.1.4.1.1. REDUCING AGENT / SOLVENT

Vanadyl pyrophosphate can be prepared in aqueous or organic medium. Hodnett [1985] states that a VPO catalyst prepared in organic medium has a higher surface area (15 - 50m^2/g) than one prepared in aqueous medium (10 m^2/g). The specific activity of the catalyst prepared in organic medium is also higher as shown in Figure 1.13. This can be explained by the stronger Lewis acid sites found on catalysts prepared in organic medium [Centi et al, 1988]. As mentioned in section 1.1.3, several investigators propose that n-butane activation (the rate determining step) takes place on a Lewis acid site.

Busca et al [1986] showed that, at the same reaction temperature, a catalyst prepared with HCl (aqueous reducing agent) gives a lower yield of maleic anhydride than a catalyst prepared in organic medium. He also found that, for 1-butene oxidation, similar yields of maleic anhydride could be obtained with both catalysts, but with the catalyst reduced in the aqueous medium, 100°C higher temperatures were needed. The surface area of the organically prepared catalyst was higher than that of the catalyst prepared in aqueous medium (27 and 6 m^2/g respectively) and the specific rate of n-butane depletion was about 6 times higher. During organic preparation, alcoholates become entrapped inside the sheets of the precursor. This results in increased disorder in the stacking-fold, causing preferential exposure of the reaction surface. The catalyst prepared in organic medium also showed the presence of strong Lewis acid sites as opposed to medium-strong Lewis sites for the catalyst prepared in aqueous medium.

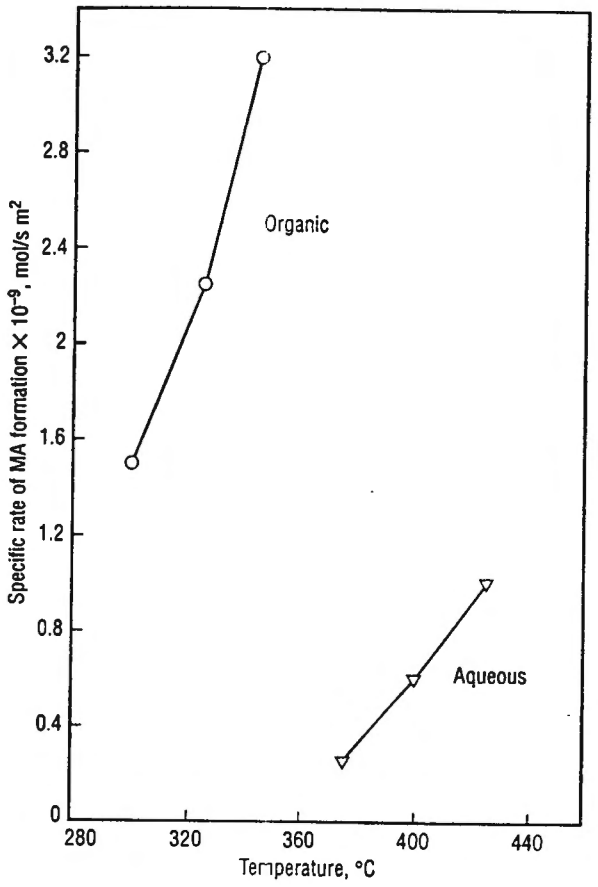

FIGURE 1.13:

COMPARISON OF THE SPECIFIC RATE OF MALEIC ANHYDRIDE FORMATION IN n-BUTANE PARTIAL OXIDATION FOR CATALYSTS PREPARED IN AQUEOUS VS ORGANIC MEDIUM

[Cavani et al, 1994]

High surface areas can be obtained when using a mixture of isobutanol and benzyl alcohol as reducing agent [Cornaglia et al, 1993, US Patent 4132670 (1979)]. Although high surface areas can also be obtained with the use of many other organic reducing agents, improved catalytic activity for the oxidation of n-butane to maleic anhydride does not necessarily follow. When methanol, acetic acid or tetrahydrofuran are used, typically 50 to 90°C higher reaction temperatures are needed to achieve comparable activities and selectivities, although BET surface areas are similar to that of the isobutanol/benzyl alcohol mixture [US Patent 3864280 (1975)]. It should be noted that the organic reducing agents which give the best yields are the stronger reducing agents such as allyl alcohol and isobutyl alcohol, as opposed to methanol. No correlation between the strength of the organic reducing agent and the resulting vanadium oxidation state is however given [Hodnett, 1985], although it is hypothesised that the different strengths of the reducing agents result in different average valence states in the precalcined precursor. This is however refuted by later authors. Busca et al [1986] claim that aqueous and organic reducing agents both give the same $VOPO_4.0.5H_2O$ hemihydrate precursor although the one prepared in organic medium is less crystalline. The differences in reactivity of catalysts reduced with different organic reducing agents but having similar BET surface areas therefore remain unexplained and may be a result of differences in surface Lewis acid strength.

Cornaglia et al [1993] showed that varying the isobutanol/benzyl alcohol ratio of the organic reducing mixture results in different degrees of disorder in the precursor as shown by XRD: "The extent of disorder is a function of the proportion of aromatic alcohol in the mixture... the disorder in the precursor lattice is related to the retention of benzyl alcohol between the layers of the precursor." It is therefore hypothesised that different alcohols will vary in the way in which they are retained between the layers. This will result in differences in the occurrence of defect sites. However, Cornaglia et al do not show a comparison in catalytic activity between catalysts prepared with different isobutanol/benzyl alcohol ratios.

1.1.4.1.2. METHOD OF ACTIVATION AND CONDITIONING AT HIGH TEMPERATURES

During the reduction step, the catalyst precursor $VOHPO_4.0.5H_2O$ is formed and needs to be transformed to $(VO)_2P_2O_7$. This is done by calcination. There are three main methods of catalyst calcination: i) activation in an oxygen-free atmosphere at 673-723K, followed by introduction of the reaction mixture; ii) single step or multi step calcination in air until 653K; iii) activation in the reaction mixture. In air, the transformation of $VOHPO_4.0.5H_2O$ to the pseudomorphically layered $(VO)_2P_2O_7$ by topotactic reaction takes place at lower temperatures, but care must be taken to avoid excess oxidation of the amorphous phase to 5+ species [Bordes, 1987]. In nitrogen, transformation takes place at higher temperatures and sintering must be avoided. Bordes further reported that, when calcining an aqueously and an organically prepared catalyst in air, the transformation takes place at a 100°C higher for the catalyst prepared in aqueous medium.

Bosch et al [1987] compared the reactivity of catalysts calcined in N_2 (Figure 1.14a) and in air (Figure 1.14b), having been otherwise prepared in the same way. The catalyst calcined in N_2 gave a yield of maleic anhydride which peaked at a lower temperature than for the catalyst calcined in air (plotted as yield versus temperature). The best yield of maleic anhydride was, however, obtained when the catalyst was calcined under reaction feed conditions, that is 1.5% n-butane in air. Bosch et al compared the phases observed after calcination under different atmospheres for a range of P/V ratios.

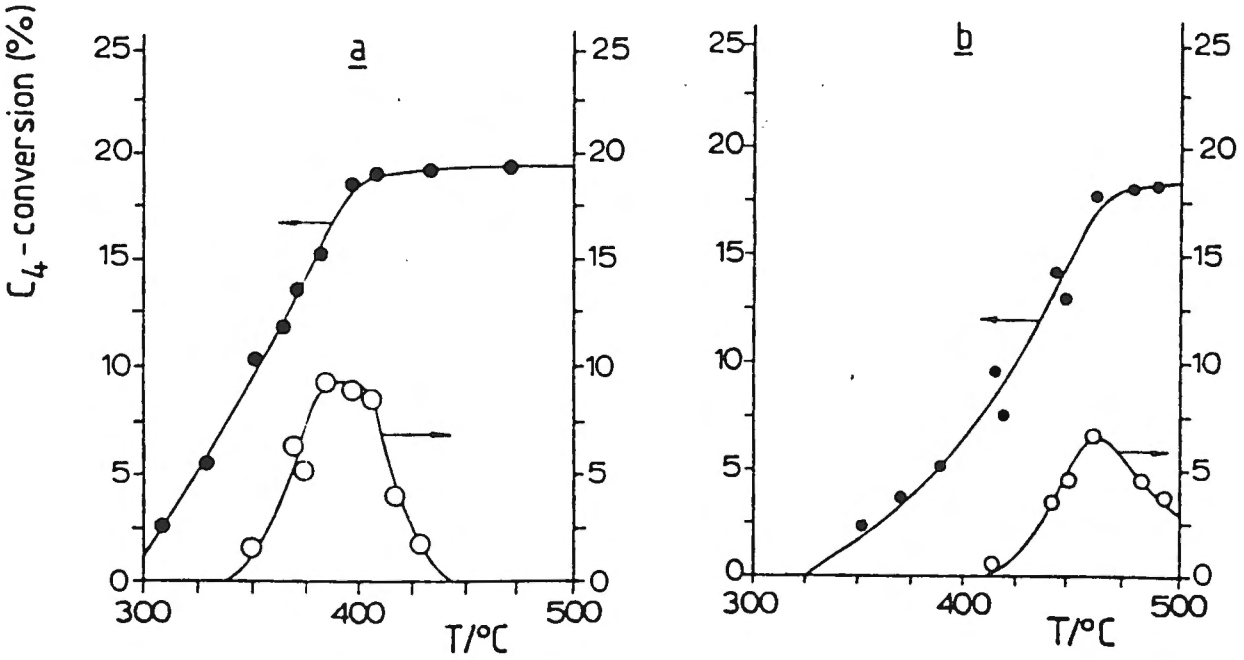

FIGURE 1.14: • CONVERSION AND ◦ YIELD OF MALEIC ANHYDRIDE VS TEMPERATURE FOR CATALYSTS CALCINED IN: a) NITROGEN b) AIR [Bosch et al, 1987]

Mass of catalyst:	**0.2 g**
Total feed rate:	**15 ml/min**
Feed composition:	**1.5% n-butane in air**
Pressure:	**1.03 bar**
P/V ratio:	**1**
Calcination conditions:	**500°C, 10 hours**
Reducing agent:	**isopropanol/benzyl alcohol**

At P/V = 0.9 and 0.7, calcination in air produced a mixture of V_2O_5 and β-$VOPO_4$ and at P/V = 1, a mixture of β-$VOPO_4$ and a so-called poorly crystalline β*-phase, which is also referred to as $(VO)_2P_2O_7$ by authors such as Bordes [1987]. The percentage of the β-$VOPO_4$ phase decreased with temperature of calcination. Over-oxidation to the 5+ $VOPO_4$ phase is known to occur at severe oxidising atmospheres such as long calcination times and high calcination temperatures in air [Bordes, 1985; Bosch et al, 1987]. The β* phase is also reported by Poli et al [1981] as a mixed-valence crystalline phase which oxidises n-butane to maleic anhydride. Hodnett [1985] also mentions this phase which features vanadium in the 4+ state and oxidises n-butane to maleic anhydride. Later authors refer to it as $(VO)_2P_2O_7$ with indefinite crystal shape [Bordes, 1987]. Nguyen et al [1996] also state that calcination in air results in the formation of an inhomogeneous $(VO)_2P_2O_7$ phase with many defect sites. It is therefore thought that the β*-phase mentioned by earlier authors is simply the less crystalline $(VO)_2P_2O_7$ phase formed after calcination and prior to equilibration.

At P/V = 1, calcination in N_2 gave only $(VO)_2P_2O_7$. At P/V = 0.9, a mixture of $(VO)_2P_2O_7$ and β-$VOPO_4$ was formed and at P/V = 0.7, a mixture of V_2O_5 and β-$VOPO_4$. In the experiments of Bosch et al, time of calcination did not play a role when calcining in N_2. However, when calcining in air, longer times resulted in over-oxidation to form larger percentages of the 5+ phase. The influence of time on stream was as follows: Conversion decreased with increased time on stream, but selectivity towards maleic anhydride increased strongly, resulting in an overall increase in yield. Abon et al [1995] also reports an increase in maleic anhydride selectivity and a decrease in total oxidation product selectivity with time on stream.

Although the above results suggest the presence of 5+ phases when calcining in air, it has been shown by diffraction and electron microscopy studies that only a single phase is present in equilibrated VPO catalysts, even if calcined in air. The nonstochiometry in the VPO catalyst is explained by defect sites associated with V^{5+} [Nguyen et al, 1996]. The 5+ phases formed during initial activation in air are therefore reduced to $(VO)_2P_2O_7$ [Kubias et al, 1992].

Where the results of Bosch et al indicate lower activity for a catalyst calcined in air (non-equilibrated), Schuurman et al [1997] find that an equilibrated catalyst shows an increase in selectivity and activity when the catalyst surface is oxidised prior to reaction. A reduction in activation energy for the reaction of n-butane is shown by Schuurman et al, who explain it as follows: "This result strongly suggests that with oxygen-treated catalyst, in the absence of gas phase oxygen, the active-selective site involves a combination of V^{4+} and V^{5+} phases". This result is not in contradiction with the results of Bosch et al and other investigators who claim that the presence of V^{5+} phases on the surface results in over-oxidation and therefore lower yields, when one considers the defect-site hypothesis of Nguyen et al [1996]. The V^{5+} species are present as defect sites and not as a separate phase.

It is therefore proposed that the presence of 5+ species as a separate β-$VOPO_4$ phase decreases activity and selectivity (Bosch et al found that β-$VOPO_4$ on its own only produces CO and CO_2 from n-butane), whereas the presence of 5+ species as defect sites in a single $(VO)_2P_2O_7$ phase enhances selectivity and activity. The exact role of these 5+ species in the mechanism is however not shown by Nguyen et al, but Bordes [1987, 1993] states that oxygens linked to V^{5+} are needed for the oxygenation step. Bordes [1993] also proposes that most active sites exist at the interface of γ-$VOPO_4$/$(VO)_2P_2O_7$, as the vanadium atoms in these phases act as redox partners. Whereas Nguyen et al mention the presence of 5+ species as defect sites, Bordes [1987] models the 5+ sites as micro-domains of γ-$VOPO_4$.

Cavani et al [1984] showed the effect of calcination temperature in air on the catalyst surface area (Figure 1.15). The surface area showed a maximum at between 350°C and 440°C. This is attributed to the formation of the $(VO)_2P_2O_7$ phase from the precursor. At higher temperatures, the formation of $VOPO_4$ results in a reduction in surface area.

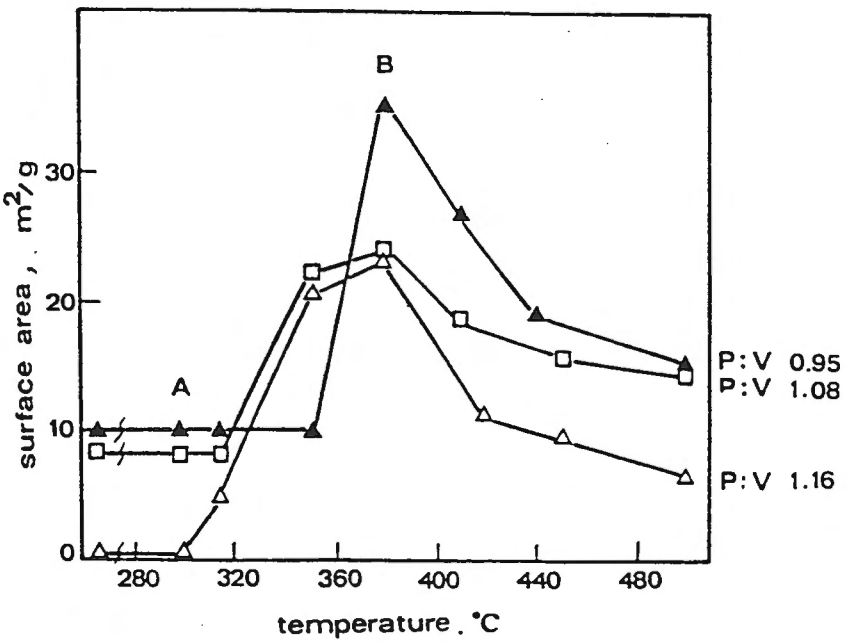

FIGURE 1.15: SURFACE AREA AS A FUNCTION OF CALCINATION TEMPERATURE IN AIR [Cavani et al, 1984]

1.1.4.1.3. PHOSPHORUS / VANADIUM RATIO

The P/V ratio influences the catalyst in the following way:

i) Influence on the redox properties, i.e. the reducibility of the catalyst by hydrogen or hydrocarbons and oxidisability by oxygen [Trifiro, 1993]. At lower P/V ratios (P/V = 0.95), oxidation of the catalyst occurs more readily (V^{4+} to V^{5+}), which results in increased activity and decreased selectivity to maleic anhydride. At P/V = 1, both oxidisability and reducibility of the vanadium remains high (i.e. all species, V^{5+} and V^{3+} will form during reaction). At ratios higher than 1, both reducibility and oxidisability of the catalyst decrease considerably (i.e. mostly V^{4+} species with low activity are present). "Catalysts with a slight excess of phosphorus represent a suitable compromise in the effort to obtain both high activity and high selectivity." [Cavani et al, 1994]. A survey of patents gives P/V ratios of unpromoted industrial catalysts of between 1.1 and 1.2, e.g. P/V = 1.1 [Japanese Kokai 8145815 (1981)], P/V = 1.15 [US Patent 4219484 (1980)], P/V = 1.2 [US Patent 4209423 (1986)]. Surface P/V ratios of equilibrated catalysts are typically 1.5 to 3.0 [Cavani et al, 1994]

ii) Influence on the phase composition of crystalline catalysts, as mentioned in section 1.1.4.1.2. which discusses the effect of activation [Bosch et al, 1987]. "An excess of phosphorus with respect to a P/V ratio of 1 stabilises the V(IV) phase and delays, at high temperatures the formation of $VOPO_4$." [Trifiro, 1993; Cavani et al, 1984]

iii) Influence on the distribution of vanadium oxidation states in unequilibrated catalysts: The $\%V^{5+}$ in an unequilibrated catalyst was found to decrease from 100% at P/V =0.9 to 0% at P/V = 1.12 for catalysts calcined in air at T = 380°C [Poli et al, 1981]. Although the % of V^{5+} increased with increasing temperature of calcination in air, this increase was less pronounced at higher P/V ratios [Cavani et al, 1984]. See Figure 1.16.

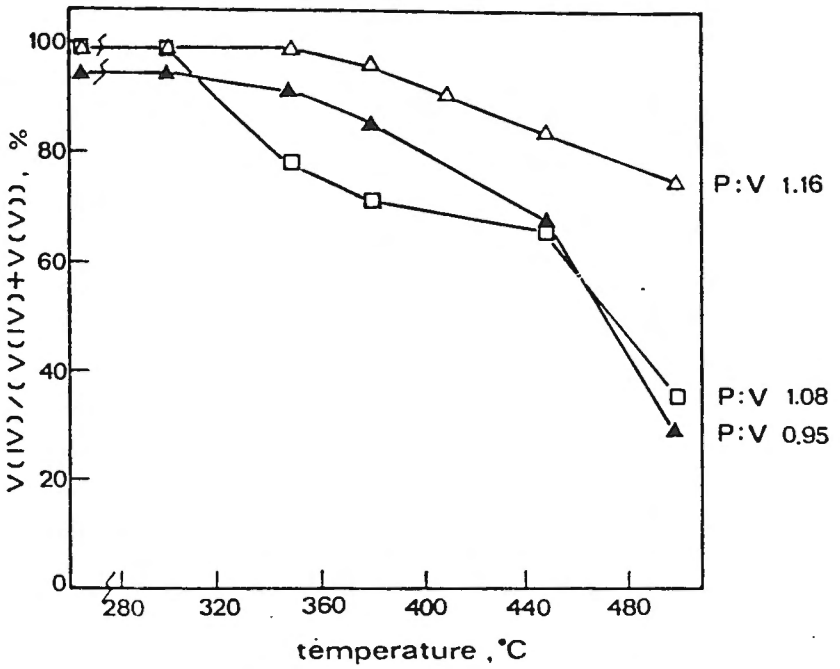

FIGURE 1.16: V(IV) CONTENT AS A FUNCTION OF P/V RATIO AND TEMPERATURE OF CALCINATION IN AIR [Cavani et al, 1984]

iv) Influence on the surface morphology as mentioned in section 1.1.3.1 discussing the active sites on the catalyst surface.

1.1.4.2. EFFECT OF THE ADDITION OF PROMOTERS ON ACTIVITY/ SELECTIVITY

The promoter can be added at different stages in the catalyst synthesis process as different species with different solvents. The solvent of addition was shown to affect the surface area and exposure of the reaction plane and subsequently the reactivity. Ye et al [1993] prepared promoted catalysts by impregnating the precursor $VOHPO_4.0.5H_2O$ with a solvent containing the promoter species. In order to study the effect of the solvent, they immersed the precipitated catalyst precursor $VOHPO_4.0.5H_2O$ in the pure solvents H_2O, CH_3OH, C_2H_5OH and C_4H_9OH, followed by drying, and compared activities and selectivities during n-butane conversion. Although selectivity to maleic anhydride was the same for all solvents, the reaction rate of n-butane changed in the following order: $C_4H_9OH > C_2H_5OH > CH_3OH > H_2O$. These samples varied in surface area and relative intensity of the (020) plane as shown by XRD. Promoter species can therefore only be compared if the same solvent is used.

1.1.4.2.1. FUNCTION OF THE PROMOTER

Ye et al report that the addition of small amounts of metal promoters improve the yield of maleic anhydride and this is thought to result from increased exposure of the (020) reaction plane and an increase in V=O species on the surface. Busca et al [1986] have shown that increased exposure of the (020) plane enhances catalyst activity. Ye et al showed an increase in reaction rate of n-butane with the addition of promoter metal species which are less electronegative than vanadium. There was also an increase in maleic anhydride selectivity. Although a direct correlation between electronegativity of promoter species and increase in yield or selectivity of maleic anhydride was not shown, a correlation between the electronegativity of the metal promoter species and the increase of V=O species on the catalyst surface was found. Another effect of promotion is the lowering of the temperature at which activation of n-butane starts [Hutchings, 1991]. Promotional effects were found to be less pronounced at higher n-butane concentrations. This led Hutchings to propose that promoters can stabilise the oxygen anions present in the structure and the average vanadium oxidation state. This would enable improved initial dehydrogenation of n-butane.

Takita et al [1991] found that for promotions of up to 10 atomic % of Zn, no XRD peaks other than $(VO)_2P_2O_7$ are present, with slight variations in line positions according to the degree of substitution. Several studies suggest that promoters such as Ce, Co, Cr, Cu, Fe, Hf, La, Mo, Nb, Ni, Ti and Zr form solid solutions with $(VO)_2P_2O_7$ to form compounds of the type $((VO)_xM_{1-x})_2P_2O_7$ where M = promoter [Brutovsky et al, 1982; Otake, 1982].

1.1.4.2.2. METAL SPECIES AND SOLVENT SPECIES USED IN ADDITION

Although a large number of metal promoter species are reported in the patent literature, the most widely used are: Mo [US Patent 4416802 (1983)], Co [US Patent 3987063 (1976)], Zn [US Patent 3862146 (1974)], Ti [US Patent 4382876 (1983)] and Fe [US Patent 4337173 (1982)].

Ye et al [1993] compared different promoters with respect to activity and selectivity towards maleic anhydride (atomic content of additive 5%, M/V = 1/19). The increase in V=O species on the surface is thought to have been caused by the promoter, but the increase in surface area and exposure of the reaction plane may also have been the result of the impregnation method used. In their comparisons, the solvent and the species which contained the metal promoter were not always consistent. These factors should themselves influence the surface area and exposure of the reaction plane. Whereas, in general, a good correlation was shown between electronegativity and surface density of V=O species in $\mu mol/m^2$, the increase in surface area and exposure of the reaction plane is not as clear. For instance, a precursor that was immersed in a solvent without a promoter species already showed improved exposure of the reaction plane and improved performance. Catalysts that were immersed in solvent showed the following decrease in reaction rates: C_4H_9OH > C_2H_5OH > CH_3OH > H_2O > unimmersed [Ye et al, 1993].

Catalysts were promoted with different additives and compared for butane oxidation. Catalytic activity changed in the following order: Zr > Ce > La > Fe > Co > Cu > Nb > Ti > Mo > Ca > Si > W > Ni > Ge > K > VPO (unpromoted). Variation in catalytic activity was partly due to a variation in surface area. The rate per surface area changed in the following order: Ce > La = Zr > Cu > Ni > W > Co > Fe = Si = Ca > Ti > Mo > Nb > VPO (unpromoted) > K [Ye et al, 1993]. Solvents used were H_2O, CH_3OH, and C_2H_5OH. Species were added as acetates or oxalates. The order of selectivity and yield of the catalyst as a function of metal species also varies with the amount of additives [Hutchings, 1993].

1.1.4.2.3. STAGE OF ADDITION

Ye et al [1993] impregnated the precursor ($VOHPO_4.0.5H_2O$) with a solution (e.g. H_2O, CH_3OH, C_2H_5OH or C_4H_9OH) containing the promoter additive, followed by calcination. Bej et al [1991] also first produced the $VOHPO_4.0.5H_2O$ precursor and then added the species (e.g. molybdic acid, ceric ammonium nitrate), followed by drying and calcination. Alternatively, the promoter can be added in the first reflux step, before the addition of phosphoric acid.

Ai [1986] studied various methods of adding a ZrO_2 promoter as $ZrOCl_2$ in an ethylene glycol or H_2O solution. The promoter solution was added either before or after the addition of o-H_3PO_4. Alternatively, the promoter solution was first reacted with o-H_3PO_4 and then added to $VOHPO_4.0.5H_2O$. P/V ratios were also varied. The Zr/V atomic ratio was held constant at 1/10.

It was found that when adding the $ZrOCl_2$ before the o-H_3PO_4 addition step, a $ZrPO_4$ phase also formed, which separated almost immediately from the solution. This made it hard to achieve complete mixing between vanadium phosphate and zirconium phosphate. Ai also obtained better results when the precursor was first dried and then immersed in a solution containing the precursor, followed by kneading. He proposed the following reaction:

$$\text{Precursor} + 0.2\ H_3PO_4 + 0.1\ ZrOCl_2 \rightarrow \text{Precursor} + 0.1\ Zr(HPO_4)_2$$

With promotion, an increase in activity and a decrease in selectivity from an unpromoted catalyst of the same P/V ratio (P/V = 1.2) were observed. When promoted, a precursor with a P/V ratio of 1.3 gave selectivities comparable to that of the unpromoted catalyst of P/V ratio = 1.2. Ai proposed that a part of the $ZrOCl_2$ reacts with the phosphorus of the precursor, resulting in the formation of a compound with a lower P/V ratio, which might result in the increase in activity and decrease in selectivity. In order to avoid this, $ZrOCl_2$ was first reacted with o-H_3PO_4 and then kneaded with the precursor as before. The resulting catalyst showed a selectivity comparable to the unpromoted catalyst. The best results were obtained when adding two solutions of ethylene glycol simultaneously to the dried precursor, the one containing o-H_3PO_4 and the other the $ZrOCl_2$, and then kneading the mixture. It is thought that this method allows the Zr to interact more with the V than when the $ZrOCl_2$ is first added to the o-H_3PO_4.

Methods of promoter addition are thought to differ in that some involve the addition of the promoter to the bulk and others to the surface [Hodnett, 1985]. From the work done by Ai [1986], the former seems to yield better results. The stage of promoter addition affects activity. When the promoter is added before the addition of o-H_3PO_4 in the preparation step, the promoter is incorporation in the bulk structure. Impregnation after the precursor formation, on the other hand, results in impregnation on the surface.

1.1.4.2.4. QUANTITY ADDED

Quantities added range from 0 to 0.5 mol % and activity goes through a maximum which is different for each promoter metal [Brutovsky et al, 1982]. After the optimum, there is a sharp decrease in activity. Hutchings [1991] proposes that these optima relate to the maximum concentration of the promoter that can form a solid solution with the VPO compound. The additional promoters are then thought to form separate phases, which are oxides forming total oxidation products.

1.1.5. EFFECT OF REACTION CONDITIONS ON ACTIVITY/SELECTIVITY

1.1.5.1. FEED COMPOSITION

The effect of the O_2/n-butane ratio at low n-butane concentrations (0.84 vol%) is shown in Figure 1.17 [Centi et al, 1984a]. Total conversion and yields of CO and CO_2 decrease steadily with a decrease in the amount of oxygen available. The selectivity towards maleic anhydride does not change much.

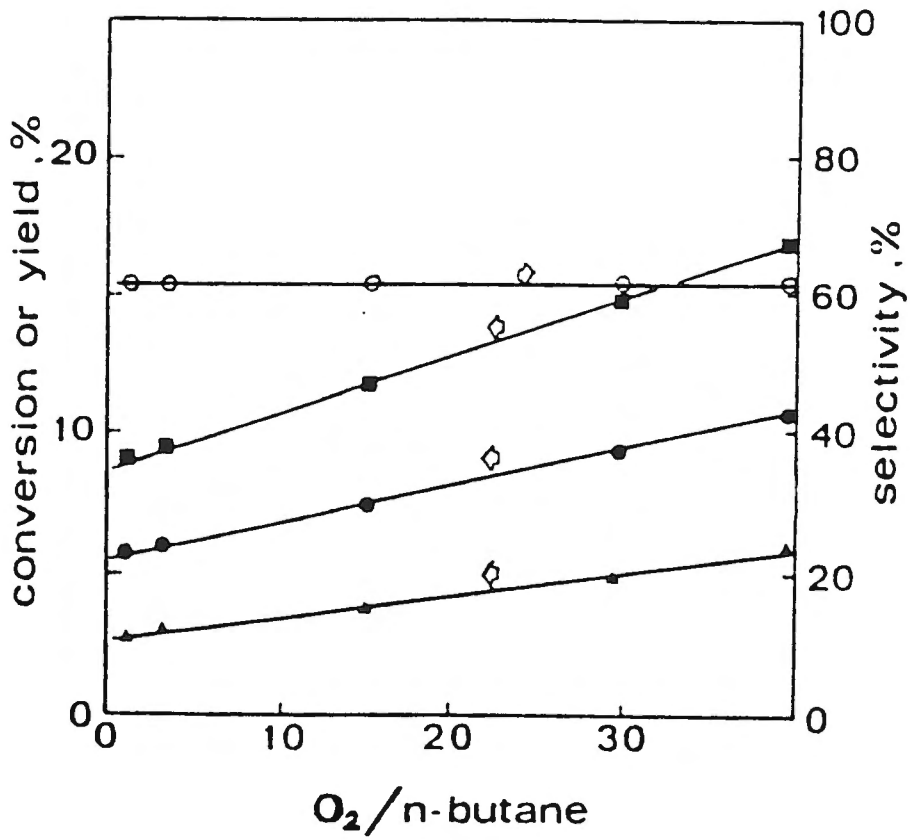

FIGURE 1.17: EFFECT OF O_2/n-BUTANE RATIO ON THE CONVERSION ■
YIELD OF MALEIC ANHYDRIDE ●
YIELD OF CARBON OXIDES ▲
SELECTIVITY TO MALEIC ANHYDRIDE ○
IN n-BUTANE OXIDATION [Centi et al, 1984a]

Temperature: 320°C
Contact time: 0.2 seconds
n-Butane conc: 0.84 vol%

Bosch et al [1987] studied the effect of butane/oxygen ratio at 450°C. Their findings are given in Table 1.5.

TABLE 1.5: INFLUENCE OF BUTANE/OXYGEN RATIO AT 450°C, SV 47 min^{-1} [Bosch et al, 1987]

n-Butane/O_2	n-Butane Conversion	Yield of MA	Yield of CO/CO_2	MA selectivity
	(%)	(%)	(%)	(%)
0.7	18.9	7.5	10	39
0.9	16.6	8.2	6.9	49
1.8	12.4	5.4	5	44
3.1	7.3	2.4	3.5	32

An optimal yield and selectivity of maleic anhydride is found at an n-butane/O_2 ratio of 0.9. n-Butane/O_2 ratios of more than 0.9 give lower yields of maleic anhydride and carbon oxides, whereas ratios of less than 0.9 favour the production of CO and CO_2, with a concurrent decrease in the yield of maleic anhydride.

The influence of partial pressures of n-butane and oxygen at constant butane/oxygen ratio was also studied by Bosch et al and is given in Table 1.6.

TABLE 1.6: INFLUENCE OF PARTIAL PRESSURES OF BUTANE AND OXYGEN AT CONSTANT BUTANE/OXYGEN RATIO OF 0.9 [Bosch et al, 1987]

P butane	P oxygen	Maximum yield of MA	Maximum selectivity of MA
(atm)	(atm)	(%)	(%)
0.16	0.18	9	80
0.08	0.09	4	27
0.04	0.04	2	9
0.01	0.01	0	0

A decrease in selectivity to maleic anhydride is observed with decreasing partial pressures of both n-butane and oxygen.

Figure 1.18 [Cavani et al, 1994] shows the effect of n-butane feed concentration on the yield of maleic anhydride. At 20% oxygen, the space yield (mol maleic anhydride/h.g catalyst) begins to level off at about 1 mol% butane in the feed, suggesting oxygen limiting. An increase in the oxygen concentration from 20% to 30% (at 1.6 mol % butane) almost doubles the space yield of maleic anhydride. Conversely, reducing the concentration to 10% halves the space yield.

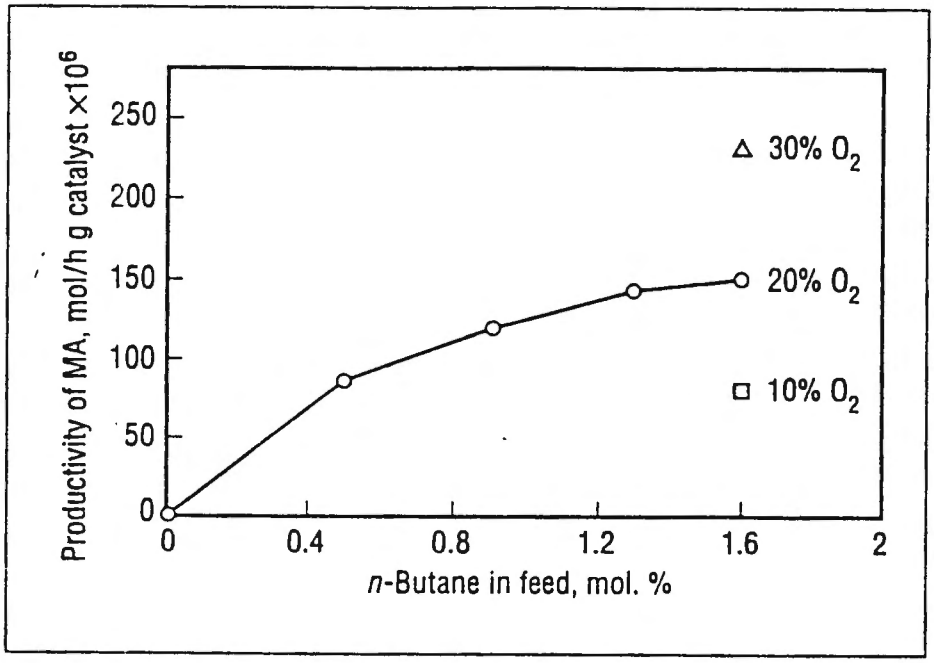

FIGURE 1.18: EFFECT OF MOL% n-BUTANE IN THE FEED ON MALEIC ANHYDRIDE PRODUCTIVITY [Cavani et al, 1994]

Temp: **340°C**
Residence time: **3 seconds**

1.1.5.2. EFFECT OF REACTION TEMPERATURE

The work of Bosch et al [1987] shows an increase in the yields of total oxidation products with temperature (Figure 1.14). The yield of maleic anhydride goes through a maximum, depending on the preparation method, as mentioned in section 1.1.4.1.2. Centi et al [1984a] (Figure 1.19) studied the effect of temperature on n-butane and 1-butene conversion. The yield of maleic anhydride initially increases with temperature. At the point where 100% conversion of n-butane is reached (T = 350°C), the yield of maleic anhydride reaches a maximum. A further increase in temperature at this point results in a lower maleic anhydride yield and greater yields of total oxidation products. This could be the result of further oxidation of maleic anhydride or of an increase in the rate of total oxidation of butane.

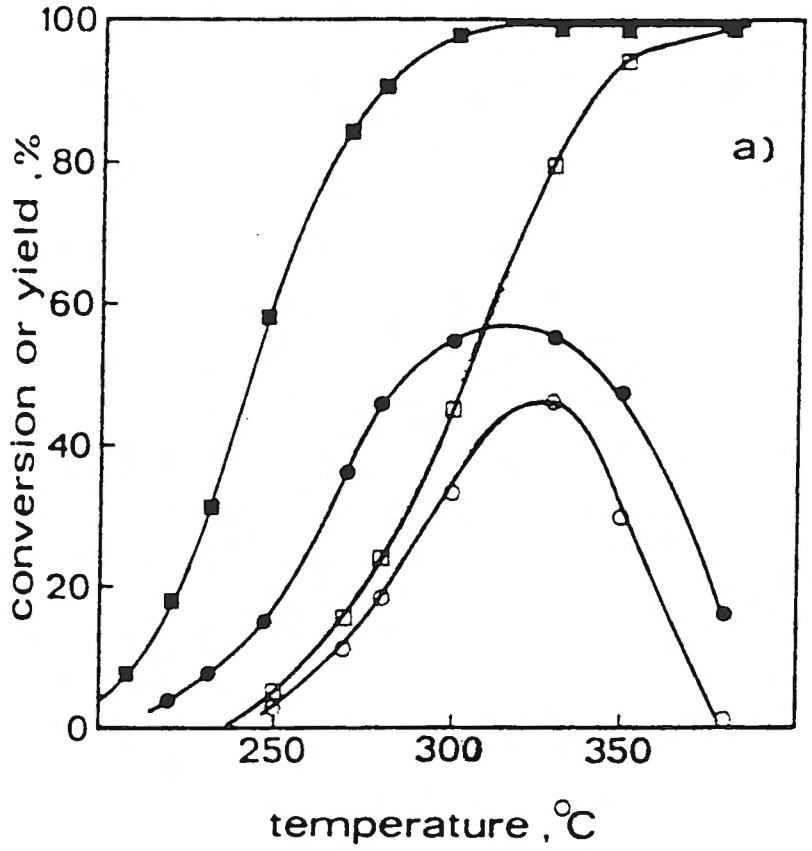

FIGURE 1.19: EFFECT OF TEMPERATURE ON THE OXIDATION OF n-BUTANE (OPEN SYMBOLS) AND 1-BUTENE (CLOSED SYMBOLS) [Centi et al, 1984a]

□ ■ = conversion
○ ● = yield of maleic anhydride

Hydrocarbon conc.:	**0.48 vol%**
Oxygen conc.:	**12.9 vol%**
Contact time:	**1.36 sec**
Mass of catalyst:	**1.9 g**
P/V ratio:	**1.0**
Solvent:	**isopropyl alcohol**
Catalyst surface area:	**30 m^2/g**

1.1.5.3. EFFECT OF STEAM

The effect of steam on the activity and selectivity of the catalyst was investigated. When steam was used along with nitrogen during activation, it was found to play a role in the development of the solid structure and the evolution of crystallinity and surface area. This effect is irreversible and manifests itself after several days. After activating the catalyst with dry feed for a week, the subsequent introduction of wet feeds resulted in a substantial increase in surface area from 4.8 m^2/g to 9.7 m^2/g after prolonged exposure [Arnold et al, 1988]. Increased surface area (from 54 m^2/g to 63.9 m^2/g) was also shown by Ye et al [1993] when treating the catalyst with water, but this was done by washing the precursor with water prior to calcination, rather than treating a calcined catalyst with wet feed.

The inclusion of steam in the reaction feed also results in site blocking, which increases the selectivity towards maleic anhydride and results in a drop in activity. This effect is reversible. In addition to site blocking, water vapour alters the selectivity characteristics of the catalyst in a beneficial and almost completely reversible manner. The water vapour alters the P/V ratio of the surface layer by moving hydrophilic P-species to the surface. This effect is more lasting than the site blocking effect, and reversible on a time scale in the order of hours [Arnold et al, 1988].

1.1.5.4. CO-FEEDING SO_2

The effect of the co-feeding of SO_2 was studied by Centi et al [1989]. SO_2 was added to a feed of 1.5% n-butane in air in order to provide a feed containing 0.48% SO_2. The presence of SO_2 had a minimal effect on the conversion of n-butane, but caused a significant increase in the yield of maleic anhydride. The presence of SO_2 had little effect on the formation of CO. At low conversions, the behaviour in the absence and presence of SO_2 was similar. When conversion was increased in the absence of SO_2, the yield of maleic anhydride started to decrease, whereas in the presence of SO_2, the yield of maleic anhydride continued to increase. Centi et al [1989] proposes that the effect of sulphur dioxide is therefore connected with the inhibition of the rate of the consecutive reaction of maleic anhydride to carbon oxides.

1.1.6. PROPOSED REACTION MECHANISM OF n-BUTANE OXIDATION

Centi et al [1988] states: "The n-butane to maleic anhydride reaction is a fascinating and complex system. The catalytic system performs a 14-electron oxidation involving the abstraction of 8 hydrogen atoms and the insertion of 3 oxygen atoms. Compared to other industrially practised hydrocarbon selective oxidation reactions, it is the most complex. It is the only example of an industrially practised selective oxidation reaction involving alkane activation."

It is generally agreed [e.g. Matsuura, 1993; Bordes, 1987] that adsorption takes place on a Lewis site provided by a V=O of which the oxygen goes into the plane of reaction. The truncation of the crystal structure at this point provides a Lewis acid site.

Bordes [1987] explains the interaction of the reactant molecule with the catalyst surface (See Figure 1.20): "n-butane is activated on the V^{4+} site with breaking of the C-H bond of methylene and of the methyl groups, the hydrogen of which is caught by OH-(V=O) of the V^{4+} pair and OH-(P) respectively. Adsorbed 1-butene and 2-butene can result (shown as the adsorbed species in diagram number 2 of Figure 1.20). Alternatively, the preceding mechanism could proceed on both V^{4+} centres, yielding directly adsorbed butadiene, trans or cis." These are cyclised by closing of the ring on an O-(P) species of a γ-$VOPO_4$ micro-domain, yielding adsorbed dihydrofuran or furan respectively. Furan is then dehydrogenated by acid phosphate and can then react with oxygen adsorbed on V^{5+}.

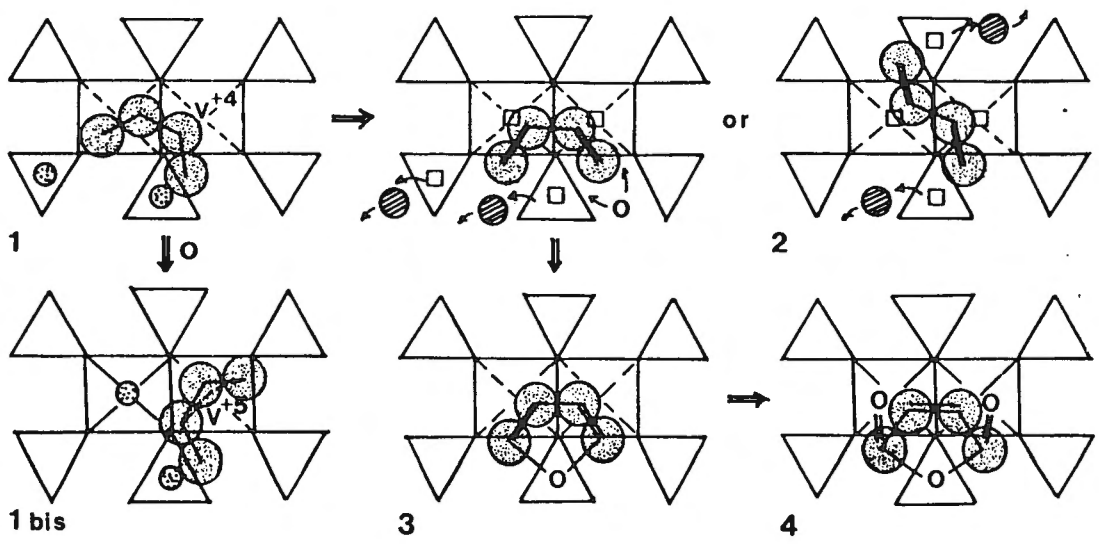

FIGURE 1.20: POSSIBLE MECHANISMS OF THE FORMATION OF MALEIC ANHYDRIDE ON AN ELEMENTARY UNIT OF $(VO)_2P_2O_7$ OR γ-$VOPO_4$. STEP 1 bis CORRESPONDS TO ALLYLIC ADSORPTION ON A V^{5+} CENTRE [Bordes, 1987]

⊘ = **desorbing H_2O**
⊙ = **OH co-ordinated to P**
□ = **vacancies left by desorbing H_2O**

TAP results, using labelled oxygen-18, show that surface $O^{\delta-}$ associated with the structure is involved in the dehydrogenation and oxygen insertion reactions of unsaturated C_4's, forming five-membered oxygen containing rings. Ebner and Thompson [1993] proposed that an activated oxygen is required to cleave the sp^3 C-H bond of n-butane. This species is suggested to arise from the irreversible dissociative adsorption of oxygen, producing a surface vanadium 5+ site. However, Abon et al [1997] have since proven with isotopic labelling that only lattice oxygen and no adsorbed oxygen, is involved in the reaction of n-butane to maleic anhydride, CO and CO_2.

Ebner and Thompson describe the mechanism as follows:
"Once butane is activated, the ensemble of $O^{\delta-}$ with V-O-P, bonding in the surface cleft, dehydrogenates the activated hydrocarbon to butadiene, at which point the $O^{\delta-}$ of the surface $V^{4+}=O$ inserts to form a five-membered, oxygen containing ring. This species reacts further with $O^{\delta-}$ associated with V-O-P bonding, or with surface activated $(O_2)^{\delta-}$ species, associated with vanadium, to form maleic anhydride."

Cavani et al [1994] propose the first step to be the activation of the n-butane (Figure 1.21). n-Butane adsorbs on the Lewis acid site and reacts with lattice oxygen to form butene, water and reduced vanadium. Oxygen from the gas phase then regenerates the catalyst.

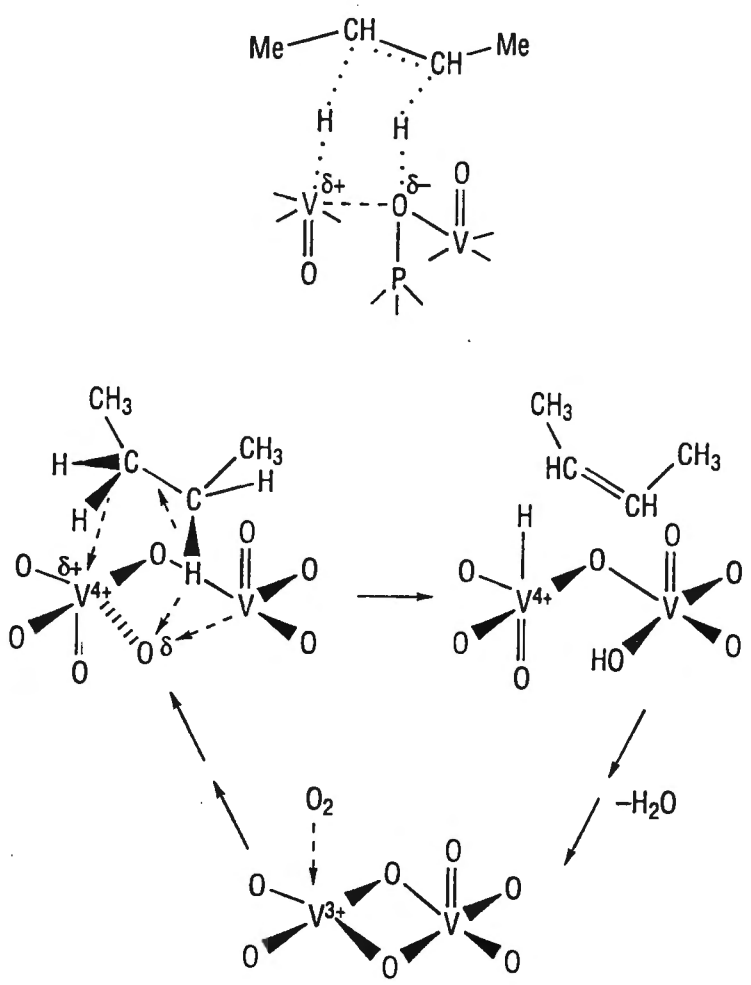

FIGURE 1.21: PROPOSED REACTION MECHANISM FOR THE FIRST STEP IN THE OXIDATION OF n-BUTANE TO MALEIC ANHYDRIDE. [Cavani et al, 1994]

The following reaction studies were carried out to reveal mechanistic information:

1) A comparison was made between the rates of 1-butene oxidation and n-butane oxidation over the same VPO catalyst [Centi et al, 1984a]. With 1-butene oxidation, interaction with the olefinic hydrocarbon leads to a rapid loss of catalyst surface area together with a decrease in activity. Initial rates were therefore compared and the initial rate of 1-butene oxidation was found to be 60 times higher than that of n-butane. Except for a loss of selectivity at conversions higher than 80%, n-butane is more selective than 1-butene. The maximum yield of maleic anhydride was 50% at an n-butane conversion of 80% and 55% at a 1-butene conversion of 100% [Centi et al, 1984a]. These differences in rate can therefore justify the rapid transformation of the proposed olefinic intermediates after activation of n-butane, before they can desorb from the catalyst. [Centi et al, 1988]

2) Butenes, butadiene and furan have been detected in the oxidation of n-butane over VPO catalysts under selected conditions such as high n-butane concentrations and a deficiency of oxygen. Concentrations of byproducts were at a maximum for an oxygen conversion of 100% [Centi et al, 1984a].

3) In the oxidation of butenes, butadiene and furan, at the same conditions as for n-butane oxidation, maleic anhydride and all the intermediates except 2, 5-dihydrofuran and lactone have been observed [Centi et al, 1984a].

4) 2, 5-Dihydrofuran reacts to form furan at T = 473K with high selectivity.

5) Intermediates for n-butane oxidation cannot be detected under normal reaction conditions for kinetic reasons as mentioned in point (1) [Centi et al, 1984a].

6) Using a temporal analysis of products (TAP) reactor, intermediates butene, butadiene and furan were observed for $(VO)_2P_2O_7$ and n-butane feed [Ebner et al, 1986]. The TAP reactor is a transient catalyst evaluation system that has been designed for detection of reaction intermediates and determination of reaction sequences. The system uses high-speed injections (200 μs pulse widths) of molecular feed into a 0.5 ml reactor containing 500 μm catalyst particles. It is able to identify and track the formation of intermediates as a function of time with a millisecond time resolution and is therefore thought to overcome the kinetic constraints which normally prohibit the observation of intermediates. The reaction sequence is also indicated and peak maxima are observed at 8.2 ms (butane), 11.4 ms (butene), 16.5 ms (butadiene), and 22.5 ms (furan) [Centi et al, 1988].

Based on the above findings, the reaction pathway given in Figure 1.22 has been postulated [Trifiro, 1993].

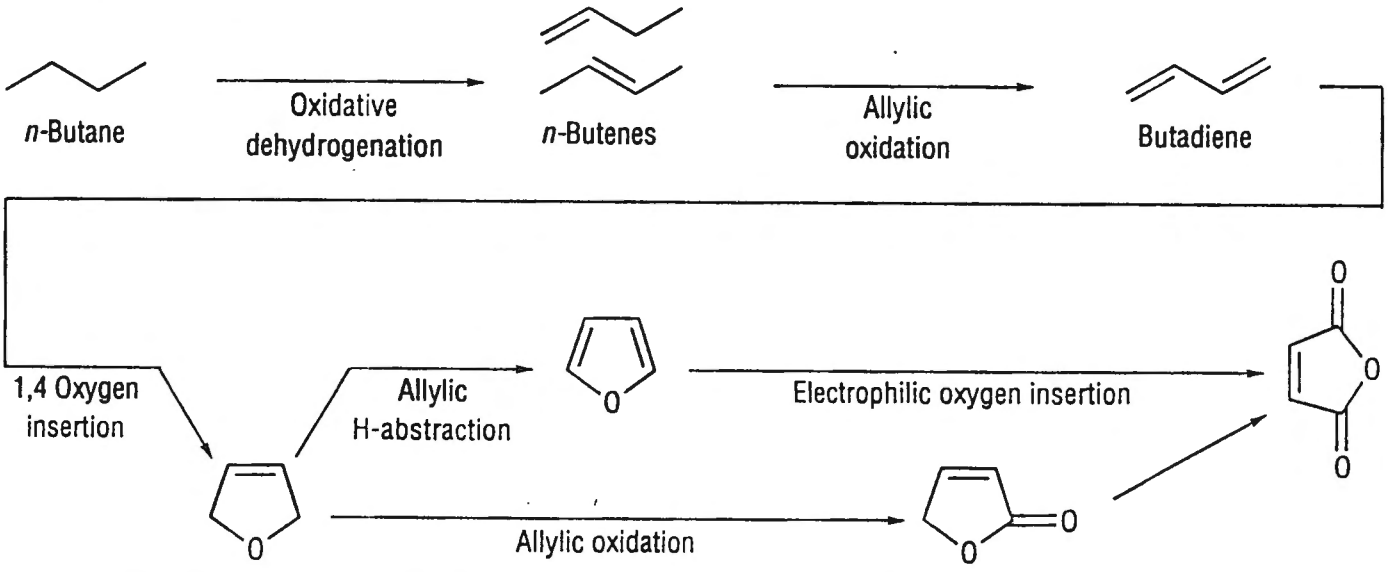

FIGURE 1.22: PROPOSED REACTION ROUTE SHOWING ALL POSTULATED INTERMEDIATES [Trifiro, 1993]

It can therefore be concluded that the n-butane molecule is activated on the surface and then oxidised as an adsorbed species. It only desorbs once maleic anhydride is formed due to kinetic reasons. Alkene activation is the rate determining step and subsequent reactions have a much higher rate.

Haber et al [1996] performed quantum-chemical calculations to obtain the energy minima along the approach of the n-butane molecule to the surface: "Upon the approach of n-butane with its plane perpendicular to the plane of the site [a pair of edge-sharing V=O groups in trans positions, linked together through six pyrophosphate groups], insertion of oxygen atoms from two opposite phosphate groups into C-H bonds of terminal carbon atoms and formation of a C-O-C bridge by vanadyl oxygen atom takes place. Dihydroxydihydrofuran is formed as the first intermediate without activation energy. This intermediate may transform by losing two hydrogen atoms twice to form maleic anhydride."

1.2. ISOBUTANE CONVERSION TO METHACRYLIC ACID OVER THE HETEROPOLY ACID CATALYST

Ninety percent of the methyl methacrylate used for organic polymers today is produced via the hydrolic esterification of acetone cyanohydrin. However, increasing difficulty in obtaining the required amount of feed from the acrylonitrile plant due to the improvement of the ammoxidation catalyst, has resulted in increased production costs. The production of an environmentally hazardous by-product, ammonium bisulphate, also creates a problem. This has resulted in the search for alternative routes, such as the oxidation of isobutyric acid or even isobutane to methacrylic acid [Otake et al, 1981]. It has been reported that heteropolyacids are good catalysts for the one-step synthesis of methacrylic acid [Akimoto et al, 1984; McGarvey et al, 1991].

1.2.1. ECONOMICS OF METHACRYLIC ACID PRODUCTION

Proprietary industrial technology has been reported by Otake et al [1981] for the process developed by Mitsubishi Chemical Industries, whereby methyl methacrylate can be manufactured with high purity (≥99.9%) (See Figure 1.23). The overall yield of methacrylic acid from an isobutyraldehyde feed is between 60 and 70 mol %. The three-stage process utilises isobutyraldehyde, which is a by-product in the oxo-reaction of propylene for the manufacture of butanols and 2-ethylhexanol.

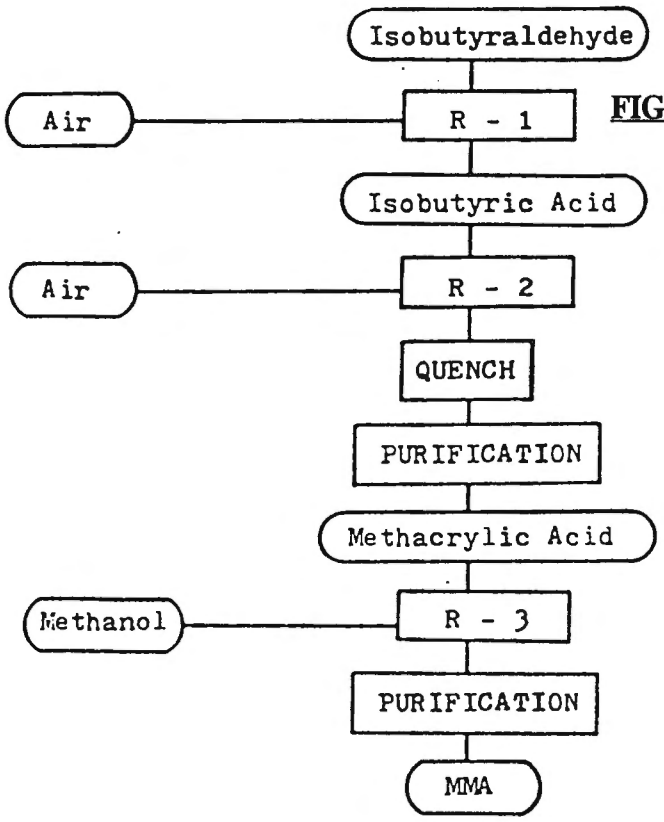

FIGURE 1.23: BLOCK-FLOW DIAGRAM OF THE MCI PROCESS [Otake et al, 1981]

R-1 = Liquid phase oxidation of isobutyraldehyde to isobutyric acid
R-2 = Gas phase dehydrogenation of isobutyric acid to methacrylic acid
R-3 = Esterification to methacrylates

The MCI process comprises the following steps [Otake et al, 1981]:

R-1) Exothermic liquid phase aerial oxidation of isobutyraldehyde to isobutyric acid. Reaction temperature = 40-80°C

R-2) Gas phase oxidative dehydrogenation of isobutyric acid (IBA) to methacrylic acid on a Keggin-type heteropoly acid catalyst of the form $M_3Mo_{12-x}V_xPO_{40}$ where M = cation. Reaction conditions are:

Feed:	$IBA/O_2/H_2O$ = 1/1-2/1-3
Temperature:	300°C
Space velocity:	1000-4000 h^{-1}
IBA conversion:	96-99%
MAA selectivity:	72%

R-3) Esterification to methacrylates. Gas phase reaction over a SiO_2-TiO_2 catalyst. Overall yield of methyl methacrylate from isobutyric acid = 60-70%.

The catalyst for step 2 has been studied by several investigators [Akimoto et al, 1981 and 1984; Ernst et al, 1987; McGarvey et al, 1991; Albonetti et al, 1993]. Albonetti et al reported yields of methacrylic acid of as high as 70% at a total isobutyric acid conversion.

Another route to methyl methacrylate which has been studied recently is the direct oxidation of isobutane to methacrylic acid [Cavani et al, 1995, Mizuno et al, 1994]. Patents have reported selectivities of higher than 50% using the abovementioned Keggin-type heteropoly acid salts and Mizuno et al [1994] have reported yields of up to 9% of methacrylic acid. The catalyst used for the direct oxidation is also a Keggin-type heteropoly acid of the type $M_3Mo_{12-x}V_xPO_{40}$, where M = Cs or a mixture of K and NH_4.

It is believed that the same modifications (e.g. choice of cation, vanadium substitution and doping) which enhance catalyst activity for the reaction of isobutyric acid to methacrylic acid are valid for the reaction of isobutane to methacrylic acid. This can be seen in the similarities in optimal catalysts used by investigators Akimoto et al [1981 and 1984] and Ernst et al [1987] for the isobutyric acid dehydrogenation and Cavani et al [1995] and Mizuno et al [1994] for the alkane oxidation.

1.2.2. STRUCTURE OF THE HETEROPOLY ACID CATALYST

Heteropoly acids are a group of acids with a complex anion structure. These compounds and their corresponding salts exhibit a combination of acidic and redox properties and are used as both heterogeneous and homogeneous catalysts.

The structure of the heteropoly acid is given in Figures 1.24 and 1.25. Heteropoly acids in the solid state consist of heteropoly anions (called the primary structure), counterions and water of hydration. In this research, the heteropoly anion, or primary structure, is made up of oxygen, phosphorus and molybdenum molecules bonded together covalently (Figure 1.24).

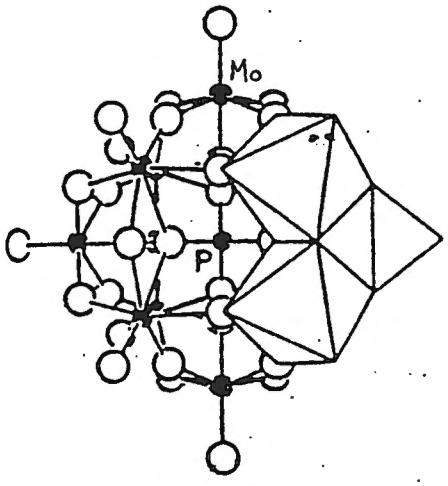

FIGURE 1.24: THE HETEROPOLY ACID ANION CONSISTS OF O, Mo AND P BONDED TOGETHER COVALENTLY

In the case of molybdophosphoric acid, the anion can be represented by polyhedra that share corners, edges and faces (See Figure 1.25). For the compound molybdophosphoric acid, the anion consists of twelve MoO_6 octahedra, surrounding a central PO_4 tetrahedron.

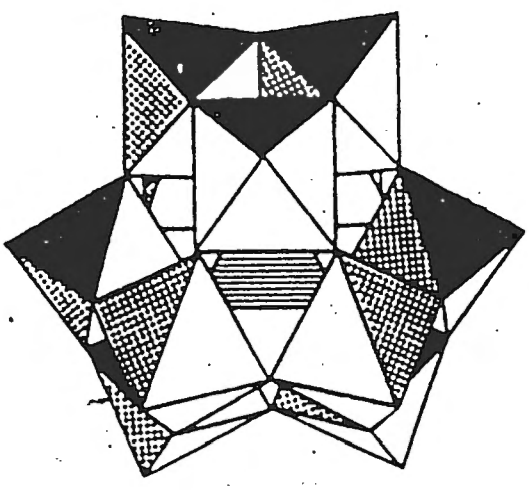

FIGURE 1.25: THE HETEROPOLY ACID ANION CAN BE REPRESENTED BY POLYHEDRA SHARING CORNERS, EDGES AND FACES. THE ANION CONSISTS OF TWELVE MoO_6 OCTAHEDRA SURROUNDING A CENTRAL PO_4 TETRAHEDRON

The anions are linked together with cations in an ordered three-dimensional arrangement called the secondary structure (See Figure 1.26).

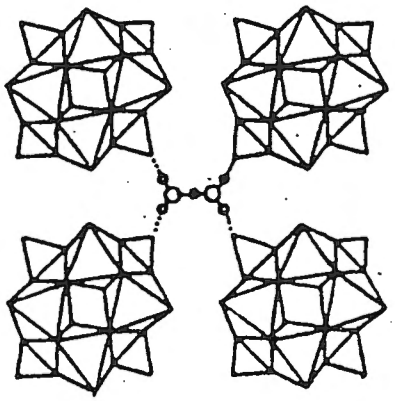

FIGURE 1.26: ANIONS ARE BONDED TOGETHER IN A THREE-DIMENSIONAL ARRANGEMENT CALLED THE SECONDARY STRUCTURE

The electronic interaction between the cations and anions is thought to influence redox properties. For example, cations with different electronegativities result in different activities of the total heteropoly acid [Akimoto et al, 1981 and 1984]. Heteropoly acids vary in the ratio of central atoms to peripheral atoms in the primary structure. Elements capable of acting as central atoms are H^+, Cu^{2+}, Be^{3+}, Zn^{2+}, B^{3+}, Al^{3+}, Ga^{3+}, Si^{4+}, Ge^{4+}, Sn^{4+}, Ti^{4+}, Hf^{4+}, Ce^{3+},Ce^{4+}, N^{4+}, P^{3+}, P^{5+}, As^{3+}, As^{5+}, V^{4+}, Sb^{3+}, Bi^{3+}, Cr^{3+}, S^{4+}, Te^{4+} , Te^{6+}, Mn^{2+}, Mn^{4+}, I^{7+}, Fe^{3+}, Co^{2+}, Co^{3+}, Ni^{2+}, Ni^{4+}, Rh^{3+}, Pt^{4+} [Zhang et al, 1993].

Heteropoly acids with a ratio in the anion (e.g. P/Mo or P/W) of 1:12 form the so-called Keggin structure, which is the most common.

1.2.3. PREPARATION OF THE HETEROPOLY ACID FOR THE CONVERSION OF ISOBUTANE

Albonetti et al [1994] describe the preparation method employed to produce the potassium/ammonium salts of molybdophosphoric acid:

16.95 g of $(NH_4)_3Mo_7O_{24}$ and 0.78 g of H_3PO_4 were dissolved in 40 ml of water at 333-343K. After cooling, KNO_3 was added in order to obtain the desired final composition, and finally 10 ml of HNO_3 was poured into the solution. This resulted in a yellow precipitate, which was dried overnight. The catalyst was calcined for an hour in oxygen at 300°C. Slow heating rates are required to obtain the desired Keggin structure. It was also shown that higher calcination temperatures result in lower activity for the oxidative dehydrogenation of isobutyric acid. Cavani et al [1995] studied mixed ammonium/potassium salts of 12-molybdophosphoric acid as prepared above and modified it by the addition of Fe. The salts were thermally stable at up to 400°C.

Mizuno et al [1994] used a 12-molybdophosphoric acid, ion-exchanged with Cs and Ni, and obtained a maximum methacrylic acid yield of 9% in the isobutane conversion. The substitution of molybdenum atoms with vanadium was also found to enhance activity. $H_{3+x}PMo_{12-x}V_xO_{40}$ was commercially obtained from Nippon Inorganic Colour and Chemical Co. To an aqueous solution of this acid (0.06 mol/dm^3), 0.08 ml/dm^3 nickel nitrate was added dropwise, followed by the addition of an aqueous solution of Cs_2CO_3 (0.08ml/dm^3). The resulting suspension was evaporated to dryness at 50°C.

Vanadium-containing heteropoly acids can also be prepared according to the method of Tsigdinos and Hallada [1968]:

7.1 g of Na_2HPO_4 was dissolved in 100 ml of water and mixed with 6.1 g of sodium metavanadate that had been dissolved by boiling in 100 ml of water. The mixture was cooled and acidified with 5 ml of concentrated sulphuric acid. To this mixture was added 133 g of $Na_2MoO_4.2H_2O$, dissolved in 100 ml of water. Finally, 85 ml concentrated sulphuric acid was added slowly with vigorous stirring of the solution. The heteropoly acid was then extracted with 400 ml of ethyl ether, after the water solution had been cooled. After separation, air was passed through the heteropoly etherate layer to free it of ether. The sample was analysed as $H_4PMo_{11}VO_{40}$. The vanadium composition was changed by varying the amounts of sodium metavanadate and $Na_2Mo_4.2H_2O$ that was added.

1.2.4. FACTORS AFFECTING ACTIVITY AND SELECTIVITY

Free heteropoly acids are strong acids. Heteropolyanions are multi-electron oxidants and those having Mo or V as peripheral atoms are strong oxidants. Usually a Keggin structure with a P/Mo ratio of 1:12 is used. The replacement of one of the peripheral Mo atoms with vanadium results in increased activity towards partial oxidation products [Mizuno et al, 1994].

A summary of partial oxidation reactions that have been studied over Mo-containing heteropoly acids is given in Table 1.7. Alkanes are oxidised to carboxylic acids, revealing the strong oxidising properties of the catalyst. The production of carboxylic acids from alkanes also shows the ability of the catalyst to activate alkanes. However, product yields for the reactions involving alkane activation are typically lower than for other feeds. This seems to indicate that the activation step has a lower rate than the oxidation step as is the case in the conversion of n-butane over the VPO catalyst.

The co-feeding of steam has been reported by several investigators for the partial oxidation reactions of isobutane [Cavani et al, 1995], isobutyric acid and n-butane [Ai, 1984] over molybdophosphoric salts, as well as over VPO catalysts. However, these investigators do not offer any comparative studies with and without steam over the heteropolyacid salts. The reason for the co-feeding of steam is not given, but it is presumed to enhance activity and selectivity as with the VPO catalyst. In the experiments done in this work, steam was not co-fed and yields obtained were therefore lower than those of Cavani et al [1995]. Vanadium substitution was also not carried out as the aim of the research was not to optimise the catalyst but to do mechanistic studies. Low conversions were preferable, as the aim of mechanistic studies was to determine the effect on selectivities of different products when conversion tends to zero.

TABLE 1.7: PARTIAL OXIDATION REACTIONS STUDIED OVER MOLYBDENUM-CONTAINING HETEROPOLY ACID CATALYSTS

FEED	PRODUCT	AUTHOR(S)	Rxn T (C)	pO2/pHC	CONVERSION (mol%)	SELECTIVITY (mol%)	WHSV (l/gmin)
n-butane	maleic anhydride	Ai, 1984	360	9.15	31.8	31.76	0.0166
1-butene	maleic anhydride	Ai, 1984	250-400	4	90	50	0.05
butadiene	maleic anhydride	Ai, 1984	250-400	4	98	60	0.05
furan	maleic anhydride	Ai, 1984	250-400	4	98	61	0.05
acrolein	acrylic acid	Ai, 1984	250-400	4	40	61	0.05
propane	acrylic acid	Mizuno et al, 1995	300-400	1.33	47	27.65	0.03
methacrolein	methacrylic acid	Ai, 1984	250-400	4	60	60	0.05
isobutyric acid	methacrylic acid	Mizuno et al, 1984	300	1.72	80.6	60.5	0.0053 (gmol/gmin)
isobutane	methacrylic acid	Mizuno et al, 1994	340	1.94	32	28	0.03
butadiene	furan	Ai, 1984	250-400	4	98	60	0.05
crotonaldehyde	furan	Ai, 1984	250-400	4	95	45	0.05

The role of the heteropoly acid cation was studied by several investigators [Akimoto et al, 1981 and 1984; Ernst et al, 1987; McGarvey et al, 1991; Albonetti et al, 1993; Mizuno et al, 1994; Cavani et al, 1995]. Akimoto et al examined the effect of the electronegativity of the cation of the molybdophosphoric acid salt on the vapour-phase oxidative dehydrogenation of isobutyric acid. The conversion of isobutyric acid was found to increase with decreasing electronegativity of the cation. The yield ratio of acetone to methacrylic acid showed a similar trend. It was proposed that the cation has an affect on the electrochemical properties of the molybdenum atom, the strength of the Mo-oxygen bond (participation of the lattice oxygen), and the acid-base properties of the catalyst. A comparison of the oxidising activity of heteropoly acid salts with cations of different electronegativity, as well as ESR spectra of the catalyst surface during reduction with H_2 and reoxidation with O_2, led to the speculation that the Keggin anions interact electronically with the cations.

It must be added that the properties of the vanadyl pyrophosphate catalyst follow a similar trend where promotion with a less electronegative metal cation species enhances the yield to maleic anhydride [Ye et al, 1993], although the correlation between electronegativity and reactivity is not as exact as with the molybdophosphoric acid catalyst. For the heteropoly acid catalyst it is not yet known how the addition of less electronegative cations affects acidity as opposed to redox properties. It is not clear why a combination of cations such as NH_4^+ and K^+, as prepared by Albonetti et al [1994], should give higher yields than for example K^+ or NH_4^+ alone (an increase in yield of up to 10%).

Cavani et al [1996] studied the effect of doping the catalyst with iron, and found that the acidity of the salt increased with iron content. Whereas Cavani et al [1995] proposed that the iron replaces one of the cations, e.g. the K^+ or NH_4^+, Busca et al [1996] later suggested that the iron is present as a $FeO_{1.5}$ Lewis acid species on the surface. It is therefore proposed that the iron surface species contributes to the acidity of the catalyst, which is important in the alkane activation step.

Albonetti et al [1994] studied the effect of calcination temperatures of between 650K and 770K on the yield of methacrylic acid in the oxidative dehydrogenation of isobutyric acid for catalysts of the type $K_x(NH_4)_{3-x}PMo_{12}O_{40}$. A monophasic system was formed, but progressive decomposition of the Keggin structure resulted in a corresponding decrease in methacrylic acid selectivity with increasing calcination temperature. A better understanding of the evolution of the catalyst during activation and equilibration may lead to the development of improved activation procedures and improved yields.

1.2.5. PROPOSED REACTION MECHANISM OF METHACRYLIC ACID FORMATION

Otake et al [1981] proposed a mechanism for the reaction of isobutyric acid to methacrylic acid (See Figure 1.27). They also showed that aliphatic carbonyl compounds, which are singularly branched at the α-position of the carbonyl group, are effectively dehydrogenated over the heteropoly acid to form allyl derivatives. The Keggin anion is strongly basic, which explains the H^+ abstraction. The positive charge on the heteropoly acid cation, in the vicinity of the adsorption site, may stabilise the resulting intermediate carbanion and finally liberate the H^-. The model of Otake et al was confirmed by ESR of the reduction of the heteropoly anion [Otake et al, 1973 and 1975].

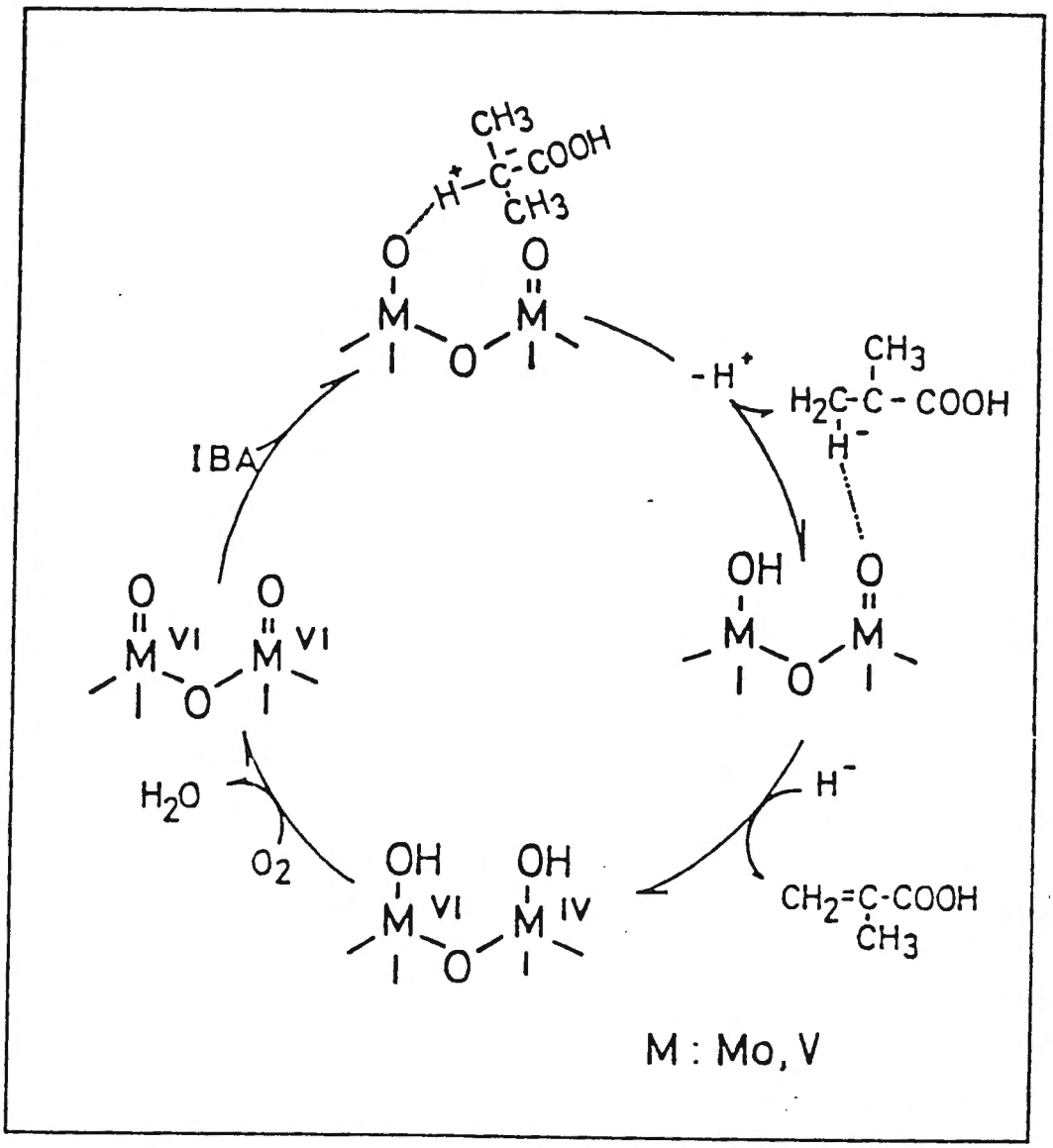

FIGURE 1.27: PROPOSED MECHANISM OF THE OXIDATIVE DEHYDROGENATION OF ISOBUTYRIC ACID [Otake et al, 1981]

Akimoto et al [1981] propose a scheme whereby the dehydrogenation of isobutyric acid takes place via a homolytic mechanism analogous to allylic oxidation:

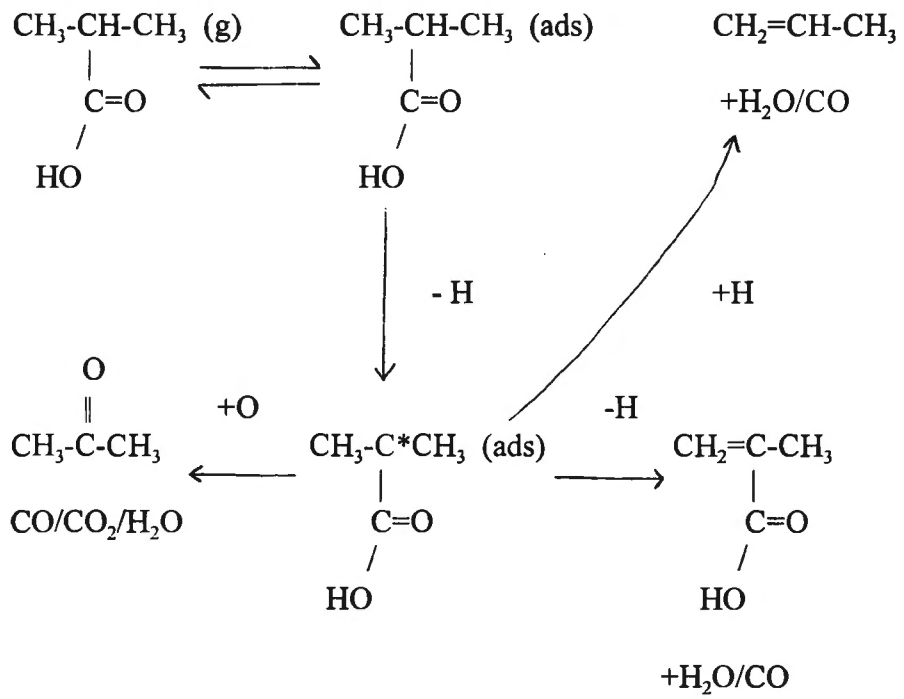

The decomposition to propylene, CO and H_2O is the result of interaction with a Brønsted acid site. Dehydrogenation takes place by lattice oxygen, and acetone is formed when the surface lattice oxygen adds to the carbon atom C^*. The carbon then acquires a positive charge, donating its electrons to the catalyst (as in the case of aromatic hydrocarbons adsorbing on heteropoly acids) and to the negative -COOH group.

Akimoto et al used this mechanism to explain the yield ratios (acetone/methacrylic acid) and selectivities to propylene as a function of catalyst composition. Yield ratios of acetone to methacrylic acid were found to increase with increasing Pauling electronegativity of the cation, i.e. as a result of the effect of electronegativity of the cations on the acidic properties of the molybdenum atoms and on the reactivity of the lattice oxygen. Surface lattice oxygen addition to the carbon atom proceeds readily when it has a high positive charge and when the bond between Mo and lattice oxygen is weakened due to interaction with the cation.

The following two reaction schemes are proposed here for the direct oxidation of isobutane to methacrylic acid:

1) Dehydrogenation of isobutane followed by oxidation:

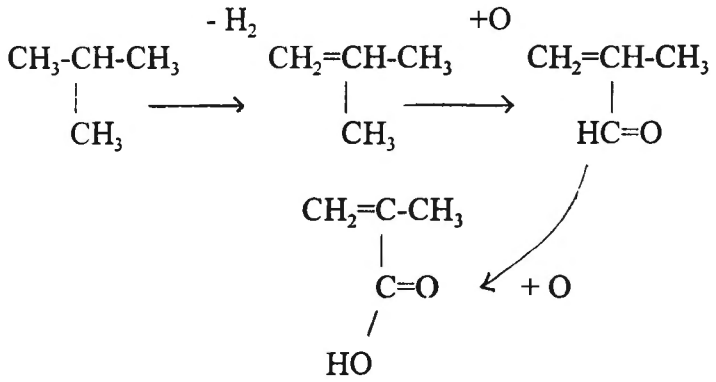

2) Oxidation of isobutane followed by dehydrogenation:

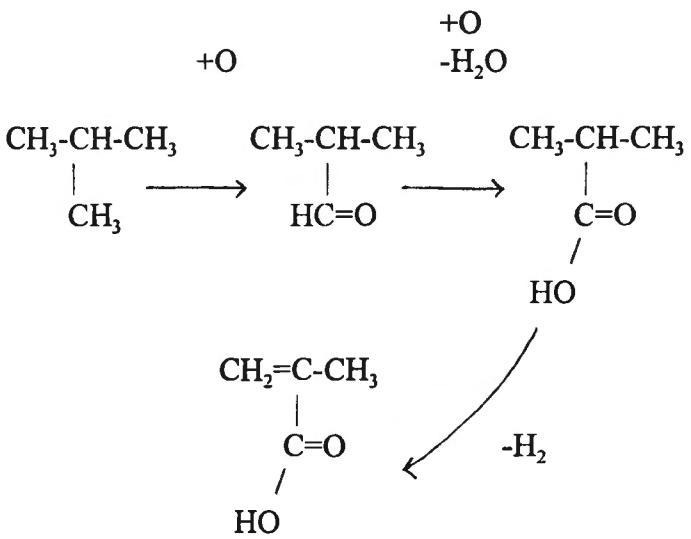

Cavani et al [1995] proposed a parallel mechanism for the oxidation of isobutane to methacrylic acid, based on his observation that the selectivities of methacrolein and methacrylic acid are different from zero for extrapolation to a residence time of zero. The zero residence time was extrapolated from a lowest conversion of 1% at a residence time of 1 second:

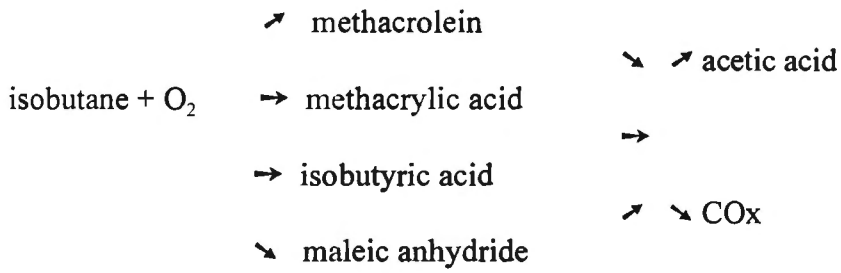

Busca et al [1996] reported FTIR studies in which they suggest that isobutane is activated at the tertiary C-H bond into an alkoxy species, which is subsequently converted to an allylic species, precursor to the formation of methacrolein and methacrylic acid. Busca et al propose that methacrolein and methacrylic acid could share the same precursor, a dioxyalkylidene, which then reacts by parallel paths to form either of the final products. Isobutene feed was shown to form the same products over the catalyst, reaching a very high conversion (65%) at a low residence time (1 second). This mechanism favours the proposed mechanism 1 above - dehydrogenation followed by oxidation - although neither Busca et al [1996] nor any other investigators have yet observed the presence of isobutene as an intermediate during space velocity studies. The proposed mechanism of Busca et al [1996] is given in Figure 1.28.

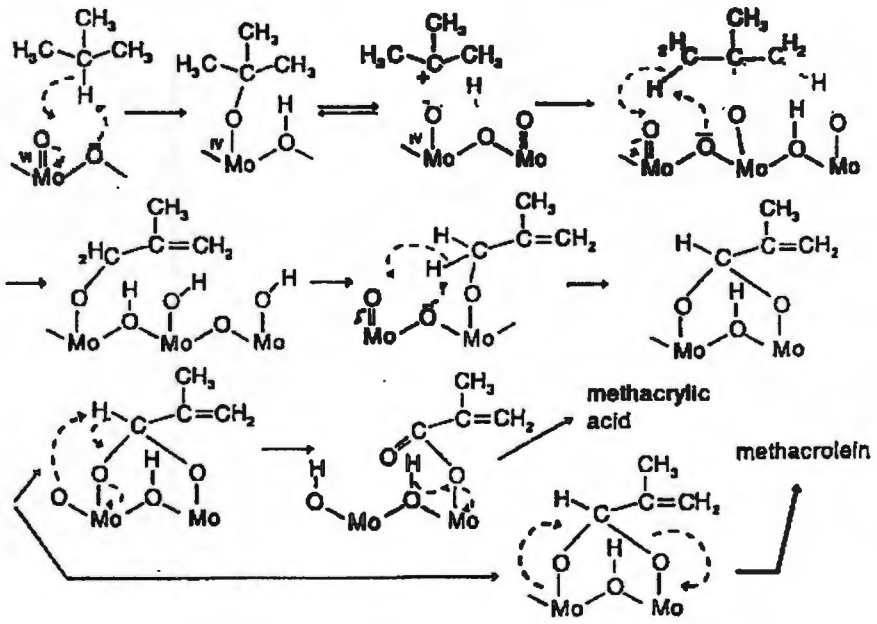

FIGURE 1.28: PROPOSED MECHANISM OF METHACRYLIC ACID FORMATION [Busca et al, 1996]

1.3. OBJECTIVES OF THE RESEARCH

The aims of the research were:

i) To synthesise a vanadyl pyrophosphate catalyst for the formation of maleic anhydride from n-butane with industrial yields (60 to 70%) and to study the effect of P/V ratio under different pretreatment conditions on the yield of maleic anhydride and how it relates to the structure of the VPO phases.

This was done by testing the catalyst for the reaction of n-butane to maleic anhydride on a reaction rig under typical industrial conditions of temperature and space velocity. Catalyst characterisation, including XRD and infrared, was used to relate changes in yields to changes in catalyst structure.

The effects of time on stream, reaction temperature and space velocity on the yields of products were also studied.

ii) To synthesise the heteropoly acid catalyst, $K(NH_4)_2PMo_{12}O_{40}/Fe_1O_{1.5}$, and to test its activity for the reaction: i-C_4 + O_2 → methacrylic acid + byproducts.

This section was aimed at studying the reaction mechanism as well as the catalyst activation. Insight into the mechanism can help with catalyst optimisation, as well as suggest optimal reaction conditions such as the separation of oxidation and reduction steps. It can also provide ideas for alternative routes for the desired product. Knowledge of the catalyst activation can give insight into catalyst preparation, e.g., if the catalyst is over-oxidised during activation and subsequently over-oxidises the feed, the activation method can be adjusted.

2. EXPERIMENTAL PROCEDURE

2.1. CATALYST PREPARATION

2.1.1. PREPARATION OF VPO CATALYST

The VPO catalyst was prepared by the reduction of V_2O_5 in either an organic reducing agent (a mixture of isobutyl alcohol and benzyl alcohol) or an aqueous reducing agent (31 wt.% HCl in water), followed by the addition of phosphoric acid.

Preparation in the organic medium was as follows: 10 g of V_2O_5 was weighed out and placed inside a cylindrical flat-bottom glass vessel (1000 ml, height = 160 mm, diameter of body = 105mm), which was placed on a hot plate/ magnetic stirrer. To this was added 100 ml of isobutyl alcohol and 50 ml benzyl alcohol. A multi-socket lid was fitted on top of the vessel and sealed with silica gel. Into the multi-socket lid was fitted a glass coil condenser, which was cooled with running tap water. The temperature in the solvent was monitored with a thermometer, which fit into the multi-socket lid with the thermometer tip inside the solvent. The setting on the hotplate was adjusted manually, and the temperature was increased from 25°C to 105°C over a period of 15 minutes. At 105°C, the mixture started to boil. The mixture was then refluxed at these conditions with constant stirring for four hours, during which time the solid suspension changed from a reddish brown powder to a black slurry. The heating plate was then switched off and the mixture allowed to cool to about 40°C. At this point, o-H_3PO_4 was introduced in such a quantity as to produce the required ratio of phosphorus to vanadium.

For instance, for a P/V ratio of 1.1 in preparation, the amount of o-H_3PO_4 added was as follows:

10g V_2O_5 = 0.055 mol V_2O_5
≡ 0.11 mol V

For a P/V ratio of 1.1 in preparation, the amount of phosphorus needed was:

Amount = 0.121 mol P
≡ 0.121 mol o-H_3PO_4
≡ 11.854 g o-H_3PO_4
≡ 13.946 g 85% o-H_3PO_4
≡ 8.155 ml 85% o-H_3PO_4 (1 litre = 1.71 kg)

After adding the o-H_3PO_4, the mixture was reheated to 105°C and refluxed for a further two hours with constant stirring. During this period, the black slurry changed colour, first to light green and then to pale blue. The colour change during reaction is not given in literature, but compared with Table 1.3, the precursor could be $VOHPO_4.4H_2O$, which is a blue powder. The green colour could be the phase $VO(H_2PO_4)_2$, which is a blue-green colour. The formation of a light blue-green suspension was also reported by Abon et al [1995].

After reflux, the catalyst precipitate was filtered and dried overnight at 75°C. Five Catalyst samples were prepared in this way with the following phosphorus/vanadium ratios: P/V = 1, P/V = 1.1, P/V = 1.15, P/V = 1.2, P/V = 1.5. These samples were labelled PV1, PV1.1, PV1.15, PV1.2 and PV1.5 respectively. It should be noted that the P/V ratios reported above are the molar ratios of phosphorus (added as phosphoric acid) to vanadium (added as V_2O_5). According to Hodnett [1985]: "A difficulty that arises in considering the P/V ratio [in patent and academic literature] is that details of the elemental analysis of the catalysts are not usually given. In cases where the precursor is isolated by evaporation of the solvent, this may not be a great problem. Where the precursor is precipitated, some uncertainty must be expressed about the composition." Elemental analysis of the precalcined precursor was therefore carried out and appears in section 3.1.1.3.

The P/V ratio used in the preparation is thought not to reflect the true P/V ratio of the final species. As mentioned by Cornaglia et al [1991]: "For organic preparations in which the solid was filtered off, a ca. 10% excess of H_3PO_4 was needed to obtain a given $(P/V)_{BULK}$ ratio." As literature reports the optimum P/V ratios to be around 1.1, ratios in the preparation of 1.2 and 1.5 were also used. PV1.2 therefore means a P/V ratio in the preparation of 1.2 but the true ratio may be closer to 1.1.

With the aqueous reducing agent, the apparatus was the same as above. 10 g of V_2O_5 powder was placed in the glass reflux vessel and to this was added 100 ml of 31% HCl. The temperature was then increased to 100°C over a period of 30 minutes, at which point the mixture started to boil. It was then refluxed at this temperature for four hours with constant stirring to form a black solution. After 4 hours, the hot-plate was again switched off and the temperature allowed to cool to 40°C. At this point, the appropriate amount of o-H_3PO_4 was added. The mixture was refluxed for a further two hours and changed from a black to a dark blue solution. The liquid was then evaporated off overnight at 75°C to form a bluish-green solid. With the aqueous method, catalyst samples with a P/V ratio of 1.1 and 1.15 were prepared and labelled PV1.1HCl and PV1.15HCl.

A catalyst was also prepared by reducing V_2O_5 in organic medium, as before. It was refluxed with o-H_3PO_4 to produce a P/V ratio of 1.15. After filtering and drying, the catalyst was again refluxed in the isobutyl alcohol/ benzyl alcohol mixture to reduce any possible remaining V^{5+} species. The sample was labelled PV1.15ref. The catalyst samples and their codes are recorded in Table 2.1. below.

2.1.1.1. VPO CATALYST PRETREATMENT

After drying, the catalyst powder was calcined in either oxygen, nitrogen or the reaction mixture (1.44% n-butane, 78.56% N_2, 20% O_2) prior to reaction. It was mixed with acid washed sand (100 to 500 microns) and supported in the reactor tube with glass wool. The acid washed sand was first washed in deionised water and dried prior to use. The catalyst was then calcined in situ by switching on the calcination gas (N_2, air or reaction mixture) and heating the reactor up at about 5°C/min. The catalyst was left at the calcination conditions, typically 400°C and a flowrate of 100ml/min N_2, for four hours. After the calcination period, the reaction feed was introduced. During calcination, the catalyst changed colour from light blue to grey, which seems to indicate the change from $VOHPO_4$ to $(VO)_2P_2O_7$ (Table 1.3).

TABLE 2.1: VPO CATALYST SAMPLES PREPARED

CODE	P/V RATIO DURING PREPARATION	REDUCING AGENT
PV1	1	organic
PV1.1	1.1	organic
PV1.15	1.15	organic
PV1.2	1.2	organic
PV1.5	1.5	organic
PV1.1HCl	1.1	aqueous
PV1.15HCl	1.15	aqueous
PV1.15ref	1.15	organic

2.1.2. PREPARATION OF THE HETEROPOLY ACID CATALYST, AMMONIUM/POTASSIUM MOLYBDOPHOSPHORIC ACID

The method followed in this research was based on the one used by Cavani et al [1995] for the preparation of the mixed potassium/ammonium salts of molybdophosphoric acid, doped with iron. It was decided not to follow the method of Mizuno et al [1994] for the preparation of the cesium-salt of molybdovanadophosphoric acid, as cesium is very expensive and the promotion of the heteropoly acid with vanadium is a more complex procedure, whereas the pure heteropoly acid can be bought off the shelf.

The following procedure was used in this research:

3 g molybdophosphoric acid (Merck) was dissolved in 20 ml of deionised water at room temperature. 0.13 g KNO_3 and 0.2 g NH_4NO_3 were then dissolved and stirred together in 20 ml of water and added to the molybdophosphoric acid solution with constant stirring. 0.519 g $Fe(NO_3)_3.9H_2O$ was dissolved in water and added dropwise to the 40 ml solution with vigorous stirring, in order to obtain the mixed potassium/ammonium salt of molybdophosphoric acid, $K(NH_4)_2PMo_{12}O_{40}$, with Fe on the surface (given by Busca et al [1996] to have the form $K(NH_4)_2PMo_{12}O_{40}/Fe_1O_{1.5}$). The water was then evaporated off overnight at 75°C.

2.1.2.1. HETEROPOLY ACID CATALYST PRETREATMENT

$K(NH_4)_2PMo_{12}O_{40}$ was also prepared as above, without the addition of $Fe(NO_3)_3.9H_2O$. The yellow precipitate was filtered and dried. The catalyst was then calcined in situ at 300°C in oxygen for one hour. After calcination, reaction feed (17% isobutane, 30% oxygen, 53% N_2) was introduced and the temperature was ramped up at 5°C/5min to 380°C. The catalyst was kept on stream at this temperature for 1 hour, 1.5 hours, 3 hours and 5 hours respectively. These samples were labelled KNHPMo1, KNHPMo15, KNHPMo3 and PKNPMo5.

2.2. CATALYST CHARACTERISATION

Characterisation of the catalyst was carried out to determine if the correct catalyst phase and structure were obtained. The characterisation results were compared with literature. The effect on the structure of changing preparation parameters was also studied with techniques such as X-ray diffraction and infrared.

2.2.1. X-RAY DIFFRACTION (XRD)

XRD spectra were measured with a Philips X-ray diffractometer with Cu-Kα radiation of 40 kV and 30 mA, and a wavelength of 1.54 Å. The scanning range used was $6° < 2\theta < 50°$ for a step size of 0.1°. Slit width was 1° divergent and 1° receiving.

XRD spectra were obtained for VPO samples calcined in air or nitrogen for a range of P/V ratios. 1 g of precursor was taken from samples PV1, PV1.1 and PV1.15 and loaded into the reactor. These samples were then calcined at T = 380°C for 3 hours in a flow of 120 ml/min (STP) air and N_2 respectively. The sample PV1.1 was also calcined in N_2 for 6 hours at 475°C. 1 g samples of PV1, PV1.1, PV1.2 and PV1.5 were also calcined for 5 hours in 100 ml/min STP reaction feed (1.44% n-butane/78% N_2/20% O_2) at 400°C. XRD spectra were also taken of a deactivated commercial catalyst as well as an experimental catalyst prepared by a commercial organisation.

2.2.2. INFRARED ABSORPTION (IR)

IR measurements were carried out on a Nicolet 5ZDX FT-IR spectrometer scanning a range of between 400 cm^{-1} and 4000 cm^{-1}. The instrument uses a 632.8 nm laser with 1-4 mW power. Beam diameter is 0.63 mm and beam divergence 1.3 mrad. Operating voltage = 1700 ± 100VDC. The spectrometer was interfaced with OMNIC FTIR software version 3.0.

The VPO samples calcined in reaction feed, as prepared for XRD above (i.e. the same calcination conditions and P/V ratios), were also used for characterisation with IR. The samples were mixed with KBr in a 1/15 mixture and pressed (P = 10 tons) into wafers for IR measurement.

Samples KNHPMo1, KNHPMo15, KNHPMo3 and KNHPMo5 were also mixed in a 1/20 weight mixture with KBr and pressed as above for infrared measurement.

2.2.3. ELEMENTAL ANALYSIS

Quantitative analysis of the precursor $(VOHPO_4).0.5H_2O$ was done at MINTEK using a volumetric procedure for vanadium. Phosphorus content was determined using a UV visible spectrophotometer with ammonium molybdovanadate as colouring agent.

Qualitative analysis was performed with Energy Dispersive Spectroscopy (EDS), using the LEICA S440 with the FISONS KEVEX Energy Dispersive X-ray analysis system. Resolution is 3 nm at 40 kV with a LaB_6 filament and a BN window, allowing elemental analysis of as low as boron. Software options allow standardless analysis.

2.2.4. SCANNING ELECTRON MICROSCOPY (SEM)

A Leica S440 scanning electron microscope was used to produce photographs of the catalyst samples. Magnifications of between 1400 and 50000 were achieved, operating at an accelerating voltage of 15 keV. Stage tilt was set at 30°. A working distance of 9-12 mm and an aperture size of 30 μm were used. Samples were mounted on aluminium stubs and coated with Au/Pd film.

In order to obtain a visual impression of the macrostructure and crystal formation of the catalyst, scanning electron micrographs of the VPO phases calcined in N_2 and air (as mentioned in section 2.2.1) and precipitated in organic medium, were taken.

2.2.5. SURFACE AREA

BET surface areas were measured for the VPO catalyst using an ASAP 2000 (accelerated surface area and porosimetry). Approximately 0.5 g of the sample was dried at 120°C and the chamber was evacuated. The mass was recorded, nitrogen was introduced to the sample and it was cooled to -196°C with liquid nitrogen. Operating pressure was 760 mm Hg and the drop in pressure P/P_o was measured for 20 adsorption points.

2.2.6. PARTICLE SIZE

A malvern particle size analysis was carried out on the VPO catalyst. The sample was suspended in deionised water and agitated. A lens of size 63 mm was then inserted and the measurement taken over a size range of 0.1 to 1000 μm.

2.3. REACTION STUDIES

2.3.1. EXPERIMENTAL RIG

A diagram of the reaction rig used for the partial oxidation studies is given in Figure 2.1. Mass flow controllers were used to supply the following gases:

1) 1.89% n-butane in N_2
2) Pure isobutane
3) Pure oxygen
4) Pure nitrogen
5) 5.1% CH_4 in N_2, used as internal standard for gas chromatographic analysis

The N_2, O_2 and isobutane or N_2, O_2 and n-butane/N_2 streams are mixed before the reactor.

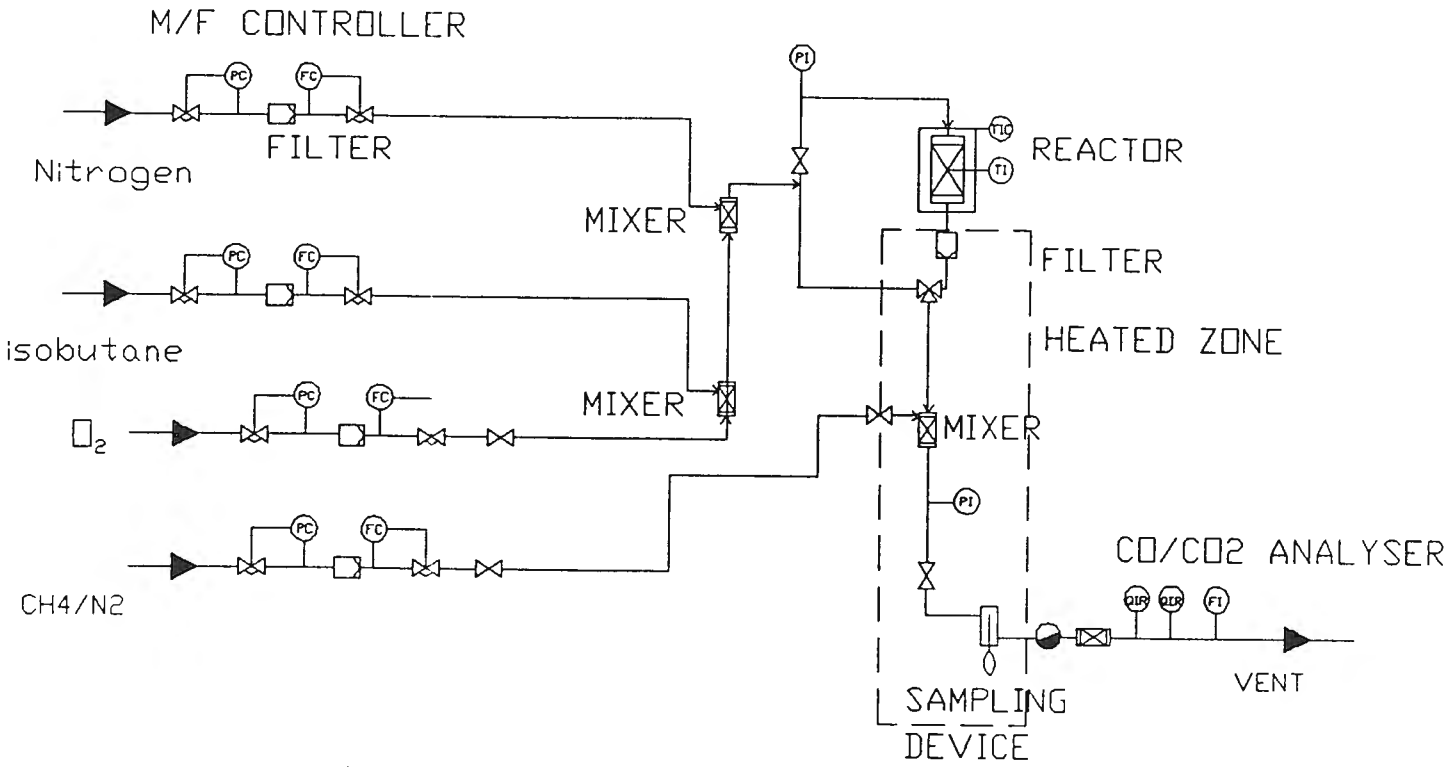

FIGURE 2.1: DIAGRAM OF THE EXPERIMENTAL REACTION RIG

mixer
valve
heated section
cold trap
infrared CO_2 measurement
infrared CO measurement
flow measurement

Two tubular fixed bed reactors were used to test the catalyst. They differ in the way that each reactor is heated: the first with a cartridge-type heating mantle (Figure 2.2) and the second with an oven.

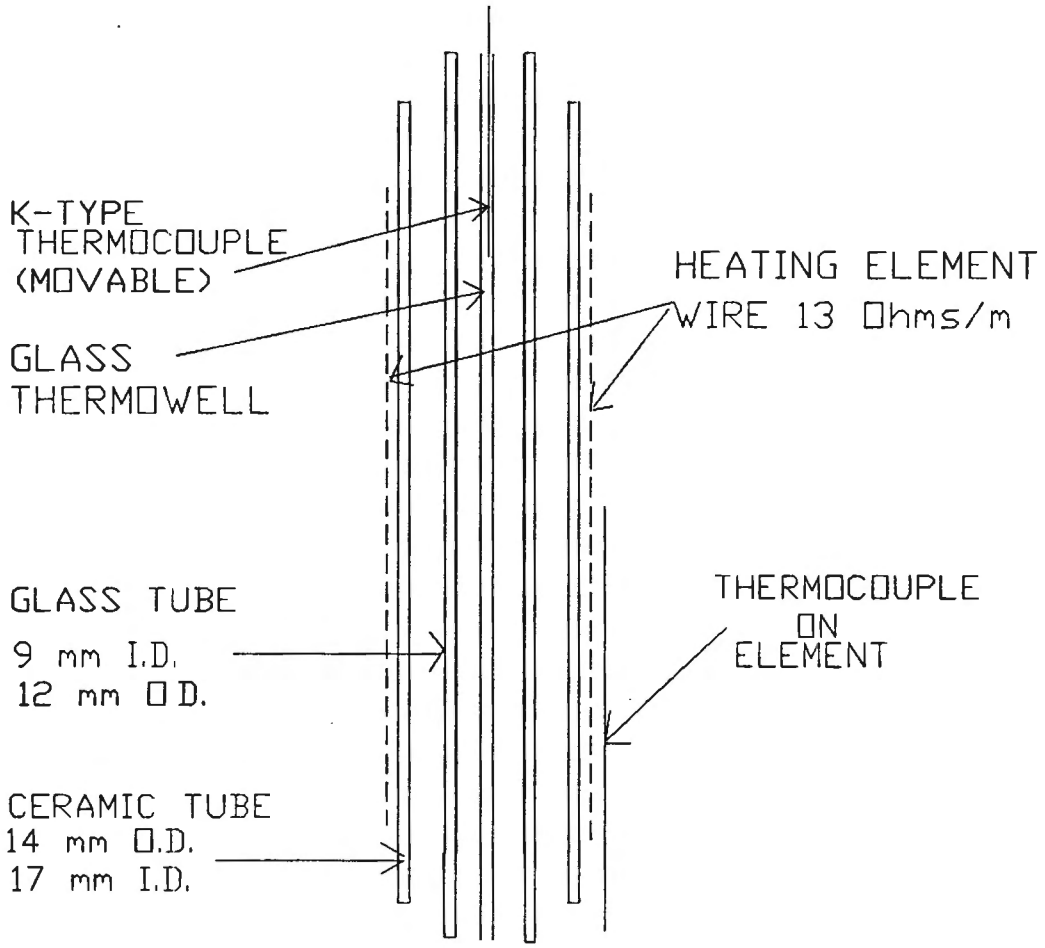

FIGURE 2.2: FIXED BED REACTOR WITH CARTRIDGE-TYPE HEATING MANTLE

The tubular reactor with a **cartridge-type heating mantle** consists of a 9 mm i.d./12 mm o.d. glass tube, loosely fitted inside a ceramic tube (13 mm i.d.). Around the ceramic tube is wound a nichrome heating wire (13 Ω/m), set with clay, which forms a 150 mm long heating zone (total resistance = 113.5 Ω). A K-type thermocouple, attached to a REX-C100 temperature controller (RKC Instrument Inc.), is placed on the element of the central heating zone. The temperature controller provides a 0/12V DC voltage pulse output to a relay (an AC switch) which controls the AC current through the element.

Due to heat transfer resistance, there is an offset between the temperature measured on the element and the actual temperature in the bed. In order to check the temperature profile through the cartridge-heated reactor bed, a glass thermowell is placed inside the glass reactor. Inside this glass thermowell another thermocouple, linked to a temperature readout, measures the more accurate temperature in the centre of the bed. The glass thermowell is sealed off on one end with glass, in order to prevent bypassing of the reactor bed. The glass reactor is sealed with rubber o-rings and stainless steel fittings on both ends and a viton ferrule seals off the thermocouple entrance. Using this method, isothermal conditions can be obtained for about 3 cm in the hotspot of the reactor bed.

One-dimensional temperature profiles, measured down the length of the reactor, are given for hot-zone temperatures of 400°C and 380°C respectively in Figure 2.3. These are the typical reaction temperatures used for the VPO and heteropoly acid catalysts, respectively. For a hot-zone temperature of 400°C in the glass thermowell, a temperature of 376°C was measured on the element. For a temperature of 380°C, a temperature of 360°C was measured on the element.

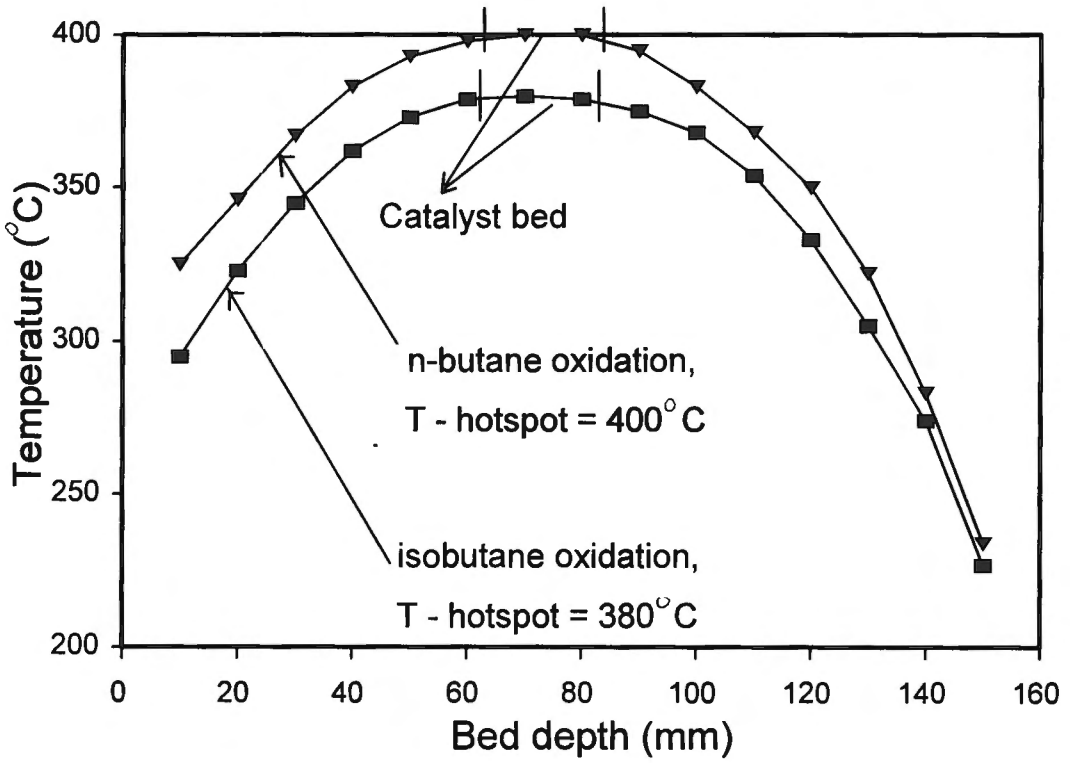

FIGURE 2.3: TEMPERATURE PROFILE IN THE CARTRIDGE-TYPE REACTOR

Catalyst powder is mixed with acid washed sand (normally 0.3 g catalyst + 1 g sand) for heat transfer purposes and supported in the glass reactor tube with glass-wool. Calcination is then carried out in situ. The calcination gas is introduced and the reactor heated up at typically 5°C/5min. After reaching the calcination temperature, the reactor is left at these conditions for the calcination period, after which the reaction feed is introduced and the reactor adjusted to the desired reaction temperature (e.g. 380°C).

The **oven-heated reactor** (Figure 2.4), on the other hand, consists of a glass u-tube, which is placed inside an oven with a fan for heat transfer. A thermocouple is placed in an inlet made into the glass u-tube for internal temperature measurement.

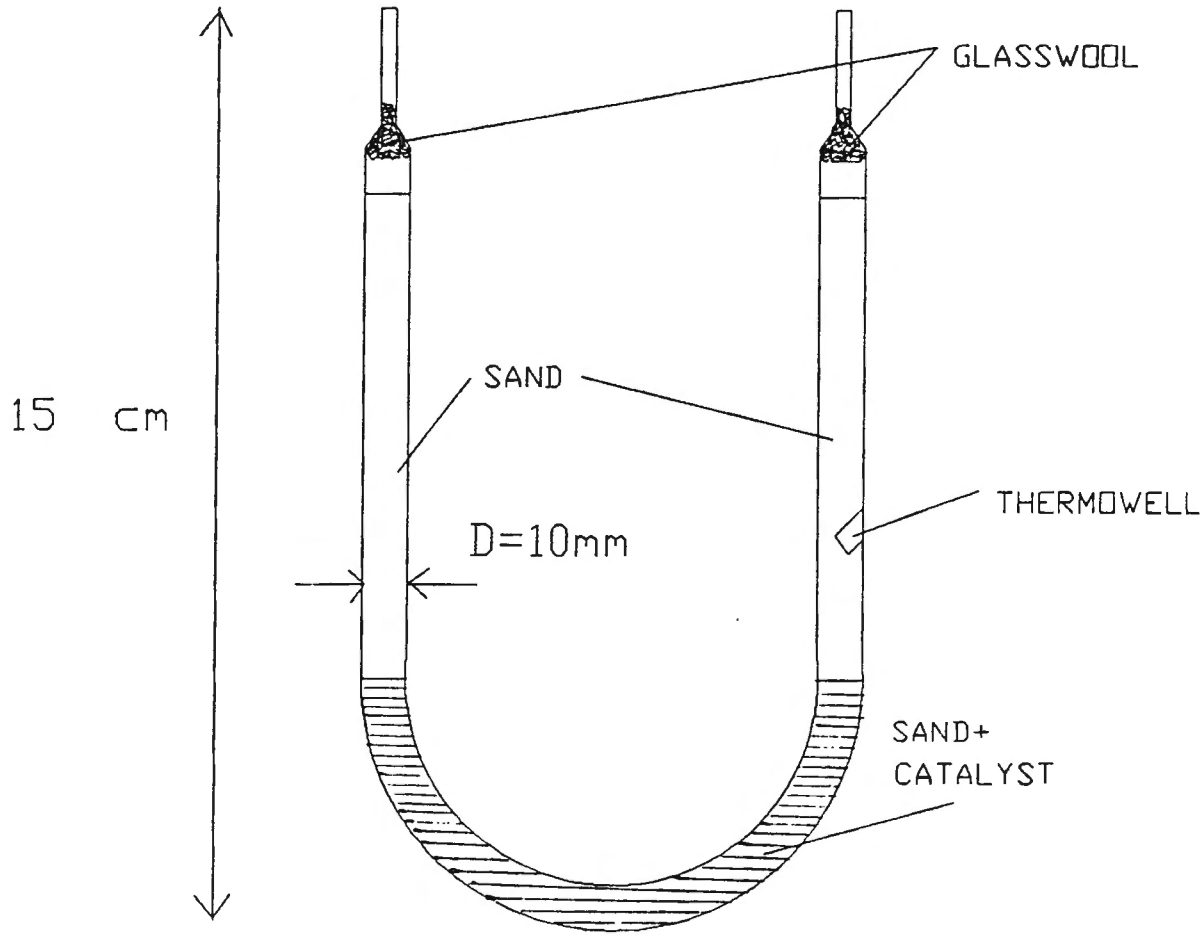

FIGURE 2.4: FIXED BED GLASS U-TUBE REACTOR IN OVEN

2.3.1.1. EVALUATION OF THE EXPERIMENTAL SET-UP

In order to test the functioning of the newly-built experimental rig, the following tests were carried out:

- Blank runs were performed by feeding n-butane in air over sand, at reactor temperatures of 380, 400 and 450°C. No conversion of n-butane was observed (Carbon balances > 99%), indicating that n-butane does not react anywhere but on the catalyst.

- Maleic anhydride was fed with a saturator to check for combustion of product in the lines. This test was carried out through outlet lines at temperatures of up to 200°C, alternatively through the reactor loaded with sand at T = 400°C and bypassing the reactor. The temperature of the saturator containing the maleic anhydride was varied between 60 and 100°C. When the reactor was bypassed, a maleic anhydride peak representing between 1 and 2 STP ml/min was observed. However, when passing the maleic anhydride over an empty reactor at T = 400°C, with the saturator at the same temperature as before, only CO and CO_2 were observed, representing 100% conversion of maleic anhydride under these conditions.

- Maleic anhydride was dissolved in a solvent (ethanol, diethyl ether and acetone) and injected into the GC. Maleic anhydride dissolved in water was also inserted into an ampoule, which was analysed on the GC to test if maleic anhydride, if formed, can be detected. When injecting the dissolved maleic anhydride into the GC FID, peaks were observed for the solvent (e.g. ethanol) and maleic anhydride as shown in Figure 2.5. (Note that quantitative analysis of the integrator printouts of Figure 2.5 was not carried out as only the retention times were compared. Similar concentrations were not used.) When breaking an ampoule with maleic anhydride dissolved in water inside the ampoule in the ampoule-breaker, a peak was observed for maleic anhydride, indicating that it can be detected with the sampling method used. The ampoule sampling method is described in Appendix E.

- To check for the formation of maleic acid, the GC retention time of maleic acid was determined and compared with the retention time of maleic anhydride. Maleic acid was found to have lower GC retention times than maleic anhydride. For those runs where product was formed, such as the test over the deactivated commercial catalyst, retention times were carefully examined and the formation of maleic acid was discounted. Only maleic anhydride formed.

2.3.2. PRODUCT ANALYSIS

The gas line leaving the reactor was heated at 180°C up to the sampling point. Samples of the effluent were taken using an ampoule sampling method [Schulz et al, 1984c] as described in Appendix E. This method employs an evacuated glass ampoule with a sealed capillary on one end. The capillary is introduced into the gas line where it is broken off, sucking gas into the ampoule, which is subsequently sealed off with a torch. The ampoule is then analysed on the GC.

FIGURE 2.5: GC TRACES SHOWING INJECTIONS OF MALEIC ANHYDRIDE DISSOLVED IN ETHANOL, DIETHYL ETHER AND ACETONE
(Analysis is not quantitative - only retention times were compared)

MALEIC ANHYDRIDE IN ETHANOL

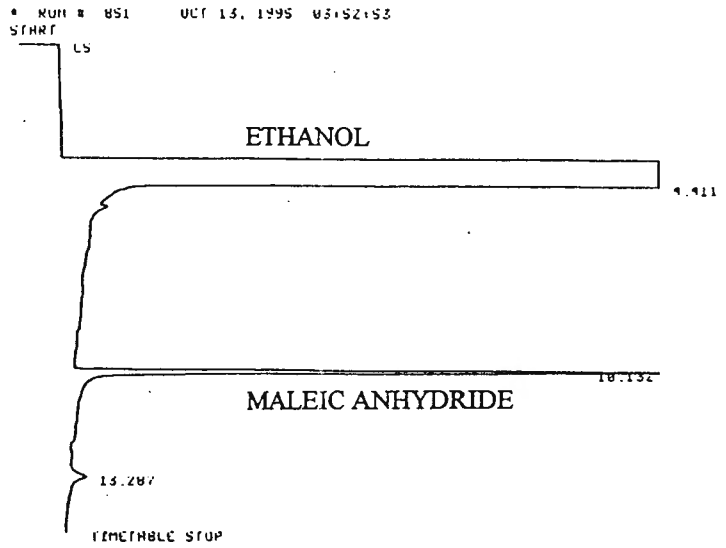

MALEIC ANHYDRIDE IN DIETHYL ETHER

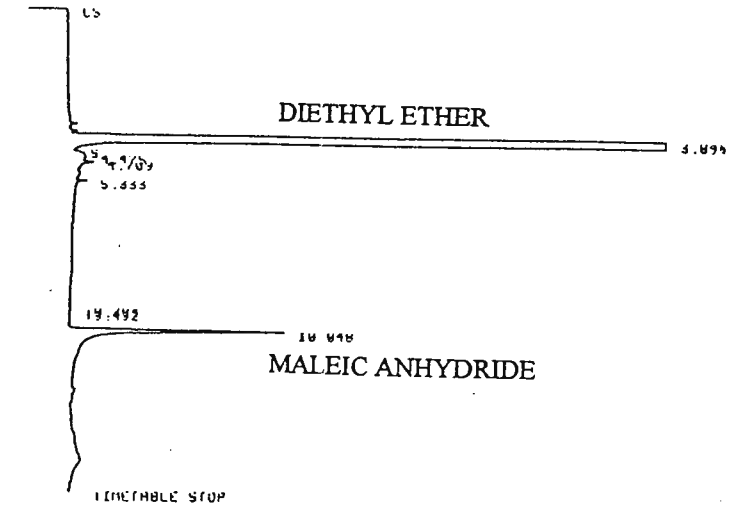

MALEIC ANHYDRIDE IN ACETONE

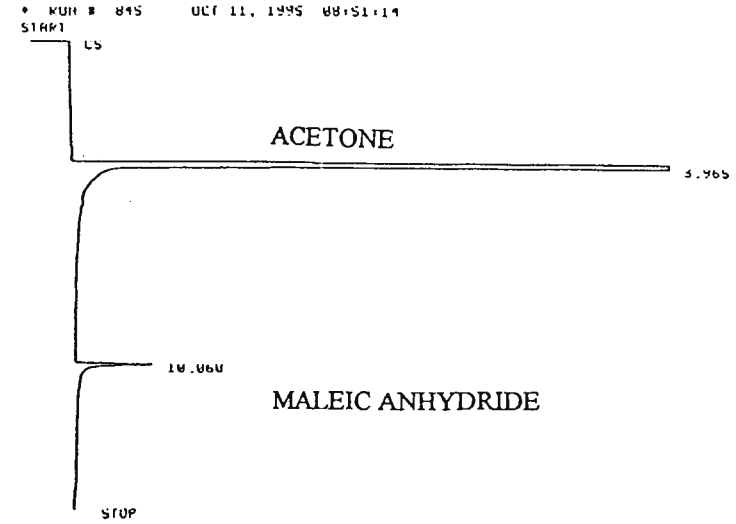

The product separation is performed using gas chromatography. Table 2.2 gives the GC specifications:

TABLE 2.2: GAS CHROMATOGRAPH SPECIFICATIONS:

GC model	VARIAN 3400
Detector type	FID
Column type	Hewlett Packard PONA
Stationary phase	Methyl silicone crosslinked
Column length	50 m
d_i	0.2 mm
Film thickness	0.5 μm
Column head pressure	20 psig
Injector temperature	230°C
Detector temperature	270°C
Split ratio	1:100
Flow of air through detector	300 ml/min (STP)
Flow of N_2 through detector	25 ml/min (STP)
Flow of H_2 through detector	25 ml/min (STP)
Flow of H_2 through column	1 ml/min (STP)
TEMPERATURE PROGRAM:	
Initial temperature	-10°C
Initial temperature holding time	5 min
Temperature ramp	30°/min
Final column temperature	250°C
Final column holding time	25 min
Method of oven cooling below room temperature	Addition of liquid nitrogen

Total combustion products were measured with an online CO/CO_2 IR analyser (Hartmann & Braun model Uras 10E).

The product was also condensed out in a cold-trap and analysed on a GC mass spectrometer.

2.3.3. DATA EVALUATION

The following formulas were used to calculate the product yields Y_i, conversions X_i and selectivities S_i. All calculations were done on a carbon basis.

$$X_i = \frac{\dot{n}_{feed,in} - \dot{n}_{feed,out}}{\dot{n}_{feed,in}} \quad (1)$$

$$Y_i = \frac{\dot{n}_{i,out}}{\dot{n}_{feed,in}} \quad (2)$$

$$S_i = \frac{Y_i}{X_i} \quad (3)$$

The molar flow was determined using the ratio of the area A_i of the peak for each component i to the area A_{ref} of the peak for the internal standard from the GC analysis.

Equations 1 and 2 change to:

$$X_i = \frac{\left(\frac{A_{feed}}{A_{ref}}\right)_{in} - \left(\frac{A_{feed}}{A_{ref}}\right)_{out}}{\left(\frac{A_{feed}}{A_{ref}}\right)_{in}} \quad (4)$$

$$Y_i = \frac{\left(\frac{A_i \cdot f_i}{A_{ref} \cdot f_{ref}}\right)_{out}}{\left(\frac{A_{feed} \cdot f_{feed}}{A_{ref} \cdot f_{ref}}\right)_{in}} \quad (5)$$

with f_i being the response factor of component i on the flame ionisation detector (FID) of the GC. The products CO and CO_2 were not detected by FID and Equation 5 cannot be applied to these products. The IR photometer measured the concentrations of CO and CO_2 in the effluent in vol-%. This reading was converted into the molar fraction x_i by dividing by 100.

The molar flows of CO and CO_2 in the effluent were calculated using the ideal gas law:

$$\dot{n} = \frac{p \cdot \dot{V}}{R \cdot T} \cdot x_i \qquad \text{i} = \text{CO}, \text{CO}_2 \qquad (6)$$

The flow $\dot{V}$ was measured using a soap bubble meter and the flow was corrected to standard conditions (T = 25°C, p = 1,013 mbar). In order to evaluate the experimental run, a carbon balance was calculated using Equation 7:

$$C\text{-}balance = \frac{\left(\frac{A_{feed} \cdot f_{feed}}{A_{ref} \cdot f_{ref}}\right)_{out} + \sum_{i=1}^{n}\left(\frac{A_i \cdot f_i}{A_{ref} \cdot f_{ref}}\right)_{out} + \frac{\frac{p \cdot \dot{V}}{R \cdot T} \cdot (x_{CO} + x_{CO_2})}{\dot{n}_{ref}}}{\left(\frac{A_{feed} \cdot f_{feed}}{A_{ref} \cdot f_{ref}}\right)_{in}} \qquad (7)$$

with n being the number of products.

Unless carbon balances were at least 95%, the experiments were rejected. An example of a carbon balance calculation is given in Appendix B.

Response factors were determined by comparing GC peak areas to that of n-heptane, the response factor of which was taken as 1.0. For each compound, a mixture of known mass ratio was prepared consisting of the desired compound, e.g. methacrolein, and n-heptane. The known mass ratio prepared was then converted to the ratio of the number of carbons. By dividing the ratio of peak areas given by the GC when this mixture was injected to the ratio of the number of carbons which was known to have been injected, the response factor based on carbon number or carbon mass was determined. For each compound, a set of mass ratios was injected and an average value determined.

Where the compound was not available and since no literature values could not be found, response factors were determined according to the method of Kaiser [1969]. According to Kaiser [1969] the signal of a CH_3- and a CH_2- group is equal to 1.0, whereas the signal of a carbon group adjacent to an oxygen is equal to 0. The values of the response factors are given in table 2.3 below.

TABLE 2.3: VALUES OF THE GAS CHROMATOGRAPH RESPONSE FACTORS

Compound	Response factor f_i
Maleic anhydride	1.666
Methacrylic acid	1.832
Methacrolein	1.666
Isobutyric acid	1.666
Propanal	1.5
Ethyl methyl ether	3
Dimethyl benzene	1

2.3.4. REACTION CONDITIONS STUDIED

2.3.4.1. VPO CATALYST

Literature reports a range of reaction temperatures and space velocities for the partial oxidation of n-butane to maleic anhydride, CO and CO_2. The range of reaction conditions studied in this work is shown in Table 2.4. Feed composition for n-butane oxidation, as given in literature, varies little between different investigators and is typically 1.5% n-butane in air. A summary of the different reaction runs carried out on the VPO catalyst, including catalyst precursor P/V ratio, calcination and reaction conditions, conversions, product selectivities and carbon balances appears in Appendix A.

TABLE 2.4: REACTION CONDITIONS STUDIED OVER THE VPO CATALYST

Temperature	350°C to 450°C
Space Velocity	3 to 24 g/g.h
Feed Composition	1.44% n-Butane, 78.56%N_2, 20% O_2 (Oxygen partial pressures were varied)
Reaction time	Reaction times of up to 40 hours were investigated for prepared VPO and 190 hours for experimental commercial catalyst
Reactors	Fixed bed glass reactor heated by a cartridge heating element Fixed bed U-tube glass reactor heated in an oven

Further catalytic tests include:

(i) A deactivated commercial catalyst tested between 350 and 440°C for a range of space velocities.
(ii) An experimental catalyst prepared by a commercial company tested at T = 390 and 400°C for different oxygen partial pressures.

2.3.4.2. HETEROPOLY ACID CATALYST

A range of reaction temperatures was studied to investigate the effect of temperature on yield of methacrylic acid and to determine the optimum operating temperature. This was followed by a series of runs investigating catalyst behaviour as a function of reaction time, in order to determine the change in catalyst structure during equilibration. A range of space velocities was examined with the aim of minimising conversion. The lowest space velocity and the widest range of space velocities allowed by the mass flow equipment were attained. A summary of all reaction runs carried out is given in Table A_{II} in Appendix A. The range of reaction conditions is given in Table 2.5. below:

TABLE 2.5: REACTION CONDITIONS STUDIED OVER THE HPA CATALYST

Temperature	330°C to 450°C
Space velocity	0.822 to 18.26 g/g.h
Feed composition	17% isobutane, 30% O_2, balance N_2
Equilibration time	Minimum 8 hours for space velocity studies
Reactors	Fixed bed glass reactor heated by a cartridge heating element

3. RESULTS

3.1. CONVERSION OF n-BUTANE OVER VPO CATALYST

3.1.1. CHARACTERISATION

3.1.1.1. X-RAY DIFFRACTION

Figure 3.1. shows the XRD spectra of the VPO samples as a function of P/V ratio (samples PV1, PV1.1, PV1.15) calcined in air and N_2 at T = 380°C for 3 hours.

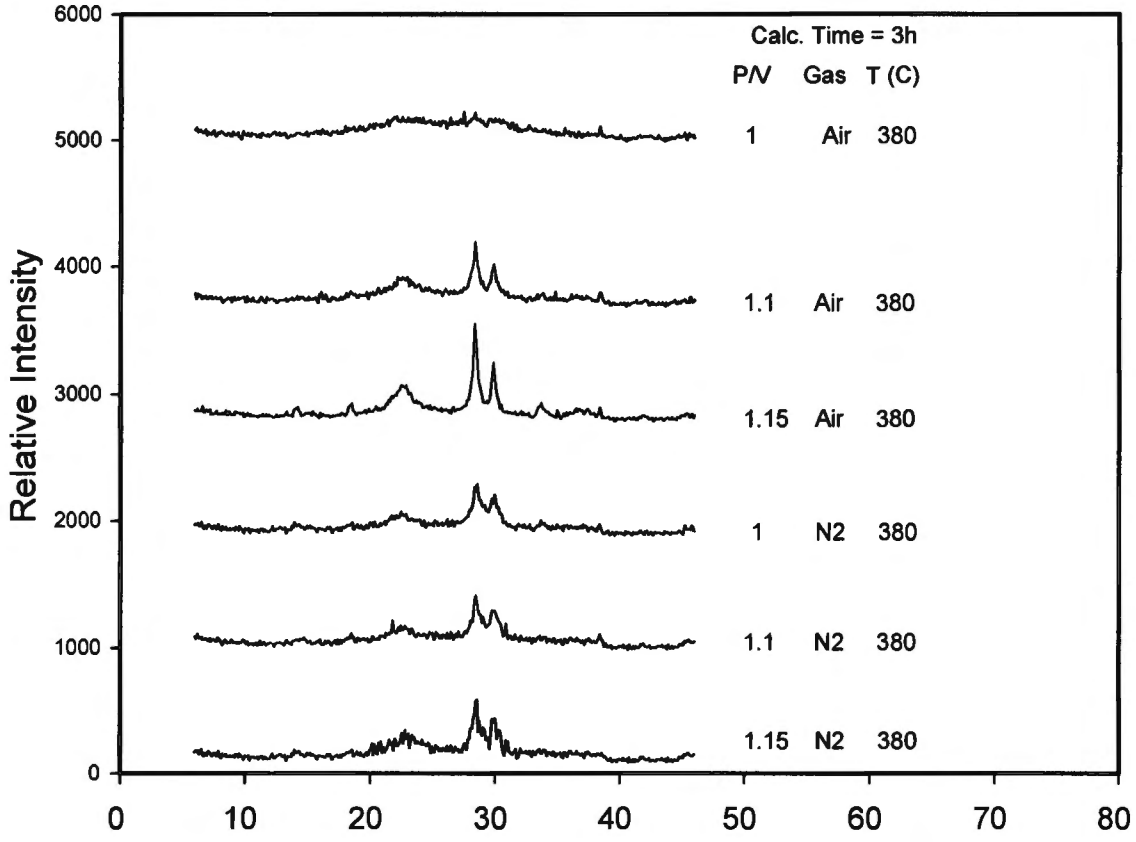

FIGURE 3.1: EFFECT OF P/V RATIO ON XRD SPECTRUM OF VPO CATALYST CALCINED FOR 3 HOURS IN AIR OR N_2 AT T = 380°C

Figure 3.2 shows the XRD spectra of VPO samples for a range of P/V ratios, calcined at 400°C for 5 hours in reaction feed.

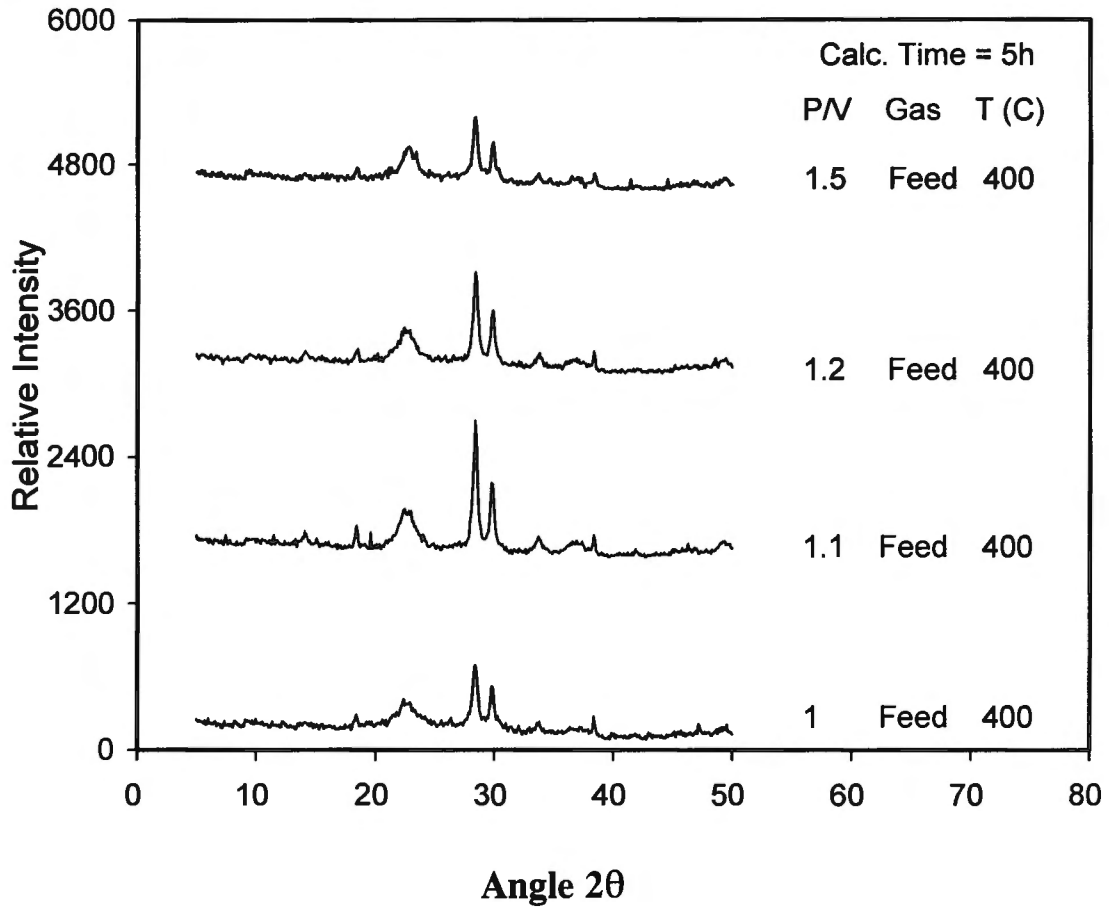

FIGURE 3.2: EFFECT OF P/V RATIO ON XRD SPECTRUM OF VPO CATALYST CALCINED FOR 5 HOURS IN $C_4H_{10}/N_2/O_2$ = 1.44/78.56/20 AT 400°C

If the XRD spectra of the calcined catalysts (Figure 3.1. and Figure 3.2) are compared with the XRD of the pure phases (Figure 1.2) and the catalysts prepared by Zhang et al [1993] (Figure 1.3), the $(VO)_2P_2O_7$ peaks can be clearly identified at 23.61°, 28.45° and 30°. The peaks of the other VPO phases of Figure 1.2 are absent. Unlike the theoretical pure phases of Figure 1.2, peak broadening (especially of the peak at 23.61°) is observed, which is similar to that of the spectrum of Zhang et al (Figure 1.3, catalyst 2) for a catalyst which gave a 60% selectivity to maleic anhydride for a feed of n-butane/O_2/He = 1.2/ 16.4/ 82.4 at 380°C. Peaks of the β-$VOPO_4$ phase do not occur. The XRD spectra of Figures 3.1 and 3.2 show the peaks of a single phase displaying peak broadening, rather than the interposition of two or more phases as is suggested by Zhang et al in Figure 1.3b. The peak broadening, especially of the peak at 23.61°, can not be the result of the interposition of another phase, e.g. β-$VOPO_4$. In order for another phase to exist, all its peaks must be present.

Since an internal standard was not used for XRD measurements, peak intensities could not be quantitatively compared. Instead, peak areas were calculated and compared. XRD spectra of catalysts calcined in air (Figure 3.1) show an increase in integrated peak area with increased P/V ratio for all three peaks, indicating a progressive development of the crystal structure. For the sample PV1, peaks can hardly be observed. Sample PV1.15 calcined in air shows the largest peak areas of all the spectra in Figure 3.1. Elemental analysis shows that the P/V ratio of this sample is in fact 1.02 (See section 3.1.1.3). XRD peaks of catalysts calcined in N_2 remain constant and do not show a change in peak area with P/V ratio as do the samples calcined in air. When calcining sample PV1 in N_2, the three $(VO)_2P_2O_7$ peaks can already be observed, whereas calcination of PV1 in air produces no peaks and the structure appears to be XRD-amorphous.

Although the average valence state was not measured, the peak broadening suggests the presence of defect sites and therefore the presence of 5+ species for the samples of Figure 3.1. Nguyen et al [1996] state that peak broadening correlates to the presence of defect sites, which in turn correlate to 5+ species as mentioned in section 1.1.3. They also state that the most active catalysts show peak broadening due to defect sites which expose 5+ species/defect sites on the surface. Most common preparation/calcination methods, such as those used for the catalysts of Figure 3.1, produce a fair degree of peak broadening, especially when organic reducing agents are used [Nguyen et al, 1996]. It is suggested here that the peak broadening also indicates the incomplete crystallisation of $(VO)_2P_2O_7$ out of its amorphous precursor.

The presence of a single crystalline phase in the case of N_2 calcination is supported by the findings of Bosch et al [1987], who used XRD for phase determination. Although a mixture of 4+ and 5+ phases was obtained by Bosch et al at P/V ratios of lower than 1 when calcining in N_2, the 4+ phase ($(VO)_2P_2O_7$) became more stabilised with an increase in P/V ratio until it was the only phase present at P/V =1. The catalyst samples of Figure 3.1 all have actual P/V ratios of about 1 or slightly in excess of 1 as shown in section 3.1.1.3. The range of P/V ratios studied by Bosch et al were P/V = 0.7 to 1.

Calcination in nitrogen does not lead to over-oxidation to the $VOPO_4$ species [Nguyen et al, 1996; Bordes, 1987]. Moreover, Nguyen et al find the N_2 atmosphere to be reducing. Over-oxidation to $VOPO_4$ does, however, take place during air calcination and the higher the temperature, the higher the degree of over-oxidation [Bordes, 1987; Nguyen et al, 1996]. The $VOPO_4$ phase was found to produce only CO and CO_2 and the percentage of the $VOPO_4$ phase was shown to increase with calcination temperature [Bosch et al, 1987]. No $VOPO_4$ was observed in Figure 3.1 for catalysts calcined in air and this can be attributed to the milder calcination temperatures - 380°C and 3 hours - as opposed to 400°C and 500°C used by Bosch et al [1987]. It is also suggested that higher P/V ratios stabilise the $(VO)_2P_2O_7$ phase and prevent over-oxidation by the scheme of Cavani et al [1994] below.

Catalyst PV1 calcined in air shows an amorphous hump from $2\theta = 16°$ to $39°$ approximately (Figure 3.1). This hump is interposed on the $(VO)_2P_2O_7$ spectrum and seems to indicate the presence of an amorphous phase out of which the $(VO)_2P_2O_7$ phase crystallises. Areas under the curve were integrated from $24.5° < 2\theta < 27°$ in order to determine if the amorphous hump decreased with P/V ratio. It was found that for air calcination this area showed a definite decrease for samples PV1 through PV1.15. The area $24.5° < 2\theta < 27°$ however showed no change for the catalyst calcined in N_2. The absence of the peaks of the precursor $VOHPO_4.0.5H_2O$ after calcination, as well as the decrease in the area assigned to the amorphous hump, suggest that the amorphous hump shown by XRD (Figure 3.1) for sample PV1 calcined in air, is due to the amorphous phase proposed by Cavani et al [1994] and Nguyen et al [1996] in the calcination step when an organic reducing agent is used:

$$VOHPO_4.0.5H_2O \rightarrow \text{amorphous phase} \rightarrow (VO)_2P_2O_7 \rightarrow \beta\text{-}VOPO_4$$
$$\searrow$$
$$V^{5+} \text{ phases}$$

It is proposed that, during air calcination, higher P/V ratios make the reaction from the amorphous phase to the pyrophosphate phase proceed further. This explains the increase in peak area with P/V ratio for air calcination. The real increase in P/V ratio for the samples PV1, PV1.1 and PV1.15 is actually very small, as shown in section 3.1.1.3 (elemental analysis). It ranges from P/V = 0.99 to P/V = 1.02, but this has a profound effect on peak area, which more than doubles for the peak associated with the (024) plane of $(VO)_2P_2O_7$ for the catalysts calcined in air (Figure 3.1). Nitrogen calcined catalysts do not show a change in peak area with increased P/V ratio and it therefore seems that the transformation is less affected by P/V ratio.

Catalyst samples calcined in reaction feed (Figure 3.2) show an increase in peak area with increased P/V ratio up to sample PV1.1. The area decreases with further increase in P/V ratio. When comparing the spectra with those obtained by Zhang et al (Figure 1.3.), peaks relating to the (016), (032), (024), (200) and (012) planes can be identified. The presence of a single crystalline $(VO)_2P_2O_7$ phase is consistent with the results of Bosch et al [1987] for calcination with n-butane in air at P/V = 1. This result is consistent with the observation that excess phosphorus stabilises the V^{4+} phase [Poli et al, 1981]. It is therefore proposed that the transformation $VOHPO_4.0.5H_2O \rightarrow$ amorphous phase $\rightarrow (VO)_2P_2O_7$ is favoured by an increase in P/V ratio up to a point, after which a further increase in P/V ratio inhibits this transformation due to the presence of excess phosphorus. The sample PV1.1 has the greatest $(VO)_2P_2O_7$ peak areas.

The X-ray diffraction patterns of the deactivated commercial catalyst and the experimental catalyst made by a commercial company are shown in Figure 3.3.

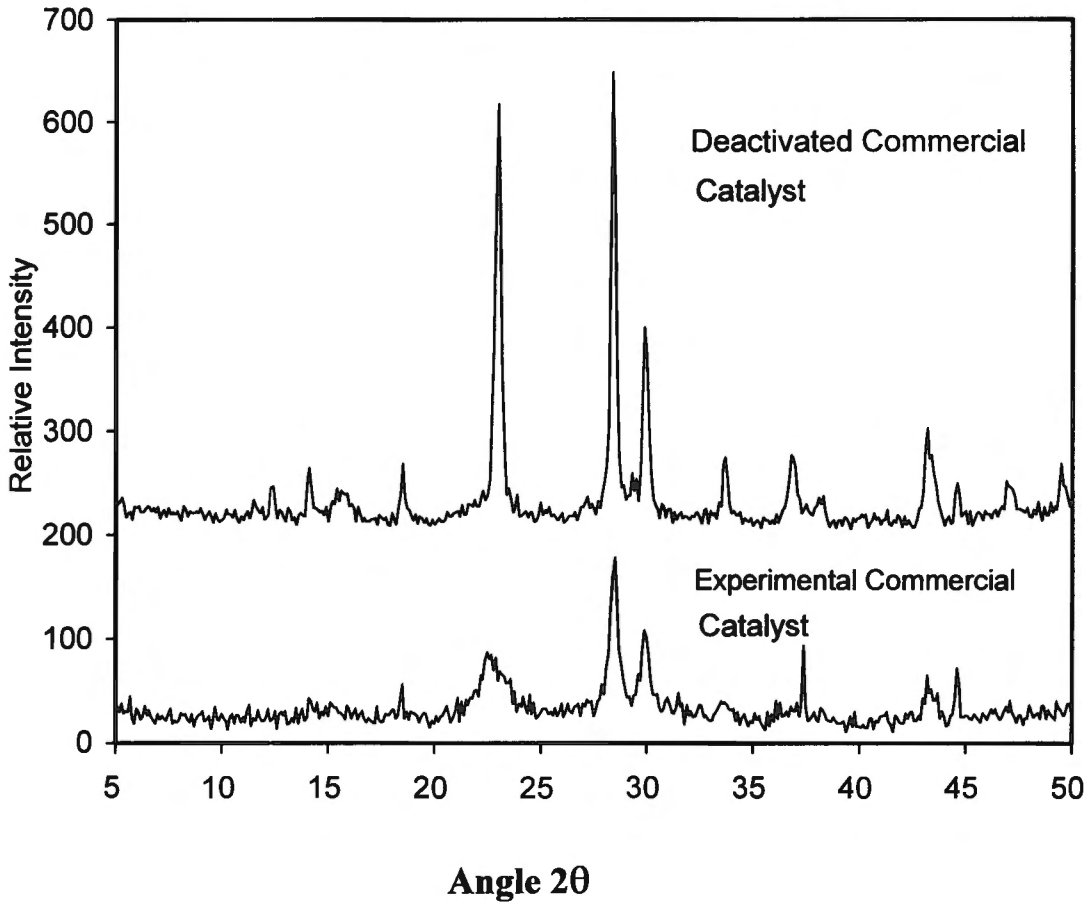

FIGURE 3.3: XRD SPECTRA OF DEACTIVATED COMMERCIAL CATALYST AND EXPERIMENTAL COMMERCIAL CATALYST

The spectrum of the deactivated commercial catalyst compares well with catalyst 3 of Zhang et al (Figure 1.3.), calcined at high temperatures in N_2, as well as that of the equilibrated VPO catalyst given in Figure 1.10 [Cavani et al, 1994]. Peaks are less broadened than for the XRD spectra of Figure 3.1. When comparing the spectra of Figures 3.1 and 3.2 with that of the deactivated commercial catalyst of Figure 3.3, the difference in the nature of the peaks is evident. The structure of Figure 3.3 is clearly more crystalline. The baseline of the spectrum is uniform and does not show changes due to the presence of an amorphous phase as for the catalysts of Figure 3.1. The spectrum of the experimental commercial catalyst (Figure 3.3), on the other hand, is less crystalline and compares favourably with the unequilibrated catalyst of Cavani et al [1994] (Figure 1.10) and the catalysts of Figure 3.1.

Although crystallinity is indicative of a selective catalyst, catalyst 3 of Figure 1.3a also has good crystallinity but low activity. This is due to the absence of V^{5+} species. The structure of catalyst 3 (Figure 1.3a) does not change with time on stream, but gives low activity due to the absence of 5+ species which are mechanistically important. The change in the nature of the 5+ species within the structure during activation is not clear. Zhang et al [1993] showed with P-NMR studies that catalyst 2 of Figure 1.3b experiences a redistribution in the V^{5+} entities with an increase in the size of the 5+ domains with time on stream. The peak broadening shown by good catalysts after initial short calcination periods (catalyst 2, Figure 1.3a) is claimed to indicate the presence of defect sites associated with 5+ micro-domains [Nguyen et al, 1996], but it could also indicate low crystallinity. It is proposed that a good catalyst will show peak broadening after initial short activation periods and will resemble catalyst 2 (Figure 1.3a) rather than catalyst 3 (Figure 1.3a). With time on stream the crystallinity increases and the structure approaches that of the equilibrated catalysts of Figures 1.10 and 3.3. It is therefore suggested that the catalyst samples of Figures 3.1 and 3.2 show the correct VPO phases for the production of maleic anhydride. These XRD spectra will approach that of the deactivated commercial catalyst and the equilibrated catalyst of Figure 1.10 with further time on stream.

3.1.1.2. INFRARED

Infrared spectra of the VPO samples PV1, PV1.1, PV1.2 and PV1.5, calcined at T = 400°C for five hours in reaction feed, are shown in Figure 3.4. The peaks at 1247- 1250 cm^{-1} (PO_3), 1136-1140 cm^{-1} ($P_2O_7^{4-}$), 1100 cm^{-1} ($P_2O_7^{4-}$), 1040 cm^{-1} ($P_2O_7^{4-}$), 968-969 cm^{-1} (V=O) and 740-744 cm^{-1} (P-O-P) can be clearly discerned. Especially the peaks assigned to the $P_2O_7^{4-}$ and V=O vibrations seem to indicate the presence of the vanadyl pyrophosphate phase.

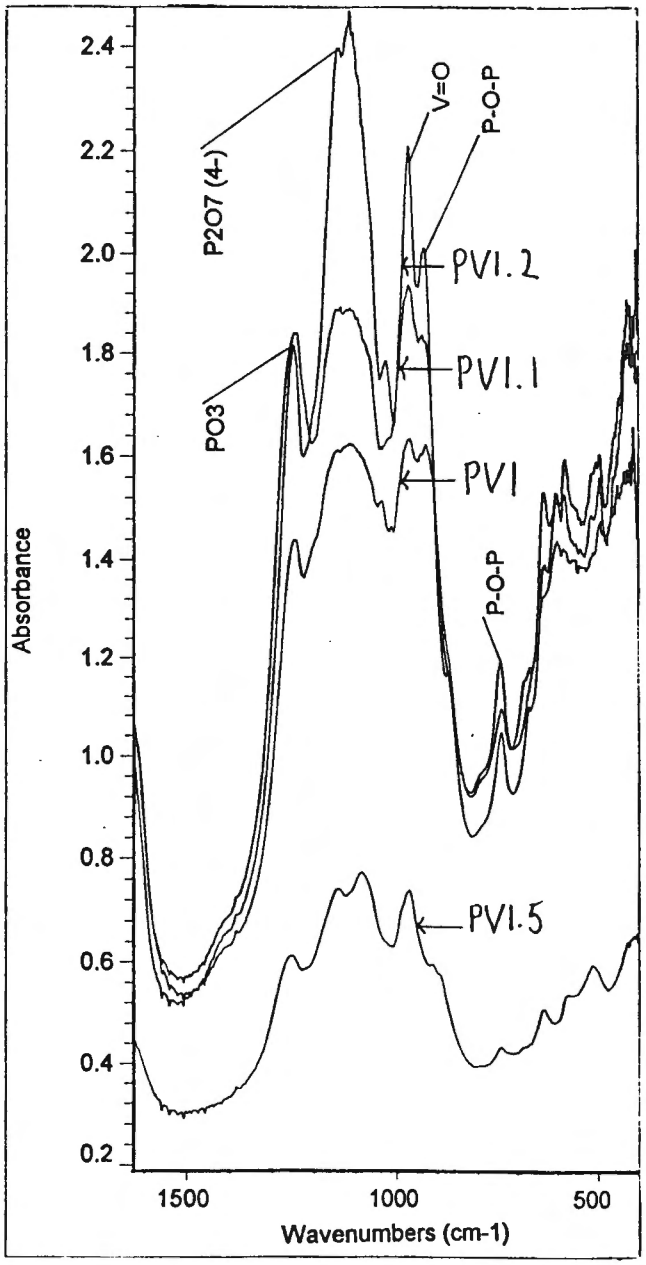

FIGURE 3.4: EFFECT OF P/V RATIO ON INFRARED SPECTRUM OF VPO CATALYST CALCINED FOR 5 HOURS AT 400°C IN $n\text{-}C_4H_{10}/N_2/O_2$ = 1.44 / 78.56 / 20

The strength of the IR absorbances of all peaks increases with increasing P/V ratio up to sample PV1.2, after which it shows a decrease for sample PV1.5. This trend is similar to that of the XRD, which gave maximum peak areas for samples PV1.1 and PV1.2 and lower peak areas for samples PV1 and PV1.5, indicating that phase formation is optimal at P/V ratios during preparation of between 1.1 and 1.2. As seen in section 3.1.1.1, the stabilisation of the V^{4+} phase by excess phosphorus [Poli et al, 1981] is also thought to play a role in the activation scheme $VOHPO_4.0.5H_2O \rightarrow$ amorphous phase $\rightarrow$ $(VO)_2P_2O_7$ of Cavani et al [1994], making the transformation to the pyrophosphate phase more facile at P/V ratios in excess of 1. From the results of XRD peak areas and IR absorbances, it appears that P/V ratios too far in excess of 1 also make this transformation less facile as shown by the lower peak areas and intensities of IR absorbances for sample PV1.5.

TABLE 3.1: IR SPECTRA OF VPO CATALYSTS IN LITERATURE AND OF THE PREPARED SAMPLES (PV1, PV1.1, PV1.2, PV1.5)

	P-O	V-O	P-O-P	V-O-V	V=O	PO_3	$P_2O_7^{4-}$	H_2O in atmosphere
Igarashi et al [1993]			740	796	960	1060-1069, 1244	1132	
Poli et al [1981]					975		1200, 1130, 1100, 1040, 920	
Bhargava et al [1977]	1211, 910	780, 990						
Cavani et al [1984]			935, 920, 740			1215, 1185		1030, 1115
PV1			741		968	1250 1040	1100, 1140, 930	1117
PV1.1			750		970	1247, 1040	1102, 1138, 938	1114
PV1.2			744		968	1247	1101, 1136, 934	1110
PV1.5			740		969	1249	1100, 1140	1120

Table 3.1 compares peak assignments obtained by other investigators with those of the samples PV1, PV1.1, PV1.2 and PV1.5 of Figure 3.4. Examples of infrared spectra by Igarashi et al [1993] and Cavani et al [1984] are given for comparison in Figure 1.12. In Figure 1.12 transmittance is given whereas Figure 3.4 shows absorbance. Therefore one has to compare peaks (absorbance) with valleys (transmittance) when comparing these graphs.
Absorbance = $-\log_{10}$(Transmittance)

The IR spectra of samples PV1, PV1.1, PV1.2 and PV1.5 gave a good correlation with spectra c and d of Igarashi et al [1993] (Figure 1.12a) and spectrum c of Cavani et al [1984] (Figure 1.12b). Cavani et al and Igarashi et al have identified these catalysts as the $(VO)_2P_2O_7$ phase with high surface areas and average valence states of close to 4 as shown in Figures 1.15 and 1.16. Since the IR spectra of samples PV1, PV1.1, PV1.2 and PV1.5 compare so well with spectrum c of Cavani et al (Figure 1.12b) and spectra c and d of Igarashi et al (Figure 1.12a), it is proposed that these samples represent the same phase, i.e. the $(VO)_2P_2O_7$.

3.1.1.3. ELEMENTAL ANALYSIS

Elemental analysis of the precursor $(VOHPO_4).0.5H_2O$, carried out at MINTEK, is given in Table 3.2. Compositional analysis showed a P/V ratio of close to 1 for all samples analysed, with a slight increase in actual P/V ratio with increase in P/V ratio of preparation. Excess phosphorus added during preparation does not seem to be incorporated into the structure and may be filtered off. This agrees with the findings of certain investigators: "For organic preparations in which the solid was filtered, a ca. 10% excess of H_3PO_4 was needed to obtain a given $(P/V)_{BULK}$ ratio." [Cornaglia et al, 1991]. Excess phosphorus has been found to congregate on the surface [Ebner et al, 1993]. A P/V ratio of close to 1 is consistent with the formation of the $VOHPO_4.0.5H_2O$ structure.

TABLE 3.2: PARTICLE CHARACTERISATION

REDUCING AGENT	organic	organic	organic
P/V RATIO IN PREPARATION	1	1.1	1.15
ELEMENTAL ANALYSIS			
V, wt %	26.75	26.55	25.2
P, wt %	16.2	16.45	15.7
Balance, wt%	57.05	57	59.1
P/V	0.996	1.01	1.02
BET SURFACE AREA	-	30 m^2/g	-
MEAN PARTICLE DIAMETER	-	10.18 μm	-

A qualitative compositional analysis was obtained with EDS spectra in order to check for impurities. Impurities can adversely affect selectivity since they concentrate on the catalyst surface and a small percentage may have a significant effect on selectivity. The EDS spectrum is shown in Figure 3.5. The presence of V, P and small quantities of carbon were shown. The elemental analysis therefore revealed the absence of impurities which might congregate on the catalyst surface and reduce selectivity. The presence of carbon, due to the formation of alcoholates entrapped in the structure, is normal for a preparation method where an organic reducing agent is used [Nguyen et al, 1996].

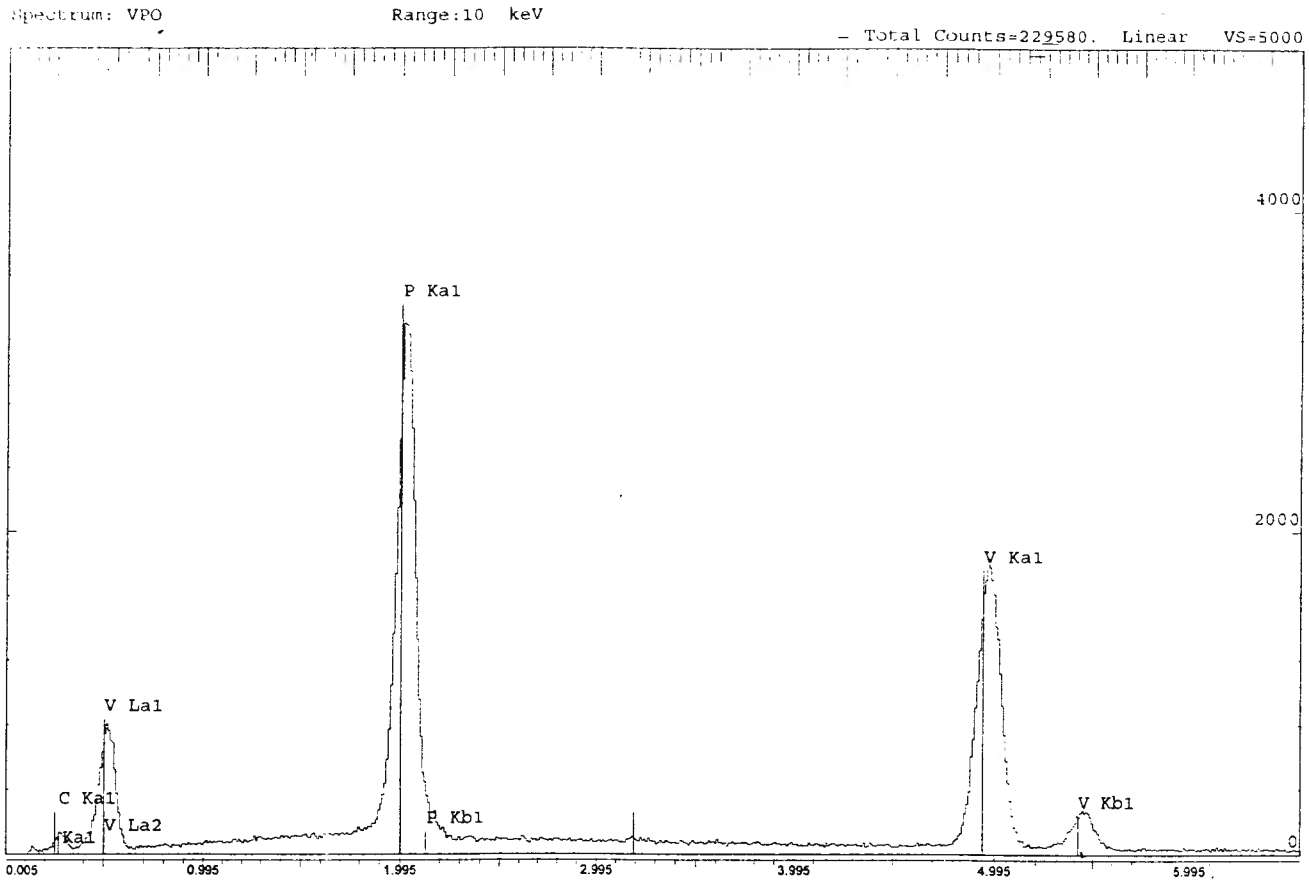

FIGURE 3.5: EDS SPECTRUM OF THE VPO PRECURSOR ($(VOHPO_4).0.5H_2O$)

3.1.1.4. PARTICLE CHARACTERISATION

In Table 3.2, the BET surface area was 30 m^2/g as opposed to approximately 10 m^2/g for the precursor of Cavani et al [1984] of Figure 1.15. The particle size should be a function of the precipitation conditions during preparation which seems to indicate faster precipitation than Cavani et al. This could be as a result of different stirring speeds.

Particle sizes obtained (Malvern: 5 μm < Particle size < 20 μm, mean dp = 10.18 μm) were lower than those obtained in literature (50 μm < Particle size < 150 μm). Particle size is also a function of the precipitation conditions. The particle size distribution is given in Appendix D.

The SEM micrographs shown in Figure 3.6 correlated well with the rose-like structures obtained by Burnett [1987], which indicate good surface area and accessibility. The rose-like structure was obtained by several investigators for the catalyst formed when using organic reducing agents.

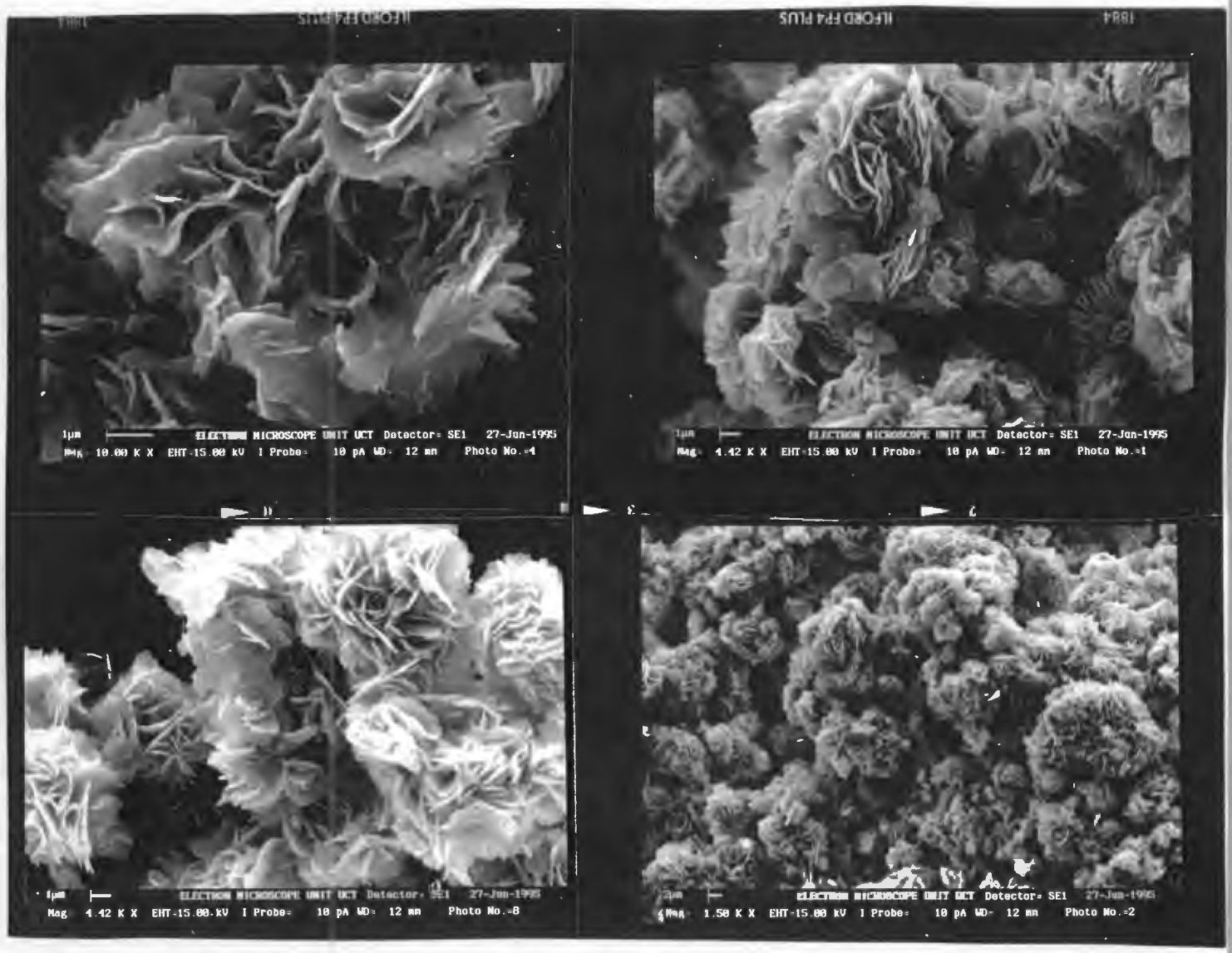

FIGURE 3.6: SCANNING ELECTRON MICROGRAPHS OF VPO CATALYST PV1.1 CALCINED FOR 3 HOURS AT T = 380°C IN AIR

3.1.2. REACTION STUDIES

3.1.2.1. VPO CATALYST IN CARTRIDGE-HEATED REACTOR

Conversions of between 0.5% and 85% were obtained for the oxidation of n-butane over the VPO catalyst. However, only CO and CO_2 were detected and no maleic anhydride. The presence of total oxidation products only, was consistent over the range of reaction conditions studied (given in section 2.3.4.1). Carbon balances were above 95% and temperatures of the outlet lines were similar to those in literature. In literature, online GC FID analysis was used, with outlet line temperatures of above 180°C.

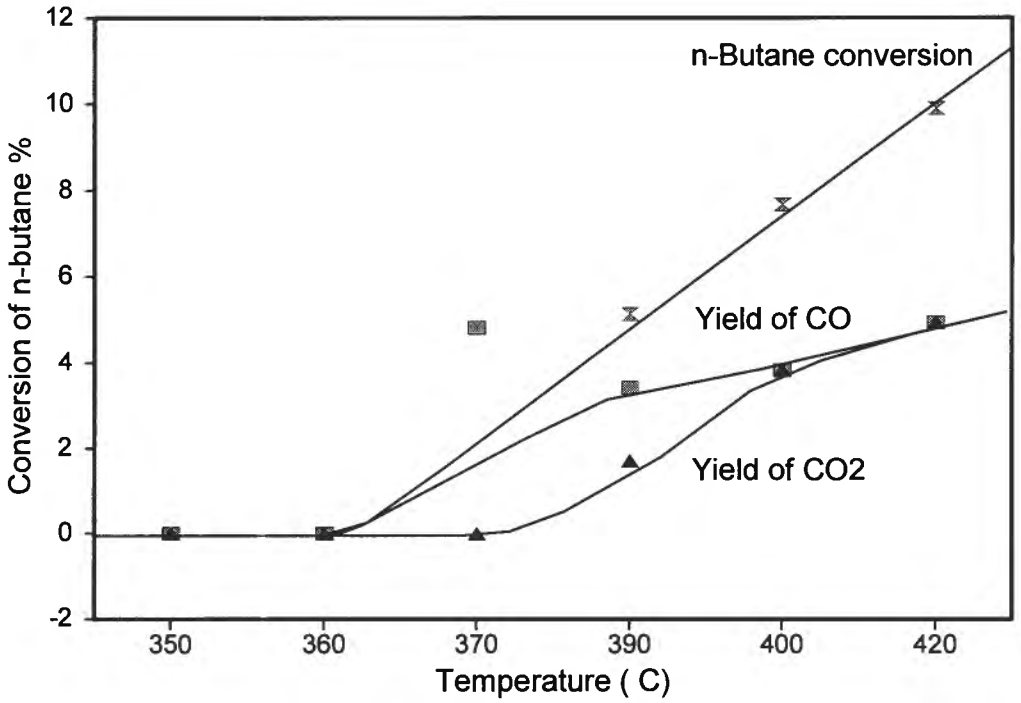

FIGURE 3.7: EFFECT OF REACTION TEMPERATURE

Feed:	**n-C_4/N_2/O_2 = 1.44/78.56/20**
Total flowrate:	**100 ml/min STP**
Mass of catalyst:	**0.25 g VPO, 3 g sand**
P/V ratio:	**1.15**
Calcination:	**4 hours in N_2 at T = 415°C**

Figure 3.7 shows the effect of reaction temperature on conversion and yields. While total n-butane conversion increased with reaction temperature, a higher selectivity of CO was shown at lower temperatures. The selectivity of CO_2 increased with temperature while the selectivity of CO decreased.

Figure 3.8 shows the effect of oxygen partial pressure on the conversion of n-butane and the yields of products. Little change is shown in the conversion and yields of CO and CO_2 with changing oxygen partial pressure. At the lowest oxygen partial pressures studied, however, the flowrates of oxygen are still at least about 10 times higher than that of n-butane. It is therefore suggested that the effect of high n-butane concentrations be studied although this will be difficult due to explosion limits.

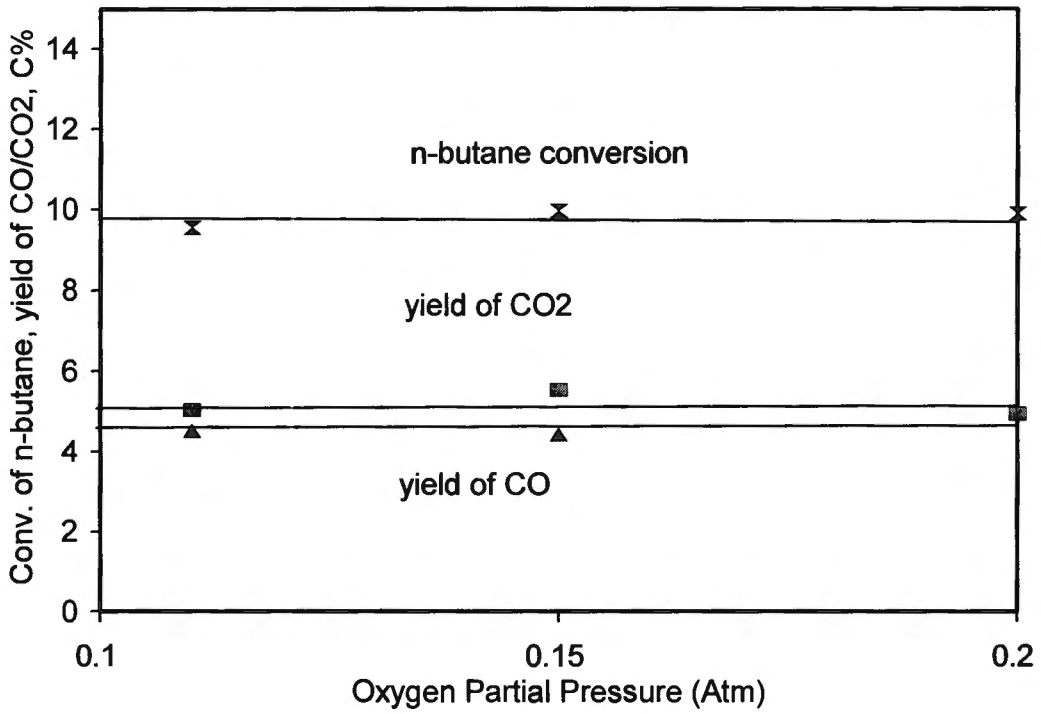

FIGURE 3.8: EFFECT OF OXYGEN PARTIAL PRESSURE

Flows (STP):	**n-C_4: 1.44 ml/min, O_2 + N_2 : 98.56 ml/min**
Mass of catalyst:	**0.25 g VPO, 3 g sand**
P/V ratio:	**1.15**
Calcination:	**4 hours in N_2 at T = 415°C**

3.1.2.2. VPO CATALYST IN OVEN-HEATED REACTOR

Figures 3.9 to 3.11 show the results of the VPO catalyst tested in the oven-heated reactor as a function of changing reaction temperature and space velocity. No maleic anhydride was detected - only CO and CO_2. At lower temperatures, the selectivity of CO was higher than that of CO_2 and at higher temperatures, the selectivity of CO_2 was higher. Yields of CO and CO_2 increased with increasing contact time and increasing temperature.

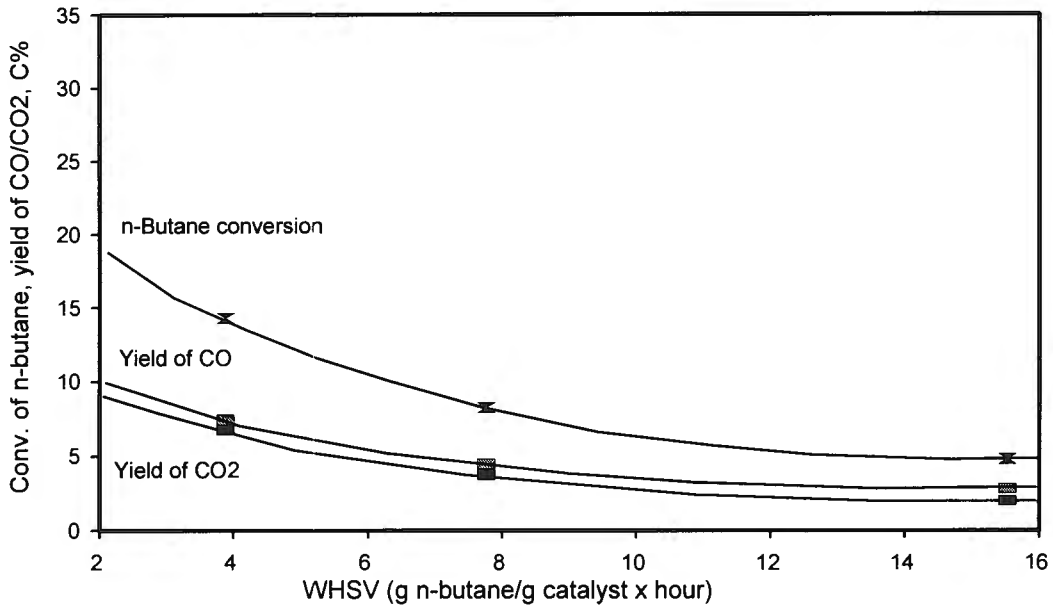

FIGURE 3.9: VPO CATALYST IN OVEN-HEATED REACTOR, T = 380°C

Feed comp.: **n-$C_4/N_2/O_2$ = 1.44/78.56/20**
Mass of catalyst: **1 g VPO, 5 g sand**
P/V ratio: **1.2**
Calcination: **4 hours in reaction feed at T = 400°C**

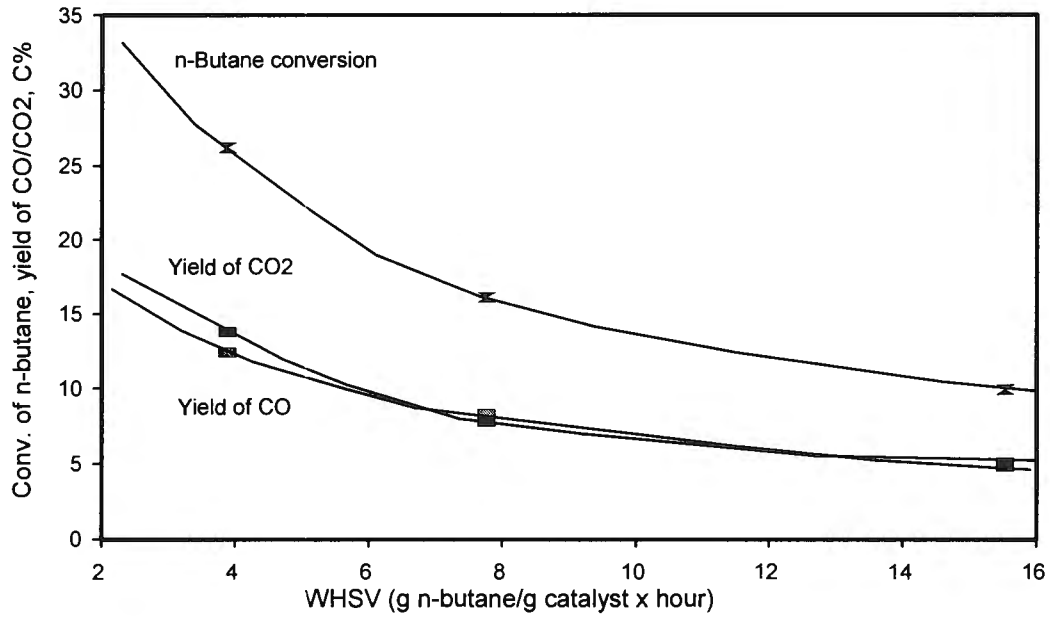

FIGURE 3.10: VPO CATALYST IN OVEN-HEATED REACTOR, T = 400°C

Feed comp.: **n-$C_4/N_2/O_2$ = 1.44 /78.56/20**
Mass of catalyst: **1 g VPO, 5 g sand**
P/V ratio: **1.2**
Calcination: **4 hours in reaction feed at T = 400°C**

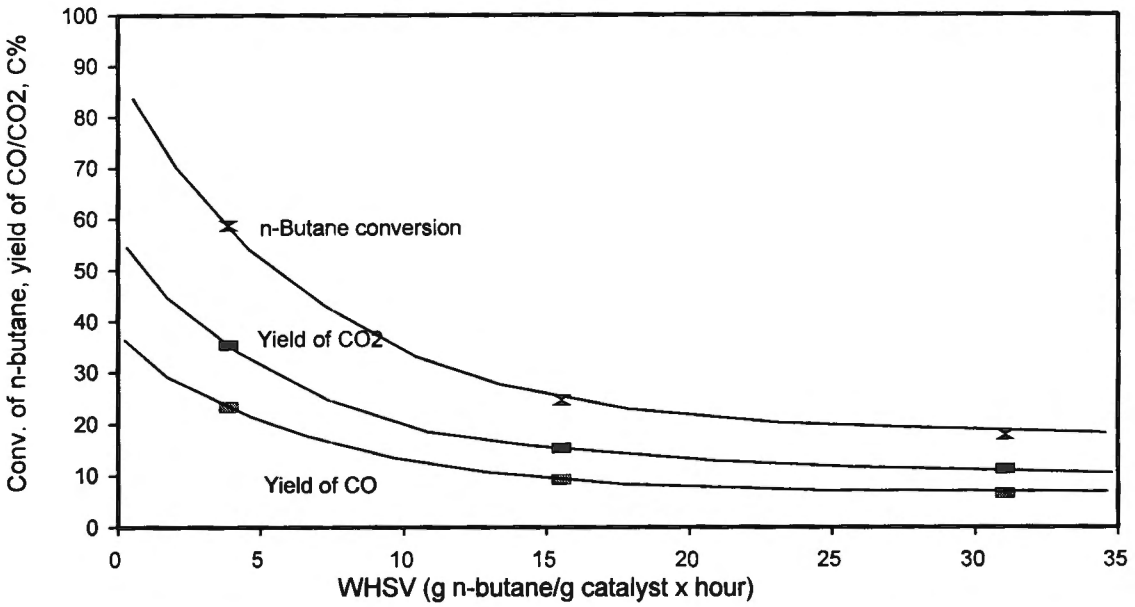

FIGURE 3.11: VPO CATALYST IN OVEN-HEATED REACTOR, T = 430°C

Feed comp.: **n-$C_4/N_2/O_2$ = 1.44/78.56/20**
Mass of catalyst: **1 g VPO, 5 g sand**
P/V ratio: **1.2**
Calcination: **4 hours in reaction feed at T = 400°C**

3.1.2.3. EXPERIMENTAL COMMERCIAL CATALYST

An experimental commercial catalyst was also tested and the effect of space velocity and oxygen partial pressure was studied. Reaction conditions, conversions, selectivities and yields are given in Appendix A. Conversions ranged from 11.7% to 22.9%. No maleic anhydride, only total oxidation products were observed. Selectivities of total oxidation products showed similar trends to the other VPO catalysts above - increased oxygen partial pressures increased the selectivity to CO_2. Higher residence times gave higher yields of CO_2 and CO and higher selectivities to CO_2.

3.1.2.4. DEACTIVATED COMMERCIAL CATALYST

Figures 3.12 to 3.14 show the results of the deactivated commercial catalyst tested in the oven-heated reactor as a function of changing reaction temperature and space velocity. Maleic anhydride yields of up to 6% were reported. At all temperatures, yields of maleic anhydride went through a maximum at a space velocity of around 8 g/gh. At higher space velocities, the lower contact times resulted in lower conversions and lower yields of maleic anhydride and total oxidation products. At low space velocities, higher contact times resulted in an increase in selectivities of total oxidation products at the expense of maleic anhydride. The low yields of maleic anhydride could be the result of the deactivated state of the catalyst. Alternatively, the actual selectivities of maleic anhydride could be higher, and a percentage of the maleic anhydride formed may oxidise further in the post-heat zone of the reactor.

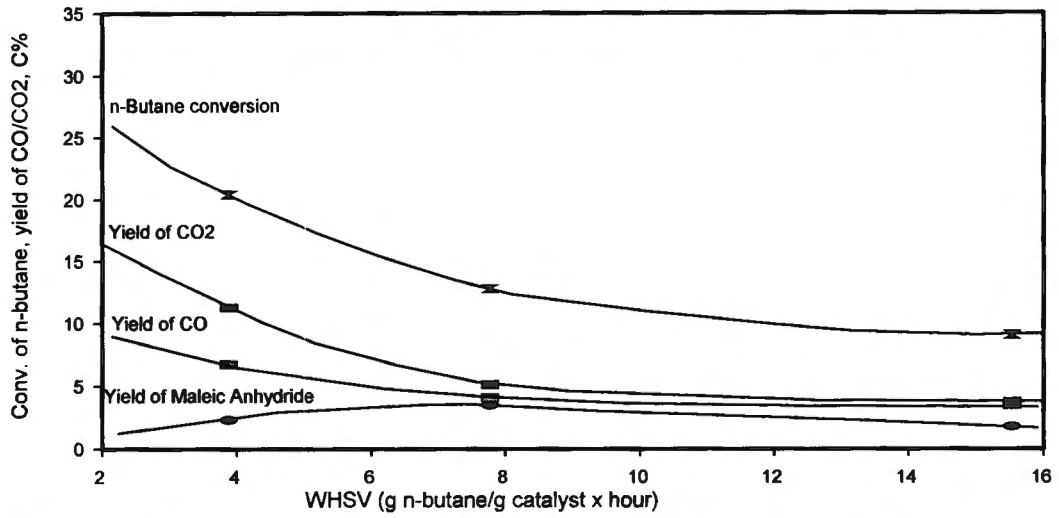

FIGURE 3.12: DEACTIVATED COMMERCIAL CATALYST: T = 380°C

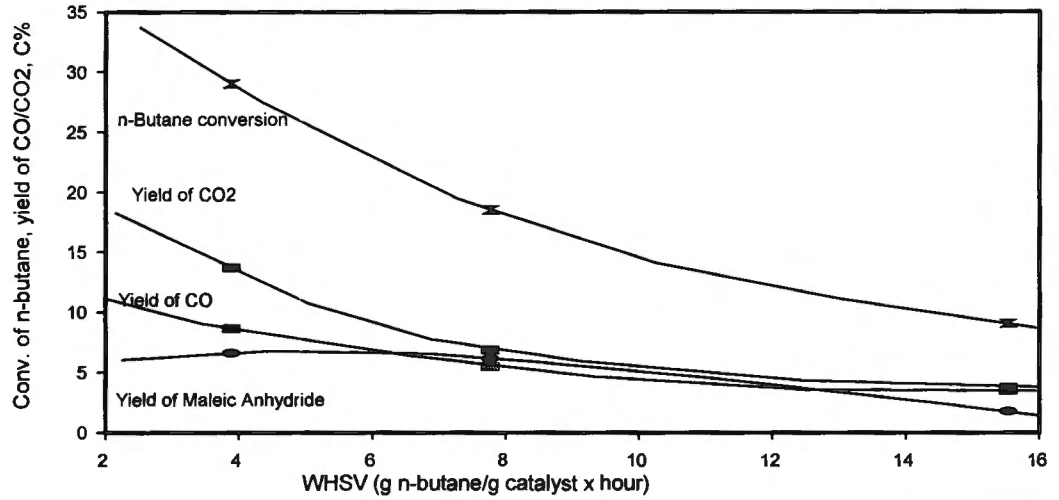

FIGURE 3.13: DEACTIVATED COMMERCIAL CATALYST: T = 400°C

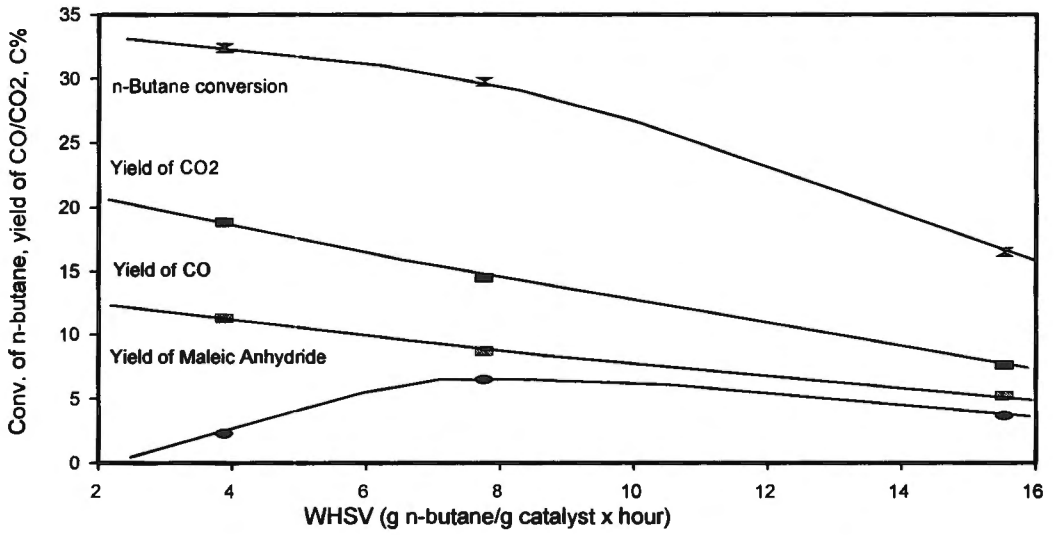

FIGURE 3.14: DEACTIVATED COMMERCIAL CATALYST: T = 420°C

3.1.2.5. EFFECT OF TIME ON STREAM

Figure 3.15 shows the results obtained for the conversion of n-butane over a VPO catalyst prepared in organic medium with a P/V ratio of 1.1. Over the 40 hour reaction period, there is little change in total conversion and yields of CO and CO_2.

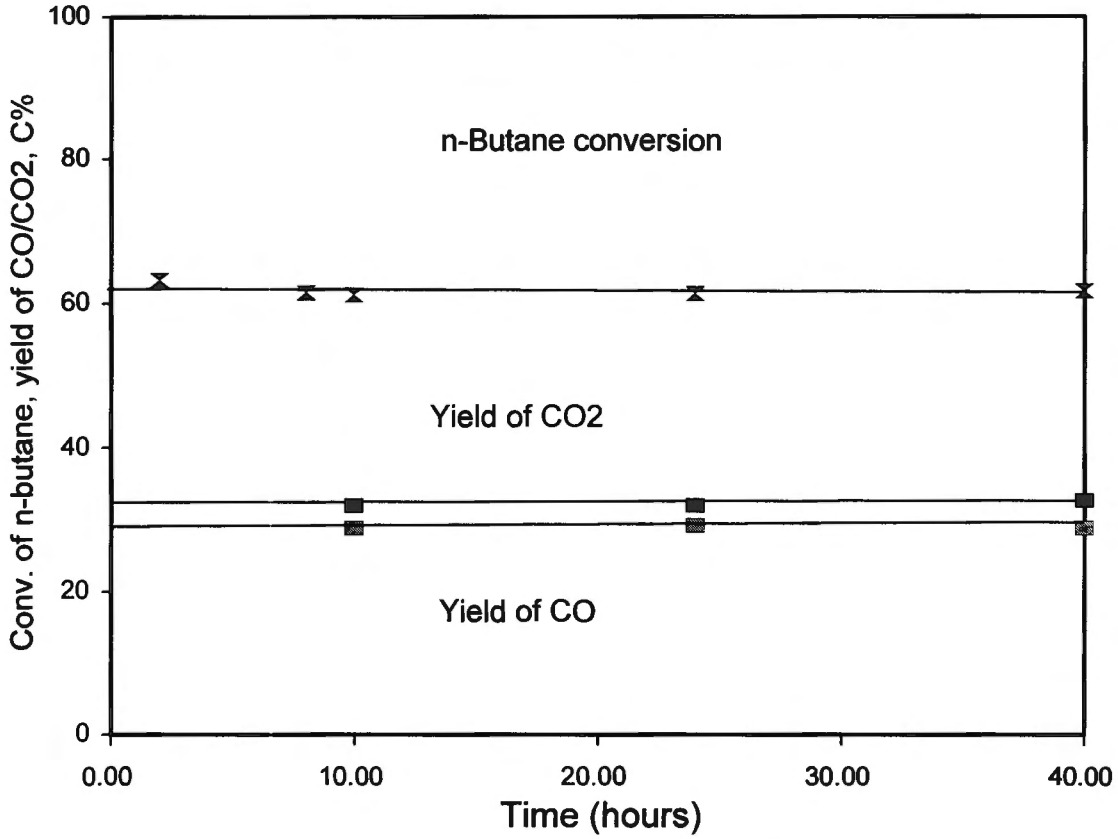

FIGURE 3.15: EFFECT OF TIME ON STREAM ON VPO CATALYST

Temperature:	**400°C**
Feed:	**n-C_4/N_2/O_2 = 1.44/78.56/20**
Total flowrate:	**100 ml/min STP**
Mass of catalyst:	**1 g VPO, 3 g sand**
P/V ratio:	**1.1**
Calcination:	**3 hours in air at T = 400°C**

Although authors such as Abon et al [1995] (Figure 1.11) observed yields of maleic anhydride after a few minutes on stream, others, for example Kubias et al [1992], mention long activation periods. During the activation period the selectivity and yield of maleic anhydride increase. Because maleic anhydride was not observed after short periods on stream, longer activation periods were studied as given in Figure 3.16.

The conversion of n-butane and the yields of products over the catalyst of Abon et al [1995] (Figure 1.11) reach a steady state after about 80 hours on stream. It is therefore suggested that the VPO catalyst tested in this work should not show any changes in product yields after this period. If maleic anhydride is not observed after about 80 hours, longer times on stream will not result in its detection.

A VPO catalyst was tested for a period of 190 hours on stream and the results are given in Figure 3.16. As with the other VPO runs, only the products CO and CO_2 were observed. A conversion of n-butane of about 12% and a selectivity of about 44% to CO and about 55% to CO_2 were obtained. A carbon balance of more than 97% was obtained. The conversion and yields showed little change over the whole reaction period. The time on stream therefore did not play a role.

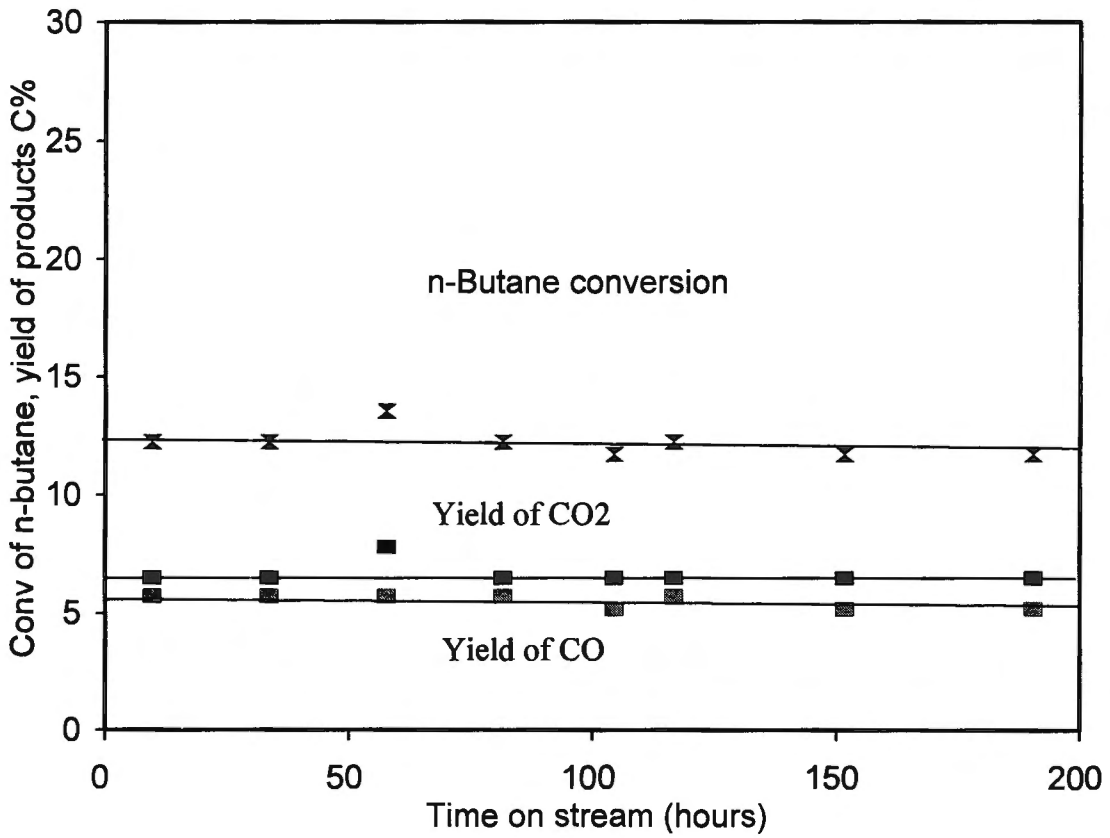

FIGURE 3.16: EFFECT OF TIME ON STREAM OVER THE EXPERIMENTAL COMMERCIAL CATALYST

Temperature: **390°C**
Feed: **n-C_4/N_2/O_2 = 1.44/78.56/20**
Total flowrate: **30 ml/min STP**
Mass of catalyst: **0.3 g VPO, 1 g sand**

3.2. CONVERSION OF ISOBUTANE OVER THE HETEROPOLYACID, $K(NH_4)_2PMo_{12}O_{40}$

3.2.1. CHARACTERISATION

3.2.1.1. INFRARED SPECTRA

Figure 3.17 shows the IR spectrum of the $K(NH_4)_2PMo_{12}O_{40}$ catalyst. The catalyst was calcined in O_2 for 1 hour, followed by the introduction of reaction feed (17% isobutane, 30% oxygen, bal. N_2). The catalyst was then kept on stream for 1 hour, 1.5 hours, 3 hours and 5 hours respectively.

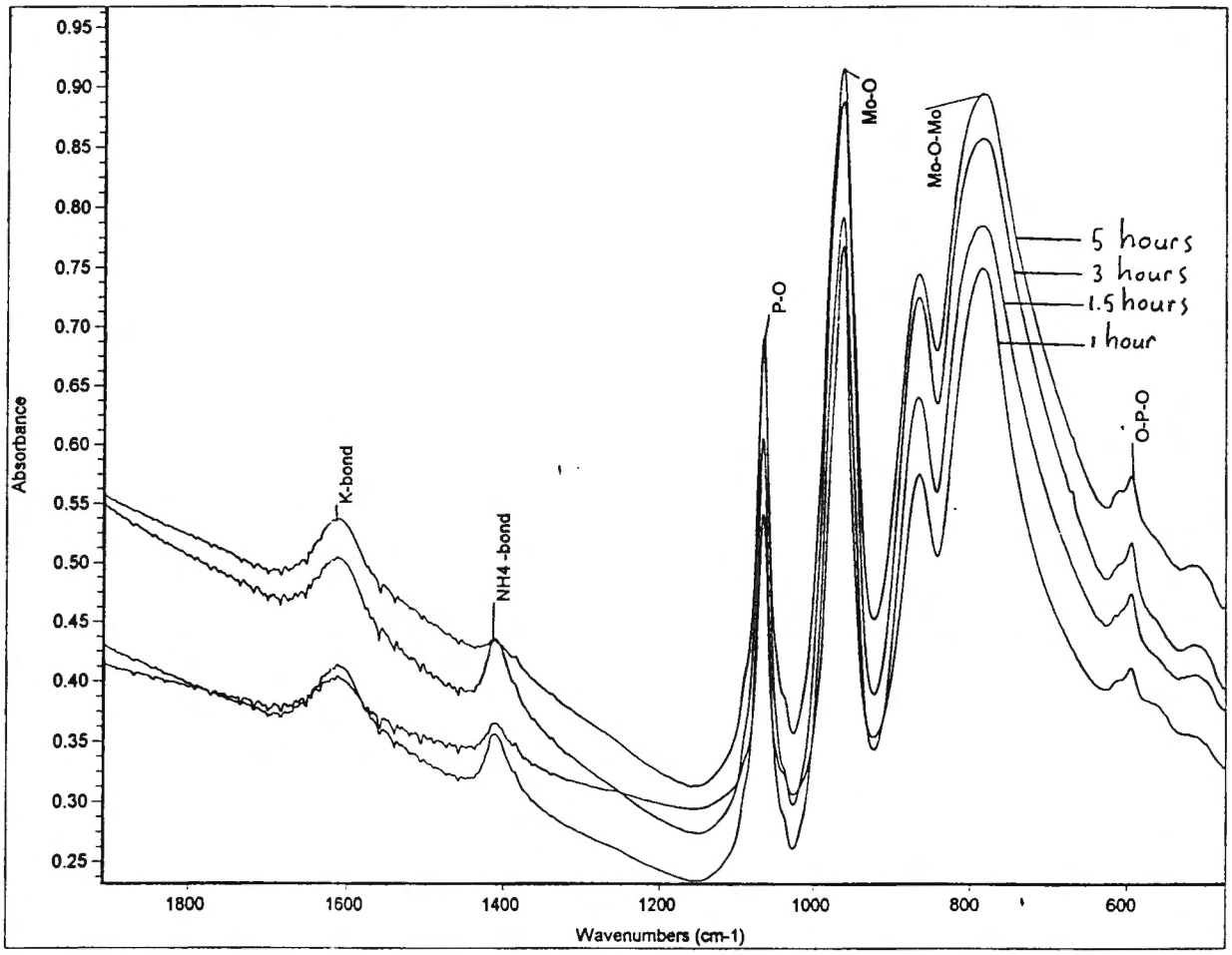

FIGURE 3.17: EFFECT OF TIME ON STREAM DURING EQUILIBRATION ON THE IR SPECTRUM OF $K(NH_4)_2PMo_{12}O_{40}$

All spectra were found to have vibrational bands at 1070, 965, 870, 790 and 590cm^{-1}, corresponding to the P-O, Mo=O, Mo-O-Mo and P-O vibrations of the Keggin structure. The intensity of all absorbance peaks was found to increase with time on stream. All peaks were found to increase by the same degree and normalisation of the different absorbance peaks showed that no peaks increased in intensity relative to any others. It is therefore suggested that the catalyst is not oxidised or reduced during equilibration but that the Keggin structure as a whole develops out of an amorphous phase.

3.2.2. REACTION STUDIES

Reaction runs for the partial oxidation of isobutane to methacrylic acid and byproducts were carried out as a function of time on stream to determine the equilibration time of the catalyst. A period of activation took place, which varied from 3 hours for a space velocity of 1.98 g/g.h, to 7 hours for a space velocity of 0.792 g/g.h. GC mass spectra identified the products (given in order of retention time with their boiling points): ethyl methyl ether (10.8°C), propanal (48-49°C), methacrolein (69°C) and methacrylic acid (163°C). A product of higher atomic mass (106) also formed on the unequilibrated catalyst for which the mass spectrum corresponds to dimethyl benzene, 5-isopropylidene-1,3-cyclopentadiene or 3-methylene-1-vinyl-cyclopentane. Although the highest mass ion for this compound is a small peak at 107, no compounds with mass 107 corresponded to the spectrum. It is therefore suggested that the compound has a structure similar to one of the abovementioned compounds of mass 106. Mass spectra of the different products are given in Appendix C. An example of the GC integrator printout with peak assignments is given in Figure 3.18.

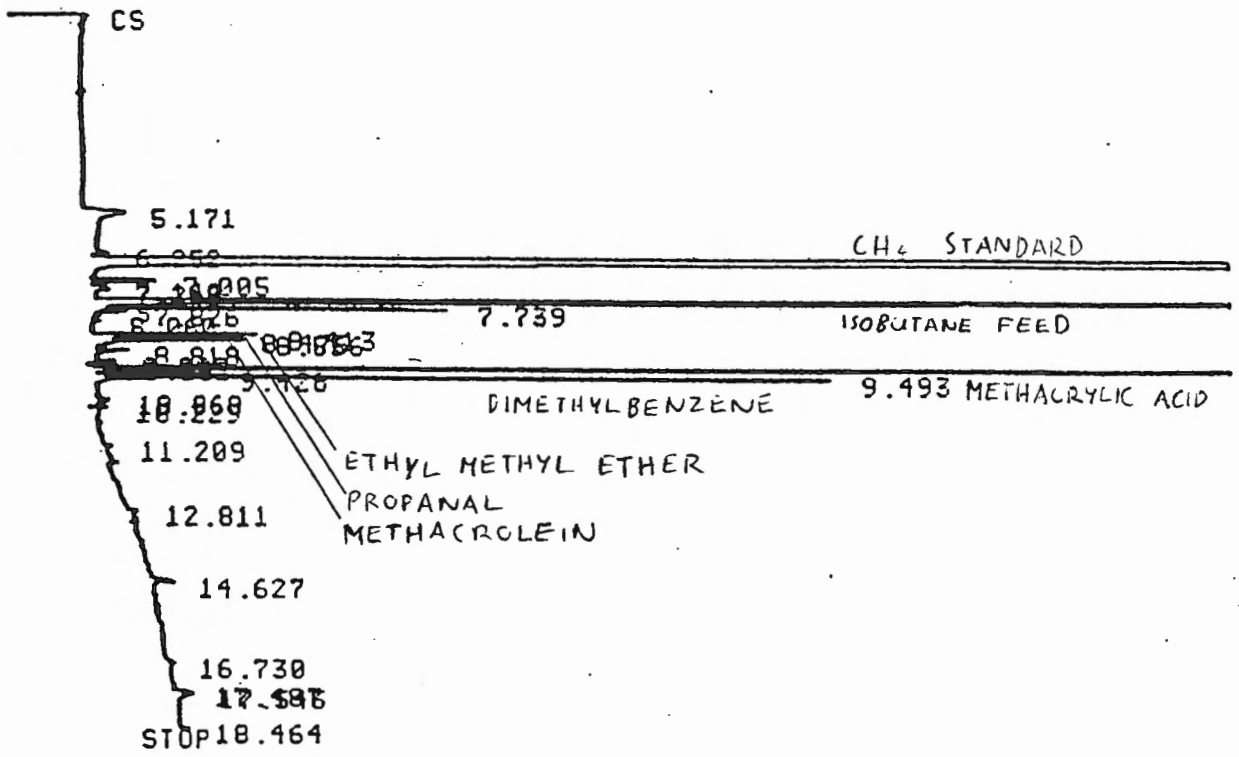

FIGURE 3.18: GAS CHROMATOGRAPH INTEGRATOR PRINTOUT SHOWING DIFFERENT ORGANIC PRODUCTS FOR THE PARTIAL OXIDATION OF ISOBUTANE AT T = 380°C

Figure 3.19 shows the yields of total oxidation products and the sum of organics as a function of time on stream at a fixed space velocity. It shows an activation period of about six hours, during which the yields of total oxidation products drop off until a steady state is reached. It is suggested that the progressive increase in crystallinity with the development of the Keggin structure during equilibration, as mentioned in section 3.2.1., results in a decrease in selectivity towards total oxidation products. At steady state, the crystallisation of the Keggin structure out of an amorphous precursor is complete and selectivities do not change with further time on stream. The high unsteady state isobutane conversion (Figure 3.21) and yields of total oxidation products (Figure 3.19) compared with steady state values, seem to indicate that total oxidation on the unequilibrated catalyst takes place on parallel sites on the amorphous precursor phase. It is later shown that total oxidation products are secondary products on the equilibrated catalyst.

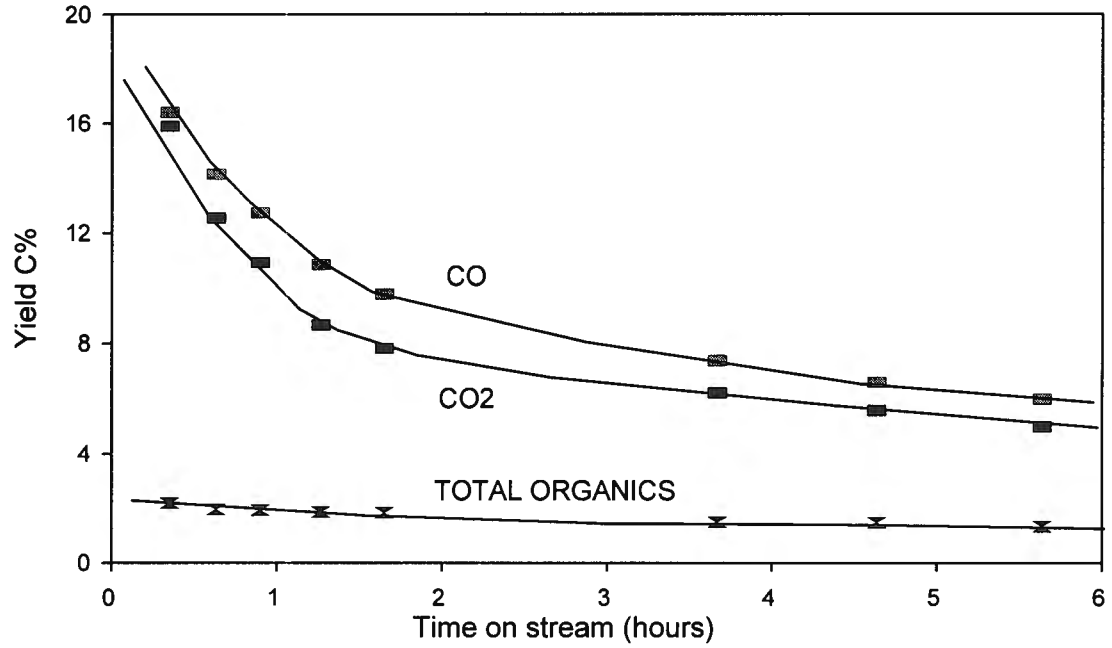

FIGURE 3.19: YIELD OF TOTAL OXIDATION PRODUCTS VERSUS TIME ON STREAM

Temp:	**380°C**
Space velocity:	**0.99 g/gh**
Feed composition:	**i-$C_4H_{10}/O_2/N_2$ = 17/30/53**
Catalyst:	**0.3 g $K(NH_4)_2PMo_{12}O_{40}/FeO_{1.5}$ + 1 g sand**

Figure 3.20 shows the yields of organic products as a function of time on stream on the unequilibrated catalyst. The yield of methacrylic acid increases to a steady state value during equilibration and this is thought to be the result of an increase in the percentage of the catalyst mass which has the Keggin structure. After equilibration, the percentage of the solid containing the Keggin structure does not increase further. Whereas the yield of methacrylic acid shows an increase of more than 50% during the activation period, yields of methacrolein and propanal remain more or less constant. Yields of ethyl methyl ether and the higher atomic mass product, which is thought to be dimethyl benzene, decrease to zero with time on stream.

Because the relative absorbance intensities of different bonds of the Keggin structure do not change during activation, there is no change in oxidation state in the Keggin crystal to account for the changes in the yields of different organic products. However, it is possible that the amorphous phase, out of which the Keggin structure crystallises, interacts electronically with the reaction sites of the Keggin species, especially at the interface of crystalline and non-crystalline material, resulting in a change in environment of the active sites. Because the organic products are thought to form by parallel routes, as is later shown in the space velocity studies of Figures 3.25, 3.26 and 3.27, the change in environment of these sites due to interaction with the amorphous precursor will affect the mechanisms of the formation of each product differently. The interaction will decrease with time on stream.

Formation of total oxidation products, as well as dimethylbenzene and ethyl methyl ether, may also take place on the amorphous phase, but yields of these unwanted byproducts will decrease with increased crystallinity. Methacrylic acid, methacrolein and propanal form on the crystalline catalyst phase as these products are still present on the equilibrated catalyst.

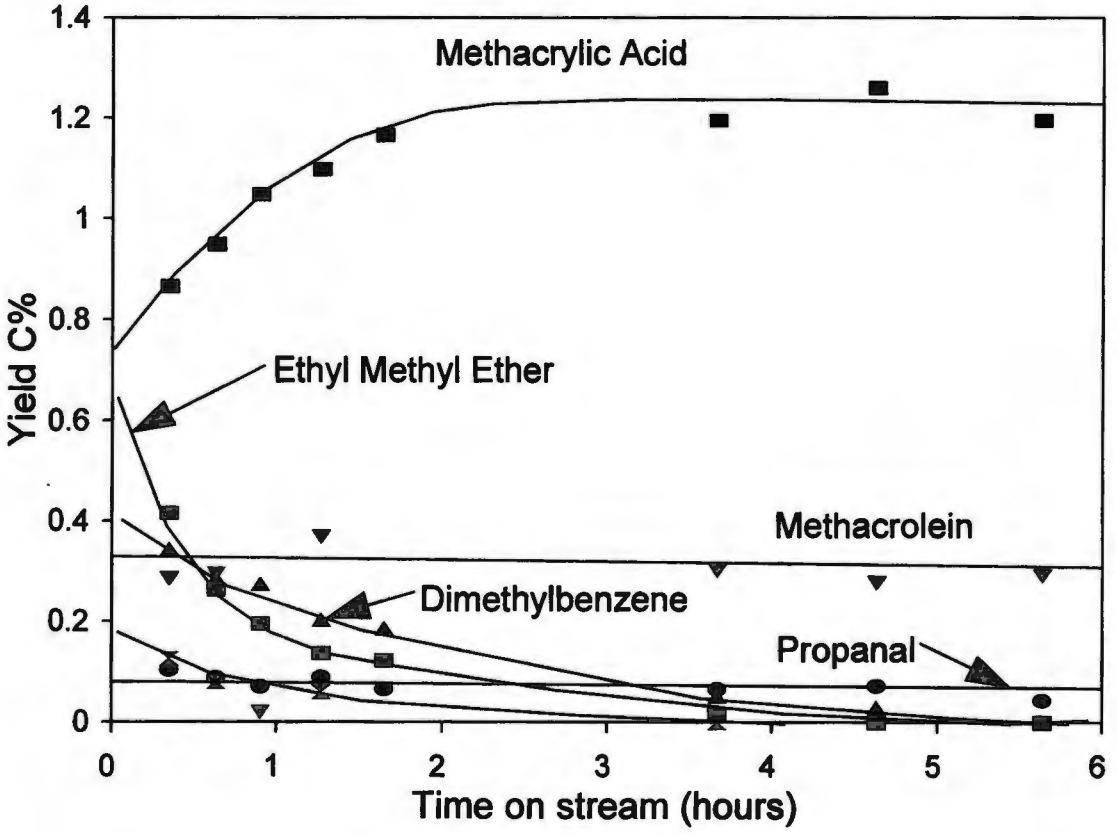

FIGURE 3.20: YIELD OF ORGANIC PRODUCTS VERSUS TIME ON STREAM

Temp:	**380°C**
Space velocity:	**0.99 g/gh**
Feed composition:	**i-$C_4H_{10}/O_2/N_2$ = 17/30/53**
Catalyst:	**0.3 g $K(NH_4)_2PMo_{12}O_{40}$ / $FeO_{1.5}$ + 1 g sand**

Figure 3.21 shows the total isobutane conversion versus time on stream for a range of space velocities. Equilibration times decrease with increasing space velocity, and this is thought to be the the result of an increased reaction rate, measured in gmols of isobutane/gcatalyst.hour. Higher space velocities give lower steady state conversions, due to shorter contact times with the catalyst.

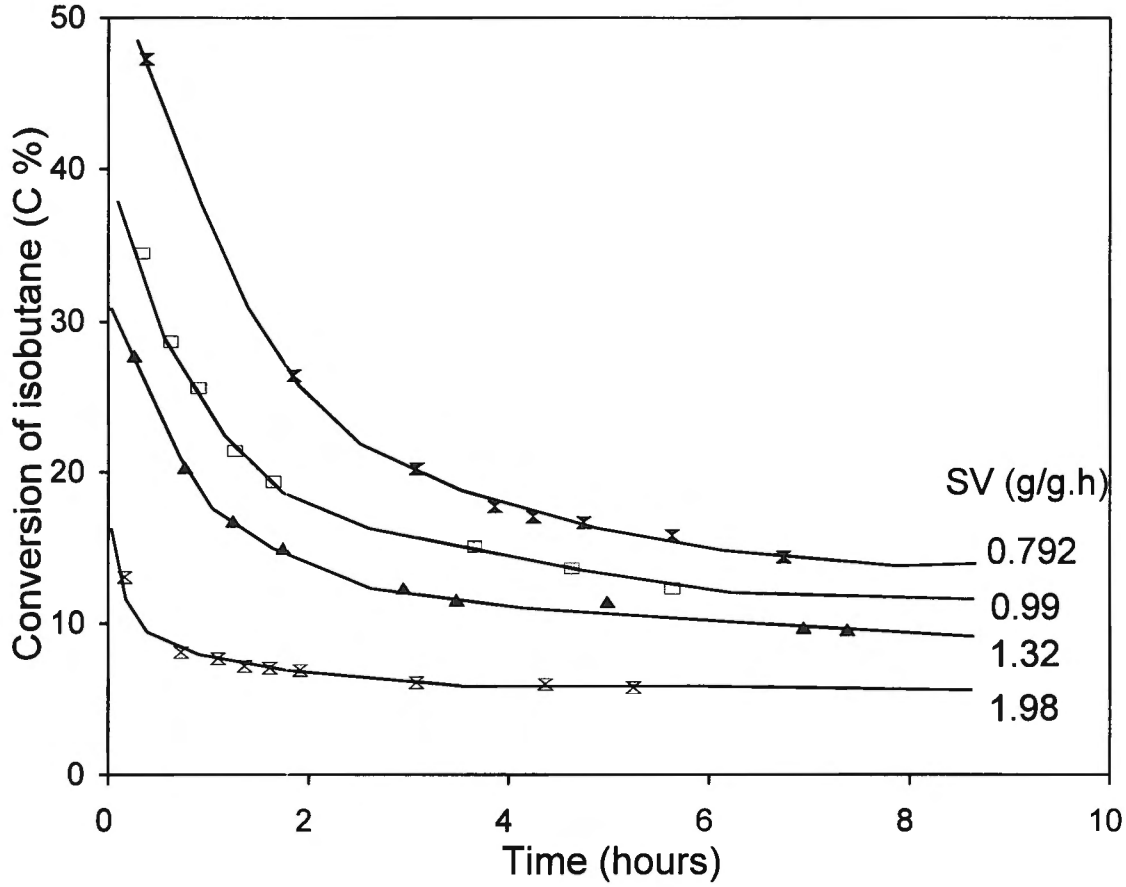

FIGURE 3.21: TOTAL ISOBUTANE CONVERSION VS TIME ON STREAM VS SPACE VELOCITY

Temp:	**380°C**
Feed composition:	**i-$C_4H_{10}/O_2/N_2$ = 17/30/53**
Catalyst:	**0.3 g $K(NH_4)_2PMo_{12}O_{40}/FeO_{1.5}$ + 1 g sand**

Figure 3.22 shows the yield of methacrylic acid as a function of space velocity and equilibration time. The steady state yield of methacrylic acid shows a slight variation with changing space velocity, although the small range of space velocities studied makes this trend difficult to see. When a wider range of space velocities is studied (Figures 3.25, 3.26, 3.27), the variation in steady state yield as a function of space velocity is more clearly shown.

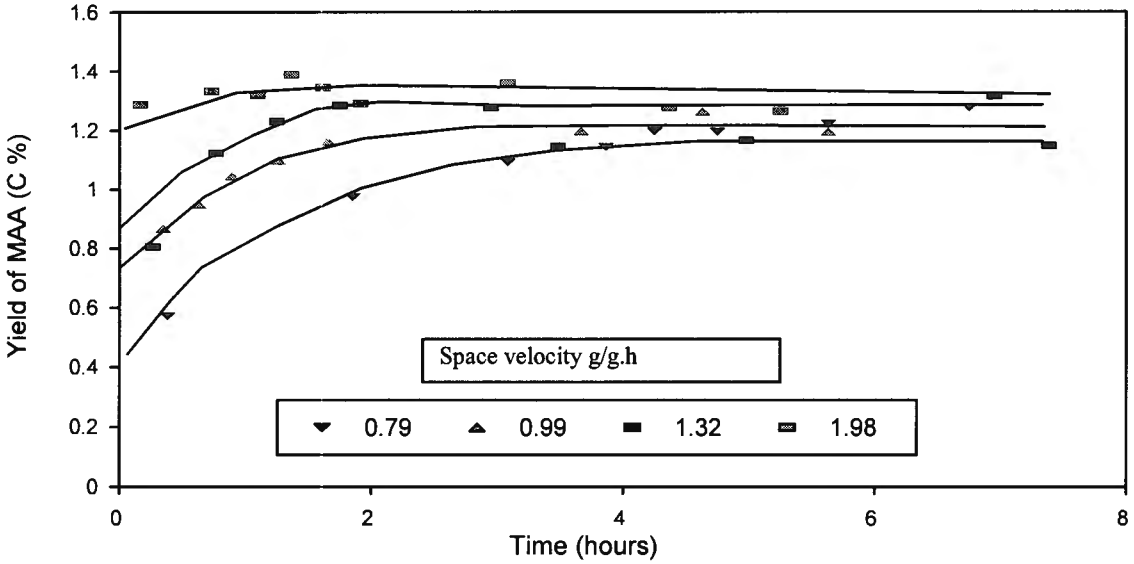

FIGURE 3.22: YIELD OF METHACRYLIC ACID VS TIME ON STREAM VS SPACE VELOCITY

Temp: **380°C**

Feed composition: **i-$C_4H_{10}/O_2/N_2$ = 17/30/53**

Catalyst: **0.3 g $K(NH_4)_2PMo_{12}O_{40}/FeO_{1.5}$ + 1 g sand**

Figures 3.23 and 3.24 show the yields of total oxidation products as a function of time on stream. Steady state yields of total oxidation products are a function of space velocity. The change of up to 50% in the yields of total oxidation products during equilibration suggests that CO and CO_2 form on parallel sites on the amorphous catalyst phase of the unequilibrated catalyst.

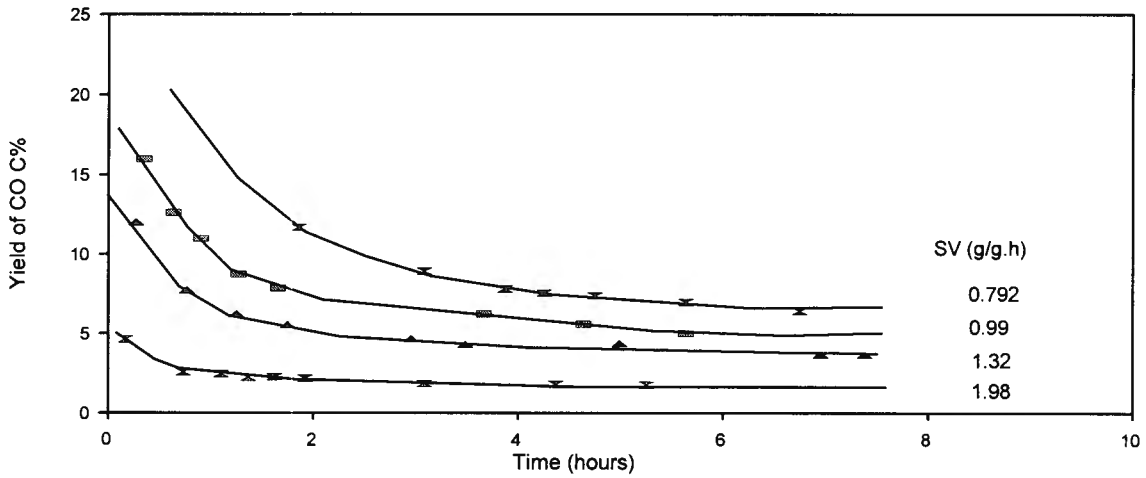

FIGURE 3.23: YIELD OF CO VS TIME ON STREAM VS SPACE VELOCITY

Temp: **380°C**

Feed composition: **i-$C_4H_{10}/O_2/N_2$ = 17/30/53**

Catalyst: **0.3 g $K(NH_4)_2PMo_{12}O_{40}$ / $FeO_{1.5}$ + 1 g sand**

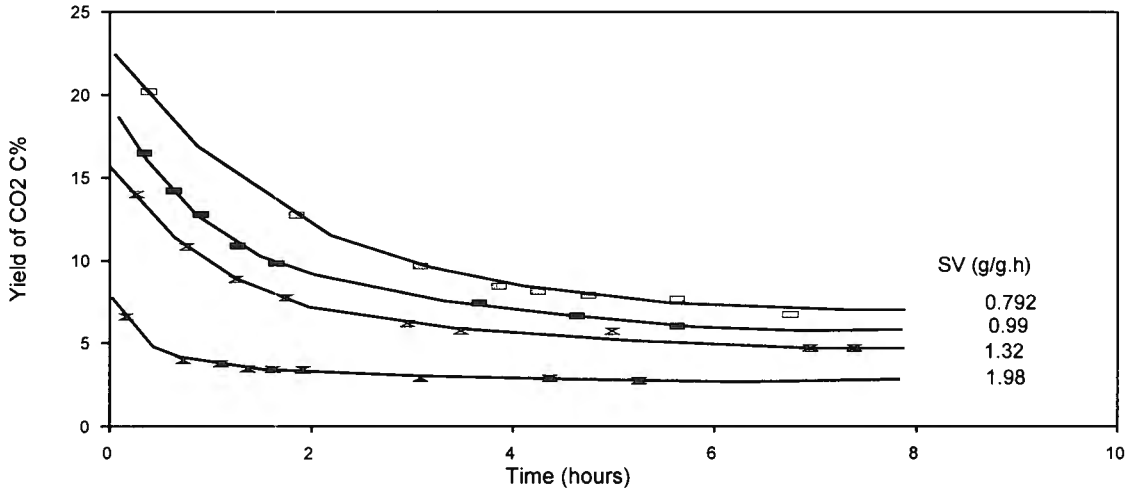

FIGURE 3.24: YIELD OF CO_2 VS TIME ON STREAM VS SPACE VELOCITY

Temp: 380°C
Feed composition: i-$C_4H_{10}/O_2/N_2$ = 17/30/53
Catalyst: 0.3 g $K(NH_4)_2PMo_{12}O_{40}/FeO_{1.5}$ + 1 g sand

Figures 3.25 and 3.26 show the effect of changing space velocity on the selectivities of methacrylic acid and total oxidation products. Selectivities of all organic products tend to a finite limit as space time tends to zero, indicating primary products. Selectivities of CO and CO_2 tend to zero as space time tends to zero, indicating secondary products. The trend is the same at both temperatures studied. It is therefore suggested that organic products form along parallel paths and total oxidation products along serial paths, except during activation, when it forms along parallel (on the amorphous precursor phase) and serial paths (on the Keggin structure).

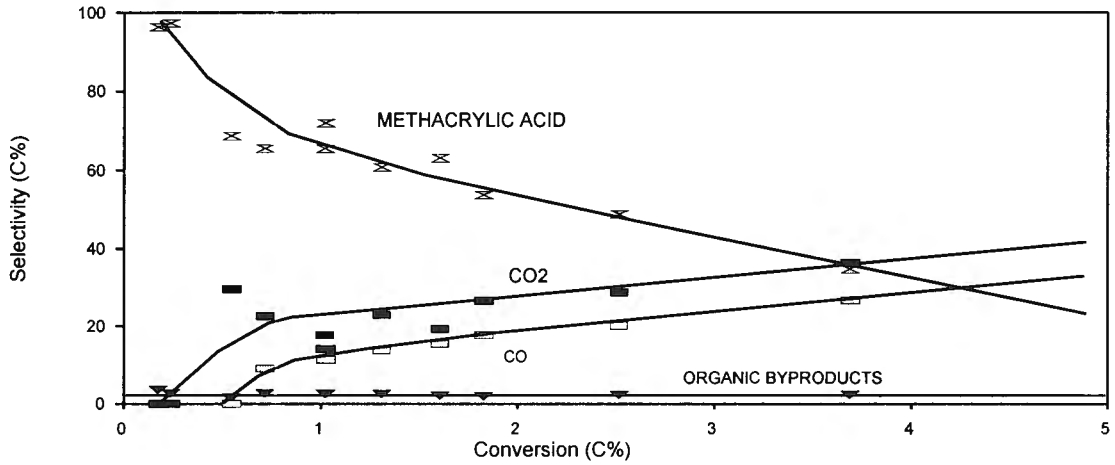

FIGURE 3.25: SELECTIVITY VS CONVERSION AS A FUNCTION OF SPACE VELOCITY AT T = 380°C

Feed composition: i-$C_4H_{10}/O_2/N_2$ = 17/30/53
Catalyst: 0.3 g $K(NH_4)_2PMo_{12}O_{40}/FeO_{1.5}$ + 1 g sand

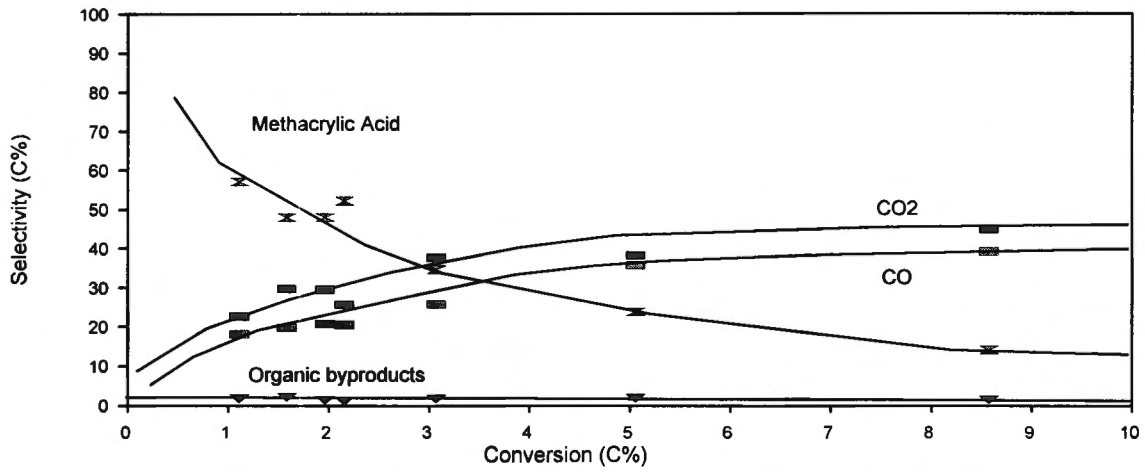

FIGURE 3.26: SELECTIVITY VS CONVERSION AS A FUNCTION OF SPACE VELOCITY AT T = 400°C

Feed composition: $i\text{-}C_4H_{10}/O_2/N_2 = 17/30/53$
Catalyst: $0.3\ g\ K(NH_4)_2PMo_{12}O_{40}/FeO_{1.5} + 1\ g\ sand$

Figure 3.27 shows the steady state selectivities of the two organic byproducts, methacrolein and propanal, as a function of conversion with changing space velocity at T = 380°C. The selectivities of both byproducts tend towards a finite limit as conversion tends to zero, indicating primary products. Scatter observed at lower conversions in Figure 3.27 should be attributed to difficulties in measuring these low yields.

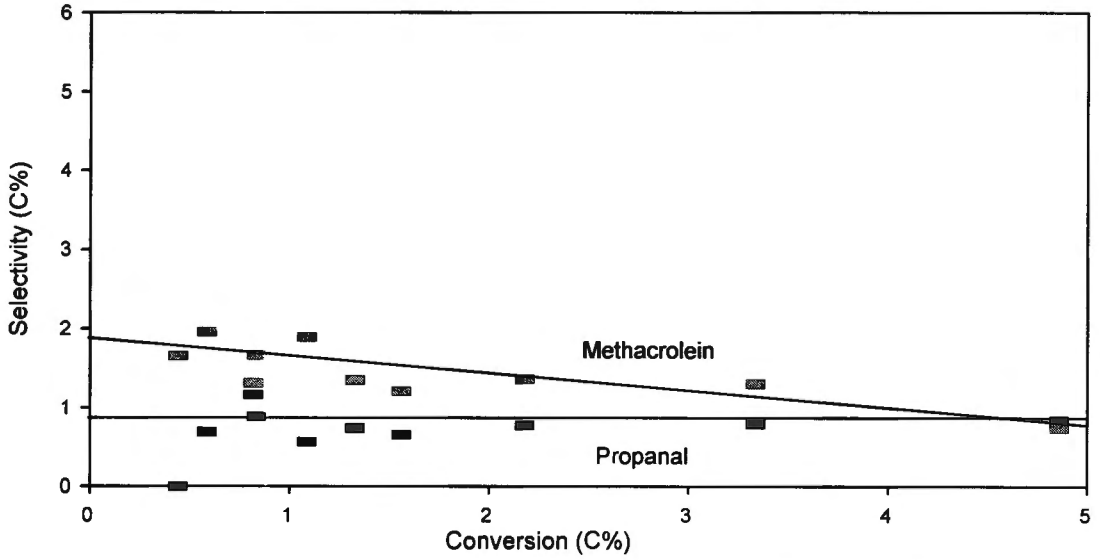

FIGURE 3.27: SELECTIVITY VS CONVERSION OF METHACROLEIN AND PROPANAL AS A FUNCTION OF SPACE VELOCITY AT T = 380°C

Feed composition: $i\text{-}C_4H_{10}/O_2/N_2 = 17/30/53$
Catalyst: $0.3\ g\ K(NH_4)_2PMo_{12}O_{40} / FeO_{1.5} + 1\ g\ sand$

4. DISCUSSION

4.1. CONVERSION OF n-BUTANE OVER THE VPO CATALYST

Infrared and X-ray diffraction indicate the presence of the $(VO)_2P_2O_7$ phase. Optimal XRD peak areas and IR absorbances associated with the $(VO)_2P_2O_7$ phase were obtained for samples with P/V ratios during preparation of 1.1 and 1.2 when activated in the n-butane/O_2/N_2 feed, and with P/V ratios of 1 15 when activated in air. Changes in peak area with P/V ratio were limited when calcined in nitrogen. XRD areas associated with an amorphous phase showed a decrease as peak areas associated with $(VO)_2P_2O_7$ increased, indicating that the $(VO)_2P_2O_7$ phase forms from an amorphous precursor. This agrees with Nguyen et al [1996], who report the presence of an amorphous precursor after calcination in organic medium. It is suggested that an excess of phosphorus facilitates the transformation from the amorphous phase to $(VO)_2P_2O_7$ during calcination. Large excesses of phosphorus (P/V ratio during preparation of 1.5), on the other hand, will again inhibit this transformation. It is suggested that this transformation is less a function of P/V ratio when calcining in a N_2 atmosphere.

To show the effect of different preparation variables on catalyst activity, rate constants were calculated for the conversion of n-butane over the VPO catalyst, using the rate equation of Bej et al [1991]:

$$-r_B = \frac{K_1 K_2 P_B}{K_1 + \alpha K_2 P_B} \tag{8}$$

where r_B = rate of n-butane conversion in $(mol_{n\text{-butane}})/(min.g_{catalyst})$
P_B = partial pressure of n-butane in Pa
K_1, K_2, α = constants

At low n-butane concentrations, the rate can be approximated as first order:

$-r_B = K_a P_B$

Integrating over the reaction bed gives the following equation:

$$K_a = \frac{-\ln(1 - X_f)F_o}{(P_o W)} \tag{9}$$

where X_f = conversion of n-butane leaving the reactor
F_0 = flowrate of n-butane entering the reactor in mol/min
P_0 = partial pressure of n-butane entering the reactor in Pa
W = mass of catalyst in g

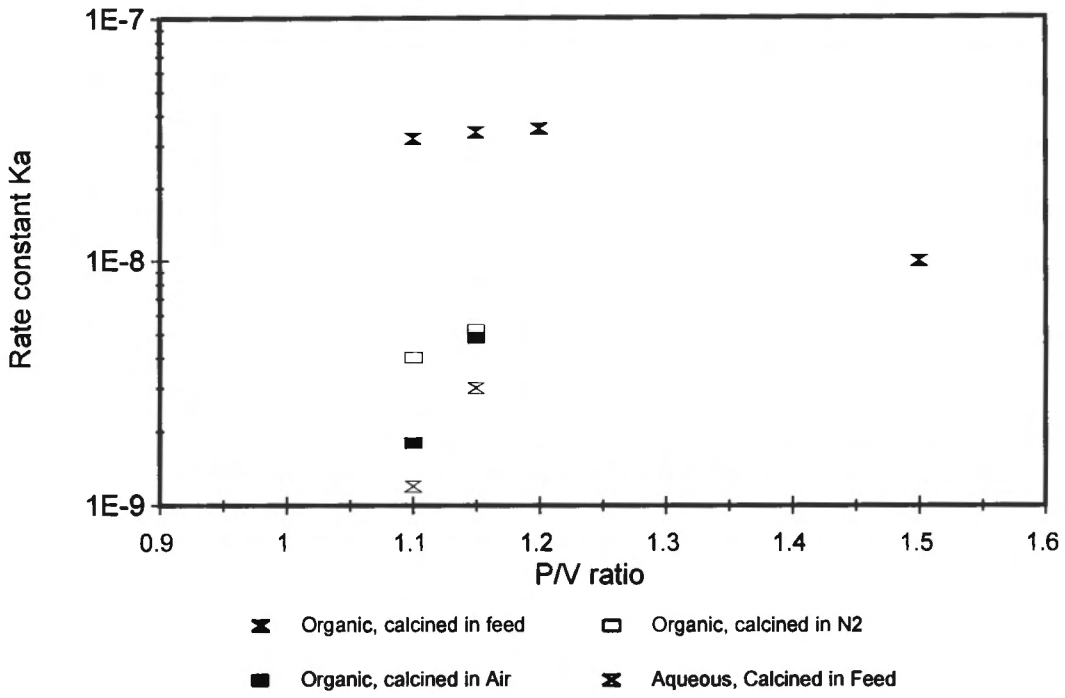

FIGURE 4.1: RATE CONSTANT Ka FOR n-BUTANE CONVERSION
Ka = (mol n-butane)/(min)(g catalyst)(Pa)

The rate constant K_a is given for different P/V ratios, reducing agents and calcination atmospheres in Figure 4.1 for reaction and calcination at 400°C. The rate constant of the catalyst prepared in organic medium and calcined in reaction feed increased with P/V ratio up to P/V = 1.2. At P/V = 1.5, the rate was much lower. This corresponds with the IR absorbances of the vanadyl pyrophosphate phases of Figure 3.4. Better crystallinity gave better conversion rates. Rates decreased in the following order: calcination in reaction feed > calcination in nitrogen > calcination in air. This agrees with the results of Bosch et al [1987]. Catalysts prepared in aqueous reducing agent and calcined in reaction feed gave the lowest rates. This is in accordance with the lower surface areas reported by Hodnett [1985] for catalysts prepared in aqueous medium.

Regardless of the wide range of synthesis variables and reaction parameters studied, only total oxidation products could be observed for the prepared VPO catalyst. This may be due to either a faulty synthesis/calcination method or oxidation of maleic anhydride in the lower part of the reactor. To determine if the synthesis method was at fault, a range of preparation and calcination variables was studied, limiting the possibility that the preparation method could be the cause of the over-oxidation. Uncertainties, such as those expressed for the P/V ratio, were compensated for by testing a range of parameters, including a P/V ratio during preparation of up to 1.5. Where a range of reaction temperatures was given in literature, tests were done over the whole range as reported in section 2.3.4.1.

Although various methods for the synthesis of unpromoted catalysts are claimed by investigators to yield maleic anhydride, the method of Katsumoto and Marquis [US Patent 4132670 (1979)] is used in most recent literature and is claimed to give the best results. The preparation methods of many recent investigators are all slight variations on this method. They describe the preparation method as a few major steps such as reduction, reaction with ortho-phosphoric acid and calcination, without further detail, or they simply refer to the method of Katsumoto and Marquis. This could mean that the preparation method is either very straightforward or that a concise version of the preparation method is given and that finer and possibly crucial details of the preparation may have been omitted. For instance, most investigators do not specify the exact amount of o-H_3PO_4 added during preparation. They merely state that o-H_3PO_4 is added so as to obtain the correct P/V ratio. This could also be the reason why investigators quoting the same preparation method get such different yields of maleic anhydride, as mentioned in section 1.1.4. However, the consistency in the description of the preparation method seems to indicate that it is complete. The preparation method is also given in detail in the patent literature.

Over-oxidation is normally associated with the presence of the β-$VOPO_4$ phase, but XRD and IR indicate that the only crystalline phase present is the 4+ pyrophosphate phase. Both IR and XRD spectra agree well with literature and indicate a $(VO)_2P_2O_7$ phase with peak broadening in the XRD. This suggests the presence of the defect sites mentioned by Nguyen et al [1996] to be present in catalysts with good reactivity. Alternatively, the peak broadening is a result of the crystallisation of the $(VO)_2P_2O_7$ out of the amorphous phase during calcination, indicating low crystallinity. A fresh catalyst shows the $(VO)_2P_2O_7$ phase, but with lower crystallinity and "clearly indicates the presence of the amorphous phase together with the $(VO)_2P_2O_7$ phase" [Cavani et al, 1994]. The non-equilibrated catalyst is less selective but more active. A more crystalline catalyst also forms when calcining at high temperatures (e.g. 880°C reported by Zhang et al [1993]), but this catalyst has low activity due to the absence of defect sites associated with 5+ species.

The change in the nature of the catalyst surface with time on stream has not been reported, although Zhang et al mention a rearrangement in the environment of the V^{5+} species. Longer times on stream will result in higher crystallinity and selectivity, which may result in the detection of maleic anhydride. Although investigators such as Abon et al [1995] (Figure 1.11) report maleic anhydride yields after minutes on stream, other investigators including Kubias et al [1992] indicate long induction periods. Although the catalyst should therefore produce maleic anhydride after short times on stream (i.e. a few minutes), longer times will improve the selectivity. Also, once the catalyst is equilibrated, it will be stable against changes in structure and will not be over-oxidised if say pure oxygen is passed over it. Stability is however not essential for the production of maleic anhydride. The catalyst of Abon et al [1995] (Figure 1.11) reaches a steady state after about 80 hours on stream. The VPO catalysts tested in this work should therefore not show any increase in maleic anhydride yield after this time. If maleic anhydride is not detected after about 80 hours on stream, longer times will not result in its detection.

The effect of time on stream over a long induction period was studied by carrying out a run over a 190 hour period. It was thought that the better selectivity resulting from a longer induction period may result in the detection of some maleic anhydride. The selectivities were, however, constant over the time period and only total oxidation products were observed. The fact that no maleic anhydride is observed after 80 hours suggests that the catalyst either does not produce maleic anhydride, or that, if it is produced, it may oxidise further in the lower part of the reactor. This would be difficult to avoid on account of the parabolic reactor temperature profile. Maleic anhydride, if formed, will also be present in low concentrations (less than 1.44 vol%). It was not possible to increase the concentration of n-butane due to explosion limits.

It is possible that impurities in the preparation chemicals may result in poisoning of the catalyst, as these impurities normally collect on the surface. This effect is normally observed for yields which are lower than expected. However, elemental analysis showed no impurities and only small amounts of carbon were observed. This may be expected prior to calcination for the organically prepared catalyst where alcoholates become entrapped in the catalyst structure [Nguyen et al, 1996]. The organic residue is removed during calcination.

As mentioned in section 1.1.3., reaction is highly dependent on the nature of the active sites on the surface. Nguyen et al mention that most catalysts prepared by traditional preparation methods show a fair degree of inhomogeneity. Since characterisation of the surface was not carried out, a layer of over-oxidised species may be present on the surface. This would not be evident in the XRD or IR spectra. However, over-oxidation, although possible when calcining in air, is unlikely to occur in the mildly reductive atmospheres of N_2 and n-butane in air. Nonetheless, it is not known if the necessary surface species (e.g. Lewis acid sites) are in fact present. The absence of the Lewis acid sites needed for activation may result in the presence of over-oxidised products.

The range of reaction temperatures, space velocities and feed compositions studied (Section 2.3.4.1), shows that the over-oxidation is not a phenomenon taking place only over a certain reaction range.

n-Butane was found not to combust over sand at the reaction conditions studied and therefore the total oxidation products are either formed over the catalyst or after the catalyst zone due to combustion of products.

In order to check for the possibility of small quantities of maleic anhydride forming and then combusting in the outlet lines, maleic anhydride was fed with a saturator. Maleic anhydride did not combust at up to 200°C in the outlet lines, but at around 400°C through an empty reactor, only CO and CO_2 were observed for maleic anhydride flowrates that were up to 2 ml/min when bypassing the reactor. It is possible, therefore, that small amounts of maleic anhydride, if formed, may combust in the approximately 5 cm of heated zone after the 3 cm hot-zone in which the catalyst is packed. The total reaction element covers a 150 mm length. It is however difficult to avoid this situation on account of the parabolic shape of the temperature profile created by the heating element.

The run carried out over 190 hours indicates that the catalyst may be producing a small amount of maleic anhydride, which is then immediately combusted. For a total reaction feed rate of 100 ml/min, the flowrate of n-butane would be 1.44 ml/min. Even if all the n-butane were converted with 100% selectivity, a flowrate of only 1.44 ml/min of maleic anhydride would be present. The small flowrate makes total combustion possible. If this is the case, higher concentrations of n-butane may result in its detection, but explosion limits make it hard to increase the n-butane concentration.

In addition, the prepared catalyst was tested for a range of conditions in the oven-heated reactor, which does not have the parabolic temperature profile. Total oxidation was also observed with these tests. It should be noted that the u-tube reactor used in the oven also has a post-heat zone in which maleic anhydride, if formed, can combust. The result of over-oxidation in the oven-heated reactor therefore does not confirm that the catalyst itself is the cause of the over-oxidation.

The possibility of maleic anhydride forming and then condensing out in the outlet lines was ruled out by good carbon balances and outlet line temperatures of above 180°C.

The possibility that maleic anhydride could be formed, but not detected, was discounted. Maleic anhydride was dissolved in a solvent and injected into the GC and a peak was observed. Maleic anhydride was built into an ampoule and again a peak was observed. A deactivated commercial catalyst was tested, showing a maleic anhydride yield of 6%, which, although low, indicates that maleic anhydride, if formed, can be observed with the sampling method.

Another cause of over-oxidation may be the development of hot-spots in the reactor bed during reaction. The heat evolved by partial oxidation could raise the temperature sufficiently for total oxidation to be ignited at some position in the reactor. However, the reactor was a thin tubular reactor and the catalyst was diluted with sand to improve heat transfer, making this phenomenon unlikely. Greater dilution of the catalyst, or the mixing of the reactor contents, as would be achieved with the use of a fluidised bed reactor, would also ensure a flat temperature profile. Diluting the catalyst would, however, result in an even lower flowrate of maleic anhydride, if formed.

4.2. CONVERSION OF ISOBUTANE OVER THE HETEROPOLYACID, $K(NH_4)_2PMo_{12}O_{40}$

Reaction runs showing product yields versus time indicate an activation period for the heteropoly acid catalyst. This period is a function of the space velocity and varied from 3 hours for a space velocity of 1.98 g/g.h to 7 hours for a space velocity of 0.79 g/g.h. During the activation period, yields of total oxidation products decreased with time on stream, while yields of methacrylic acid increased. Yields of methacrolein and propanal remained constant, while yields of ethyl methyl ether and dimethyl benzene decreased to zero.

Infrared spectra show that, with time on stream, the absorbance peaks due to bonds belonging to the Keggin structure become stronger. This indicates the formation of Keggin crystals out of an amorphous phase when reacting in an isobutane reaction feed. All IR peaks associated with the Keggin structure increase with time on stream and individual peaks such as those associated with Mo-O or P-O, for example, do not increase relative to one another. This shows that the catalyst is not oxidised or reduced during reaction on stream. The changes in yields during equilibration are therefore not a result of a change in oxidation state of the catalyst. At equilibration, crystallisation is complete and the yields remain constant. The high unsteady state yields of CO and CO_2 and the changes of up to 50% in these yields during equilibration, suggest that total oxidation products on the unequilibrated catalyst form along parallel routes - on the amorphous catalyst phase. A decrease in the percentage of catalyst mass which is non-crystalline will result in a decrease in the parallel formation of total oxidation products and an increase in the formation of methacrylic acid.

Ethyl methyl ether and dimethyl benzene could form on non-crystalline solid or on regions of interface between non-crystalline and crystalline solid. The amorphous precursor phase may also interact electronically with reaction sites on the Keggin crystal, attracting or repelling electrons and resulting in a change in the Mo-O bond strength and in the yields of organic products during equilibration. The increase of up to 50% in the the yield of methacrylic acid during equilibration, with little change in the yields of propanal and methacrolein, confirms the hypothesis that these products are formed on parallel sites, which will interact differently with non-crystalline material.

It is proposed that calcination methods which produce the most crystalline catalyst will produce the best steady state selectivities. However, it is possible that the oxygen partial pressure in the reaction feed may result in a change in steady state CO or CO_2 yields due to changes in the oxidation state of the catalyst.

Runs which compare yields and selectivities of all products as a function of space velocity, show that selectivities of methacrylic acid and the two other steady state organic products (methacrolein and propanal) tend to a finite limit as conversion tends to zero along with contact time. Selectivities of total oxidation products, CO and CO_2, tend to zero as conversion tends to zero. From this it can be concluded that methacrylic acid and the two organic byproducts are primary products and are therefore formed along parallel routes.

Intermediates in the formation of methacrylic acid do not desorb due to kinetic reasons (the high rate of oxidation of the activated species). Isobutane adsorbs on the catalyst, is transformed to organic products and once reaction is complete, methacrylic acid desorbs. Total oxidation products form as a result of serial oxidation of these organic products on an equilibrated catalyst. Because of the decrease of up to 50% in the yields of CO and CO_2 during equilibration (Figure 3.19), it is proposed that during equilibration CO and CO_2 also form on the amorphous precursor phase and that the dramatic decrease in selectivity of total oxidation products results from a decrease in the percentage of the amorphous phase present.

The following reaction pathway is proposed:

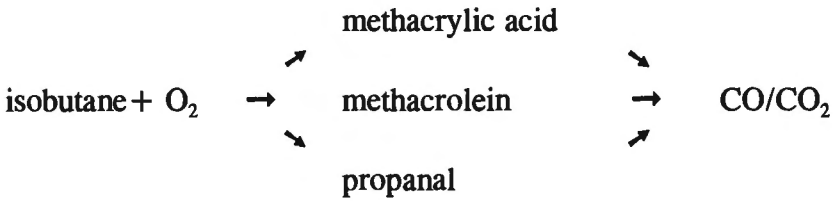

The model which is favoured is that of parallel formation of primary organic products, with serial formation of total oxidation products, as shown above. This is consistent with the findings of Busca et al [1996] who propose that methacrolein and methacrylic acid could share the same precursor, a dioxyalkylidene, which then reacts by parallel paths to form either of the final products. However, if methacrolein and methacrylic acid form on the same active site, one would expect methacrylic acid to be a product of the oxidation of methacrolein. Since methacrylic acid is shown to be a primary product, it is suggested that the two species form on parallel sites, resulting in different degrees of oxidation and different changes in yield during equilibration. This is confirmed when the yield of methacrylic acid increases during equilibration, while the yield of methacrolein shows little increase. If the two products form on different sites, these sites will differ in the way that their environments change during equilibration.

As was mentioned in Section 1.2.4., the electronegativity of the heteropoly acid cation influences the electrochemical properties of the molybdenum atom, the strength of the Mo-oxygen bond (participation of the lattice oxygen), and the acid-base properties of the catalyst, due to electronic interaction with the cation. It is therefore also suggested that the proximity of the Mo-O active site in the anion complex to the cation counterions will determine the strength of the Mo-O bond and therefore the oxidising properties of the active site. Different Mo-O active sites with differing Mo-O bond strengths will exist on the surface. This will explain the differing degrees of oxidation during methacrolein and methacrylic acid formation on parallel sites, as well as the dehydrogenation in the case of methacrylic acid and methacrolein as opposed to C-C bond cleavage in the formation of propanal on a parallel active site.

The formation of propanal along a parallel route is consistent with the lack of an initial dehydrogenation step, as opposed to the formation of methacrolein and methacrylic acid. However, since isobutene has not been observed by Busca et al [1996] as an intermediate, it is not absolutely certain whether the first reaction step is in fact the dehydrogenation to isobutene, although isobutene was shown to react with high rates towards methacrylic acid over the same catalyst.

The formation of propanal is thought to take place via a C-C bond cleavage step, followed by an oxidation step as shown in Figure 4.2. The formation of methacrolein and methacrylic acid takes place via the mechanism of Busca et al [1996], shown in section 1.2.5. The oxidation of methacrolein and methacrylic acid will take place on sites of differing Mo-O bond strength, but the difference in bond strength will not affect the activation step, which is similar for these two products. Similarly, the first step in the formation of propanal will take place on a site with a different environment to that of methacrolein and methacrylic acid, resulting in C-C bond cleavage as opposed to dehydrogenation.

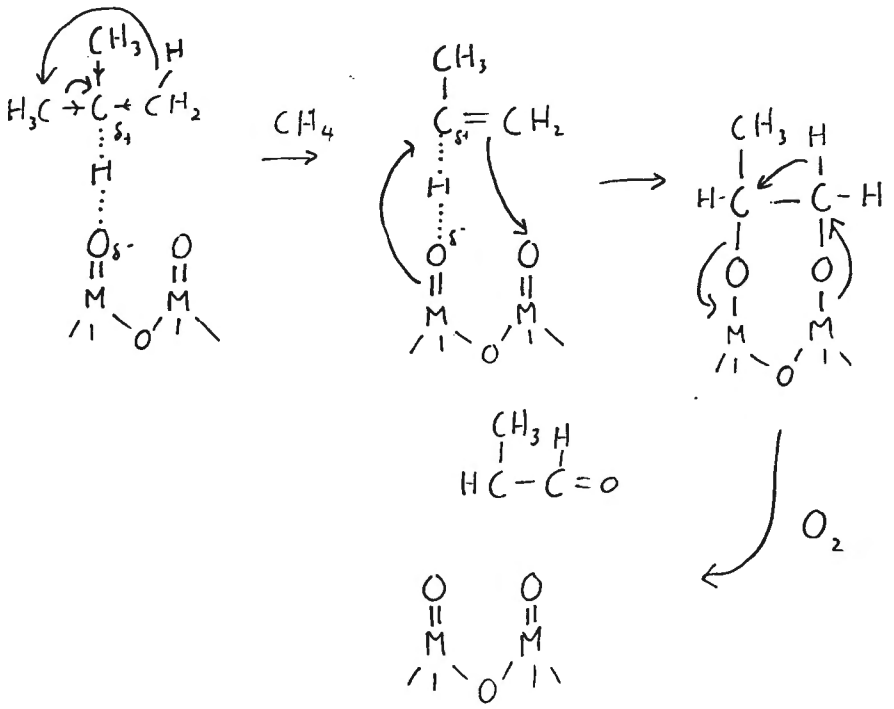

FIGURE 4.2: PROPOSED MECHANISM OF PROPANAL FORMATION

5. CONCLUSIONS AND RECOMMENDATIONS

5.1. VPO CATALYST

Characterisation of the catalyst shows good correlation with literature and indicates the presence of a bulk $(VO)_2P_2O_7$ phase. Peak broadening observed with XRD spectra can indicate the following:

1) The presence of defect sites formed during activation, as proposed by Nguyen et al [1996]. These defect sites have been correlated by Nguyen et al with the presence of 5+ sites or micro-domains in the $(VO)_2P_2O_7$ structure, which are mechanistically important.
2) A low degree of crystallisation out of the amorphous precursor, according to the activation pathway proposed by Cavani et al [1994]:

$$VOHPO_4.0.5H_2O \rightarrow \text{amorphous phase} \rightarrow (VO)_2P_2O_7 \rightarrow \beta\text{-}VOPO_4$$
$$\searrow$$
$$V^{5+}$$

The amorphous precursor is also reported by Nguyen et al when organic reducing agents are used. The presence of an amorphous precursor is confirmed by XRD, which shows a decrease in the area associated with amorphous material (Figure 3.1) with change in P/V ratio. Longer reaction times will result in greater crystallinity and better selectivity and the disappearance of the amorphous phase [Kubias et al, 1992]. The change in selectivity with time on stream may also be a result of changes on the reactive catalyst surface, which have not yet been explained by investigators.

Peak areas and IR absorbances associated with the $(VO)_2P_2O_7$ phase are optimal for samples with P/V ratios during preparation of 1.1 and 1.2., activated in the n-butane/O_2/N_2 feed and this correlates with optimal rates of n-butane conversion. Lower and higher P/V ratios gave smaller XRD peak areas, IR absorbances and rates. It is therefore suggested that an excess of phosphorus renders the transformation from amorphous phase to $(VO)_2P_2O_7$ during calcination more facile. Large excesses of phosphorus (P/V ratio during preparation of 1.5), on the other hand, will again inhibit this transformation. It has been reported that an excess of phosphorus stabilises the $(VO)_2P_2O_7$ phase against over-oxidation (Poli et al, 1981), but not that it facilitates the formation of $(VO)_2P_2O_7$ during calcination. The increase in facility of transformation from amorphous phase to $(VO)_2P_2O_7$ with increase in P/V ratio is confirmed by the XRD of samples calcined in air. These show an increase in peak area for the $(VO)_2P_2O_7$ phase with an increase in P/V ratio during preparation of up to 1.15. This increase correlates with a decrease in area associated with the amorphous phase.

XRD and IR spectra indicate the correct phase for maleic anhydride synthesis. Although these characterisation techniques are the most common in literature, they are however not surface-specific. Although the XRD spectra suggest the presence of a 4+ vanadium species, the oxidation state of the surface is not known. The n-butane/O_2/N_2 calcination atmosphere used is, however, not oxidative [Nguyen et al] and is unlikely to produce the presence of $VOPO_4$ on the surface which would result in total oxidation. The nature of other surface species such as the Lewis acid sites are also not known.

Although long activation periods are mentioned in literature, most investigators (e.g. Abon et al [1995]) show yields of maleic anhydride after only minutes on stream. The catalyst of Figure 1.11 [Abon et al, 1995] reaches a steady state after 80 hours on stream. Longer activation periods improve selectivity and stabilise the catalyst structure, but maleic anhydride should already be observed after short activation/reaction periods. It was thought that increased yields of maleic anhydride may result in its detection, if it were combusted after formation. A run over 190 hours, however, showed no change in selectivities of total oxidation products and no yield of maleic anhydride.

It is possible that maleic anhydride, if formed, combusts further to CO and CO_2 in the lower section of the reactor, as has been shown by the combustion of up to 2 ml/min of maleic anhydride fed with a saturator through the reactor at 400°C without catalyst. It is difficult to reduce the length of the post-heat zone in the cartridge-heated reactor on account of the parabolic temperature profile. The low n-butane concentrations fed also mean that, if any maleic anhydride is formed, the flowrates will be less than 1.44 ml/min for a total feed flowrate of 100ml/min, which makes combustion a greater possibility. It is therefore suggested that higher n-butane concentrations be studied. Although oxygen partial pressures in this work were varied, on account of the low n-butane concentration in the feed, the oxygen/n-butane ratios were still high. Explosion limits prevent an increase in the n-butane partial pressure.

It is also recommended that the catalyst be diluted further and that better knowledge of the temperature profile during reaction be obtained, so as to ensure a flat temperature profile and prevent the possible formation of hot-spots, which may result in over-oxidation. However, this will again result in lower concentrations of maleic anhydride, if it is formed, which in turn may make combustion more likely.

5.2. HETEROPOLY ACID CATALYST

It is proposed that the decrease in total oxidation products during equilibration results from the progressive crystallisation of the Keggin structure out of an amorphous phase. It is hypothesised that the total oxidation of isobutane takes place on an amorphous phase during equilibration and that the decrease in selectivity of total oxidation products results from a decrease in the percentage of the amorphous phase present. The amorphous phase is also thought to interact electronically with the active sites on the Keggin crystal, resulting in changes in yields during equilibration.

Space velocity studies on an equilibrated catalyst identified all organic species as primary products, formed along parallel pathways. Total oxidation products, CO and CO_2, are secondary products, which form due to combustion of organic species. Better selectivities of methacrylic acid can therefore be obtained by limiting the contact time to prevent successive oxidation.

It is proposed that the isobutane molecule is activated on the heteropoly acid surface and then undergoes reaction without the desorption of intermediates. Only final products desorb. Methacrylic acid, methacrolein and propanal are formed on parallel sites of which the environments change differently during equilibration, due to electronic interaction with the amorphous precursor phase. These parallel active sites may be caused by differences in proximity of Mo-O active sites to the heteropoly acid cation, resulting in differences in Mo-O bond strength and differences in oxidising strength and basicity between these Mo-O sites.

Increased crystallinity during activation results in increased yields of methacrylic acid. Activation procedures should therefore be aimed at optimising the crystallinity of the Keggin-structure. Further studies should involve the investigation of isobutane oxidation at low oxygen concentrations to test for the presence of isobutene. A study of the effect of calcination atmosphere on the steady state product yields is also suggested.

6. REFERENCES

6.1. ACADEMIC LITERATURE

Ai, M.; *Journal of Catalysis*; **71** (1981); 88-98:
Characteristics of heteropoly compounds as catalysts for selective oxidation

Ai, M.; in "Proceedings of the 8th International Conference on Catalysis"; Berlin, 1984; [Dechetia: EDS]; *Verlag Chemie*; Weinheim, 1984:
Partial oxidation of n-butane with heteropoly compound-based catalysts

Ai, M.; *Applied Catalysis*; **28** (1986); 223-233:
Effects of preparation variables on the properties of V_2O_5-P_2O_5-ZrO_2 catalysts used for the oxidation of n-butane.

Abdelouahab, F., Olier, R., Guilhaume, N., Lefebvre, F., Volta, J.; *Journal of Catalysis*; **134** (1992); 151-167:
A study by in-situ laser Raman spectroscopy of VPO catalysts for n-butane oxidation to maleic anhydride

Abon, M., Bere, K., Tuel, A., Delichere, P.; *Journal of Catalysis*; **156** (1995); 28-36:
Evolution of a VPO catalyst in n-butane oxidation reaction during the activation time

Abon, M., Bere, K., Delichere, P.; *Catalysis Today*; **33** (1997); 15-23:
Nature of active oxygen in the n-butane selective oxidation over well-defined VPO catalysts: an oxygen isotopic labelling study

Akimoto, M., Tsuchida, Y., Sato, K., Echigoya, E.; *Journal of Catalysis*; **72** (1981); 83-94:
12-Heteropolymolybdates as catalysts for vapour-phase oxidative dehydrogenation of isobutyric acid

Akimoto, M., Ikeda, H., Okabe, A., Echigoya, E.; *Journal of Catalysis*; **89** (1984); 196-208:
12-Heteropolymolybdates as catalysts for vapour-phase oxidative dehydrogenation of isobutyric acid

Albonetti, S., Cavani, F., Trifiro, F., Gazzano, M., Koutyrev, M., Aissi, F.C., Aboukais, A., Guelton, M.; *Journal of Catlaysis*; **146** (1994); 491-502:
Mechanism of thermal decomposition of potassium/ammonium salts of the 12-molybdophosphoric acid and effect on the catalytic performance in the isobutyric acid oxidehydrogenation

Arnold, E., Sundaresan, S.; *Applied Catalysis*; **41** (1988); 225-239:
Effect of water vapour on the activity and selectivity characteristics of a vanadium phosphate catalyst towards butane oxidation

Bej, S. K., Musti, S. R.; *Ind. Eng. Chem. Res.*; **30** (1991); 1819-1824:
Selective oxidation of n-butane to maleic anhydride: Optimisation studies

Bhargava, R., Condrate, R.; *Applied Spectroscopy*; **31(3)** (1977); 230-236:
The vibrational spectra of VPO_5 crystal phases and related glasses

Bordes, E.; *Catalysis Today*; **1** (1987); 499-526:
Crystallochemistry of V-P-O phases and application to catalysis

Bordes, E.; *Catalysis Today*; **16** (1993); 27-38:
Nature of the active and selective sites in vanadyl pyrophosphate, catalyst of oxidation of n-butane, butene and pentane to maleic anhydride

Bosch, H., Bruggink, A., Ross, J.; *Applied Catalysis*; **31** (1987); 323-337:
Selective oxidation of n-butane to maleic anhydride under oxygen-deficient conditions over V-P-O mixed oxides

Brutovsky, M., Gerej, S.; *Czechslovak Chem. Comm.*; **47** (1982); 403-408:
Effects of various modifying elements on the catalytic properties of vanadium-phosphorus catalysts in the oxidation of butane

Brutovsky, M., Gerej, S.,Vasilco, F., Gerejova, J.; *Czechslovak Chem. Comm.*; **47** (1982); 1290:
X-Ray diffractograms and infrared spectra of modified vanadium-phosphate catalysts

Busca, G., Centi, G., Trifiro, F.; *Applied Catalysis*; **25** (1986); 265-272:
n-Butane selective oxidation on vanadium-based oxides: Dependence on catalyst microstructure

Busca, G., Cavani, F., Etienne, E., Finocchio, B., Galli, A., Selleri, G., Trifiro, A.;
J. Molecular Catalysis A: Chemical; **144** (1996); 343-359:
Reactivity of Keggin-type heteropolycompounds in the oxidation of isobutane to methacrolein and methacrylic acid: Reaction mechanism

Burnett, J.C., Keppel, R.A., Robinson, W.D.; *Catalysis Today*; **1** (1987); 537-586:
Commercial production of maleic anhydride by catalytic processes using fixed bed reactors

Cavani, F., Centi, G., Trifiro, F.; *Applied Catalysis*; **9** (1984); 191-202:
The chemistry of catalysts based on vanadium-phosphorus oxides: Catalytic behaviour of catalysts prepared in organic medium in the oxidation of C_4 fraction

Cavani, F., Trifiro, F.; *Chemtech*; April 1994; 18-25:
Catalysing butane oxidation to make maleic anhydride

Cavani, F., Etienne, E., Favaro, M., Galli, A., Trifiro, F., Hecquet, G.; *Catalysis Letters*; **32** (1995); 215-226:
Enhancement of catalytic activity of the ammonium/potassium salt of 12-molybdophosphoric acid by iron addition for the oxidation of isobutane to methacrylic acid

Centi, G., Fornasari, G., Trifiro, G.; *Journal of Catalysis*; **89** (1984); 44:
On the mechanism of n-butane oxidation to maleic anhydride: Oxidation in oxygen-stochiometry-controlled conditions

Centi, G., Manenti, I., Riva, A., Trifiro, F.; *Applied Catalysis*; **9** (1984); 177-190:
The chemistry of catalysts based on vanadium phosphorus oxides: Catalytic behaviour of different phases in 1-butene oxidation to maleic anhydride

Centi, G., Trifiro, F.; *Applied Catalysis*; **12** (1984); 1:
Some aspects of the control of selectivity in catalytic oxidation of mixed oxides: A review

Centi, G., Trifiro, F., Ebner, J, Franchetti, M.; *Chem. Rev.*; **88** (1988); 55-80:
Mechanistic aspects of maleic anhydride synthesis from C_4 hydrocarbons over phosphorus vanadium oxide

Centi, G., Golinelli, G., Trifiro, F.; *Applied Catalysis*; **48** (1989); 13-24:
Nature of the active sites of $(VO)_2P_2O_7$ in the selective oxidation of n-butane: Evidence from doping experiments

Centi, G.; *Catalysis Today*; **16** (1993); 5-26:
Vanadyl pyrophosphate - a critical overview

Contractor, R., Sleight, A.; *Catalysis Today*; **3** (1988); 175:
Selective oxidation in riser reactor

Cornaglia, L.M., Caspani, C., Lombardo, E.; *Applied Catalysis*; **74** (1991); 15-27:
Physicochemical characterisation and catalytic behaviour of VPO formulations

Cornaglia, L.M., Sanchez, C.A., Lombardo, E.A.; *Applied Catalysis A, General*; **95** (1993); 117-130:
Chemistry of vanadium-phosphorus oxide catalyst preparation

Ebner, J.R., Thompson, M.R.; *Catalysis Today*; **16** (1993); 51-60:
An active site hypothesis for well-crystallised vanadium phosphorus oxide catalyst systems

Eight Peak Index of Mass Spectra; Vol 3 Part 1; 4th Edition; 1991; Mass Spectrometer Data Centre; The Royal Society of Chemistry; Cambridge

Ernst, V., Barbaux, Y., Courtine, P.; *Catalysis Today*; **1** (1987); 167-180:
Phosphomolybdic acid as a catalyst for the vapour-phase oxidative dehydrogenation of isobutyric acid: Kinetic parameters of supported and unsupported catalysts. Role of water

Gorbunova, Y. E., Linde, S.A; *Dokl. Akad. Nauk SSSR*; **245** (1979); 5864

Haber, J., Tokarz, R., Witko, M.; in "Heterogeneous hydrocarbon oxidation"; [Warren, B., Oyama, S., EDS]; *ACS Symposium Series 638*; American Chemical Society; Washington; (1996); 249-258

Hodnett, B.K., Delmon, B.; *Applied Catalysis*; 9 (1984); 203-211

Hodnett, B; *Catal. Rev.-Sci. Eng.*; **27(3)** (1985) 373-424:
Vanadium-phosphorus oxide catalysts for the selective oxidation of C_4 hydrocarbons to maleic anhydride

Hutchings, G.; *Applied Catalysis*; **72** (1991); 1-32:
Effect of promoters and reactant concentration on the selective oxidation of n-butane to maleic anhydride using vanadium phosphorus oxide catalysts

Hutchings, G.; *Catalysis Today*; **16** (1993); 139-146:
Vanadium phosphorus oxide catalysts for the selective oxidation of n-butane to maleic anhydride

Hydrocarbon Processing; **64** Nov (1985); 142:
Maleic anhydride (Alma Process) - Alusuisse Italia/Lummus Crest

Igarashi, H., Tsuji, K., Okuhara, T., Misono, M.; *Journal of Physical Chemistry*; **97** (1993); 7065-7071:
Effects of consecutive oxidation on the production of maleic anhydride in butane over four kinds of well-characterised vanadyl pyrophosphates

Irving-Monshaw, S., Kislin, A.; *Chemical Engineering News*; March (1989); 35-37:
Lively markets brighten maleic anhydride horizons

Kaiser, R.; *Chromatographie in der Gasphase*; Vol 3; Second Edition; Bibliographisches Institut; Mannheim, (1969)

Kubias B., Rodemerck, U., Wolf, G.U., Meisel, M., Schaller, W.; in: "Proceedings DGMK Conference On Selective Oxidations in Petrochemistry"; [Baerns, M., Weitkamp, J., EDS]; *DGMK*; Hamburg, (1992); 303

Matsuura, I.; *Catalysis Today*; **16**; (1993); 123-129

McGarvey, G.B., Moffat, J.B.; *Journal of Catalysis*; **132** (1991); 100-116:
The oxidative dehydrogenation of isobutyric acid to methacrylic acid on ion exchange modified 12-heteropoly oxometalates

Milmo, S.; *Chemical Marketing Reporter*; July 22 (1996); 9:
Huntsman and Condea in Maleic Venture

Mizuno N., Tateishi, M., Iwamoto, M.; *Applied Catalysis A: General*; **118** (1994); L1-L4:
Enhancement of catalytic activity of $Cs_{2.5}Ni_{0.08}H_{0.34}PMo_{12}O_{40}$ by V^{5+} substitution for oxidation of isobutane into methacrylic acid

Mizuno, N., Tateishi, M., Iwamoto, M.; *Applied Catalysis A: General*; **128** (1995); L165-L170:
Pronounced catalytic activity of $Fe_{0.08}Cs_{2.5}H_{1.26}PVMo_{11}O_{40}$ for direct oxidation of propane into acrylic acid

Morselli, L., Trifiro, F., Urban, L.; *Journal of Catalysis*; **75** (1982); 112-121:
Study of the interaction of 1-butene with V_2O_5 and mixed vanadium and phosphorus oxides by means of temperature-programmed desorption

Nguyen, P., Sleight, A., Roberts, N., Warren, W.; *Journal of Solid State Chemistry*; **122** (1996); 259-265:
Modelling of extended defects in the vanadium phosphate catalyst for butane oxidation, $(VO)_2P_2O_7$

Okuhara, T., Inumaru, K., Misono, M; in "Catalytic Selective Oxidation"; *ACS Symposium Series*; **523** (1993); 156-167:
Active Crystal Face of Vanadyl Pyrophosphate for Selective Oxidation of n-Butane

Otake, M., Onoda, T.; in "Studies in surface science and catalysis"; Vol. 7: New Horizons in Catalysis; [Seiyama, T., Tanabe, K.: EDS]; *Proc. 7th ICC*; Tokyo; Elsevier, 1981:
A new route to methacrylates from isobutyraldehyde

Poli, G., Resta, I., Ruggeri, O., Trifiro, F.; *Applied Catalysis*; **1** (1981); 395-404:
The chemistry of catalysts based on vanadium-phosphorus oxides: The role of the method of preparation

Sand, R., Varma, A.; *Journal of Catalysis*; **143** (1993); 215-226:
Selective oxidation of butane to maleic anhydride on a vanadium-phosphorus oxide catalyst: Promotional effects of Zirconium

Schulz, H., Böhringer W., Kohl C., Rahman N., Will A.; *DGMK-Forschungsbericht 320*; DGMK; Hamburg, (1984c)

Schuurman, Y., Gleaves, J.; *Catalysis Today*; **33** (1997); 25-37:
A comparison of steady-state and unsteady-state reaction kinetics of n-butane oxidation over VPO catalysts using a TAP-2 reactor system

Shelley, S., Fouhy, K., Moore, S.; *Chemical Engineering News*; December 1993; 61-64:
Seeking the best route for maleic anhydride

Takita, Y., Tanaka, K., Ichimary, S., Ishihara, T., Inoue, T., Arai, H.; *Journal of Catalysis*; **130** (1991); 347-353:
Location and functions of Zn as a promotor element in the V-P-O catalysts for n-butane oxidation to maleic anhydride

Trifiro, F.; *Catalysis Today*; **16** (1993); 91

Tsigdinos, G., Hallada, J.; *Journal of Inorganic Chemistry*; **7 (3)** (1968); 437-441:
Molybdovanadophosphoric acids and their salts: Investigation of methods of preparation and characterisation

Tsigdinos, G.; *Ind. Eng. Chem., Res. Develop.*; **13 (4)** (1974); 267-274:
Preparation and characterisation of 12-molybdophosphoric and 12-molybdosilicic acids and their metal salts

Ye, D., Satsuma, A., Hattori, A., Hattori, T., Murakami, Y.; *Catalysis Today*; **16** (1993); 113-121:
Effect of additives on the active sites of $(VO)_2P_2O_7$ catalysts

Zhang, Y., Sneeden, R.P.A., Volta, J.C.; *Catalysis Today*; **16** (1993); 39-49:
On the nature of the active sites of the VPO catalysts for n-butane oxidation to maleic anhydride

Zhang-Lin, Y., Forissier, M., Vedrine, J., Volta, J.; *Journal of Catalysis*; **145** (1994); 267-275:
On the mechanism of n-butane oxidation to maleic anhydride on VPO catalysts: A kinetic study on a VPO catalyst as compared to VPO reference phases

6.2. PATENTS

US Patent 3856824 (1974); Monsanto Co.:
Maleic anhydride production by oxidation of saturated aliphatic hydrocarbons using modified P/V/Fe catalysts

US Patent 3862146 (1974); Boghosian, E.M.; Standard Oil Co. Indiana:
Catalyst for maleic anhydride production by catalytic oxidation of butane

US Patent 3864280 (1975); Chevron Res. Co.:
Phosphorus-vanadium mixed oxide catalyst - for oxidising hydrocarbons esp. n-butane to maleic anhydride

US Patent 330354 (1975); Monsanto Co.:
Phosphorus-vanadium-oxygen catalysts - for oxidising hydrocarbons to maleic anhydride

US Patent 3987063 (1976); UCB SA:
Maleic anydride preparation from butane - using catalyst containing vanadium, phosphorus, oxygen, and nickel, cobalt or cadmium activators

US Patent 4016105 (1977); PETRO-TEX Chemical Corporation:
Vanadium-phosphorus oxidation catalyst preparation - by reducing vanadium compounds in aqueous phosphoric acid solution

German Offenlegungsschrift 2636800 (1977); Lonza AG:
Oxidation catalysts based on vanadium and phosphorus oxides - esp. for maleic anhydride production

Japanese Kokai 7843687 (1978); Umemura, S., Odan, K., Bando, Y.; Ube Industries Ltd.:
Catalyst for maleic anhydride manufacture

US Patent 4132670 (1979); Katsumoto, K. Marquis, D.M.; Chevron Res. Co.:
Vanadium(IV) phosphate catalyst for oxidation of hydrocarbon to maleic anhydride prepared by heating a vanadium feed with orthophosphoric acid, removing liquid and calcining

US Patent 4219484 (1980); Dolhyj, S.R., Milberger, E.C.; Standard Oil Co. Ohio:
Catalyst for oxidation of hydrocarbon(s) to maleic anhydride - comprises mixed oxide(s) of vanadium and phosphorus

US Patent 4244879 (1981); Bremer, N.J., Dria, D.E.; Standard Oil Co. Ohio:
Vapour phase preparation of maleic anhydride - uses catalyst prepared by reducing pentavalent vanadium compound, removing particles above specified size, adding phosphorus compound and calcining

Japanese Kokai 8145815 (1981); Mitsubishi Chemical Industries Ltd.:
Crystalline reduced phosphovanadic acid as maleic anhydride production catalyst

US Patent 4315864 (1982); Bremer, N.J., Dria, D.E.; Standard Oil Co. Ohio:
Maleic anhydride production from C4 hydrocarbon - by oxidation of vanadium and phosphorus mixed oxide catalyst

US Patent 4337173 (1982); Mitsubishi Chemical Industries Ltd.:
Crystalline vanadium iron chromium aluminium phosphate - used as gas phase oxidation catalyst, especially in production of maleic anhydride from C4 hydrocarbon

US Patent 4317778 (1982); Blum, P.R., Nicholas, M.L.; Standard Oil Co. Indiana, Standard Oil Co. Ohio:
Preparation of maleic anhydride from hydrocarbon(s) by oxidation with fluid bed catalyst containing mixed oxide(s) of vanadium and phosphorus

US Patent 4382876 (1983); Gollmer, K.D.; Chem. Werke Huels AG, Neubold K:
Vanadyl phosphate catalyst production for maleic anhydride production - from butane, butene and butadiene by reducing vanadic compound and adding promoter

US Patent 4416802 (1983); Edwards, R.C., Udovich, C.A.; Standard Oil Co. Indiana:
Phosphorus, vanadium and metal oxide catalyst production - for oxidation of butane to maleic anhydride

US Patent 4209423 (1986); Imperial Chemical Ind. Ltd.:
Vanadium phosphorus mixed oxide catalyst containing X- and B-phase - giving maleic anhydride from n-butane in improved yield and increased conversion rate

U.S. Patent 4 626 412 (1986); Ebner, J., Gleaves, J.; Monsanto:
The activation of oxygen by metal phosphorus oxides - the vanadium phosphorus oxide catalyst

US Patent 4652543 (1987); Edwards, R.C., Meyers, R.L.; Standard Oil Co. Indiana:
New phosphorus-vanadium-oxide catalyst for maleic anhydride production - by oxidation of butane, prepared by treating vanadium compound in ether solvent with phosphoryl halide and water

APPENDIX A: SUMMARY OF REACTION RUNS PERFORMED

A summary of all reaction runs carried out over VPO catalysts is given in Table A_I (following page) including catalyst precursor, calcination conditions, reaction conditions, conversion of n-butane, product selectivities and average carbon mass balance. Where no calcination conditions are given, the catalyst precursor was introduced directly to the reaction feed.

Table A_{II} gives a summary of the reaction runs carried out over heteropoly acid catalysts. Reaction and calcination conditions, conversions of isobutane, yields of CO, CO_2 and methacrylic acid, and mass balances are given. Conversions and yields are given as unsteady-state values for run 1 and steady-state values for runs 2 to 7.

TABLE A_1: SUMMARY OF REACTION RUNS OVER VPO CATALYST

RUN NO.	REACTOR TYPE	CATALYST PRECURSOR	MASS OF CATALYST (g)	MASS OF SAND (g)	CALC. GAS	CALC. GAS FLOW (STD ml/min)	CALC. TEMP (C)	CALC. TIME (hours)	FEED COMP. nC4/N2/O2	TOTAL FEED FLOW (STD ml/min)	RXN TEMP (C)	TOTAL RXN TIME (hours)	n-C4 CONV. C %	CO SEL. %	CO2 SEL. %	MA SEL. %	MASS BALANCE C %
1	Cartridge	PV1.15	0.65	5	Air	60	380	3	1.44/78.56/20	100	400	14.1	6.771	33.33	66.67	0	96.11
2	Cartridge	PV1.1	1	5	-	-	-	-	1.44/78.56/20	100	450	20	60.71	41.26	58.74	0	97.94
3	Cartridge	PV1.15	1	3	O2/N2 = 2/8	100	400	3	1.44/78.56/20	100	400	40	61.61	46.89	53.11	0	97.72
4	Cartridge	PV1.15	1	-	-	-	-	-	1.44/78.56/20	100	400	19	53.94	31.38	68.62	0	95.17
									1.44/78.56/20	100	420	3	42.43	62.77	37.23	0	
									1.44/78.56/20	100	450	1	39.5	62.86	37.14	0	
5	Cartridge	PV1.15	1	3	N2	100	400	3	1.44/78.56/20	100	400	22	56.42	52	48	0	96.71
6	Cartridge	PV1.15	0.25	3	N2	100	450	5	1.44/78.56/20	100	350	2	0	0	0	0	99.85
									1.44/78.56/20	100	360	22	0	0	0	0	
									1.44/78.56/20	100	370	2.55	0	0	0	0	
									1.44/78.56/20	100	380	1.43	0	0	0	0	
									1.44/78.56/20	100	390	1.53	3.385	66.67	33.33	0	
									1.44/78.56/20	100	400	20.26	4.514	50	50	0	
									1.44/78.56/20	100	420	0.71	8.576	47.37	52.63	0	
									1.44/78.56/10	90	420	2.38	7.917	47.37	52.63	0	
									1.44/78.56/14	94	420	0.18	7.75	44.44	55.56	0	
7	Cartridge	PV1.15	0.25	3	N2	50	400	3	1.44/78.56/20	100	400	18.433	2.934	61.54	38.46	0	96.79
									1.44/78.56/20	100	390	0.68	2.934	61.54	38.46	0	
									1.44/78.56/20	100	380	1.42	2.934	61.54	38.46	0	
									1.44/78.56/20	100	370	0.58	0.903	100	0	0	
									1.44/78.56/20	100	360	0.11	0.451	100	0	0	
8	Cartridge	PURE SAND	-	5	-	-	-	-	1.44/78.56/20	100	400	-	0	0	0	0	97.55
									1.44/78.56/20	100	420	-	0	0	0	0	
									1.44/78.56/20	100	450	-	0	0	0	0	
9	Cartridge	PV1.1	0.766	5	Air	60	380	3	1.44/78.56/20	100	350	3.72	0.451	100	0	0	95.34
									1.44/78.56/20	100	400	1	3.16	100	0	0	
									1.44/78.56/20	100	420	0.75	5.191	78.26	21.74	0	
10	Cartridge	PV1.1	1	2	-	-	-	-	1.44/78.56/20	57.79	400	1.15	71.13	30.07	69.93	0	96.41
									1.44/78.56/20	57.79	380	0.63	54.72	27.27	72.73	0	
									1.44/78.56/20	28.895	380	1.15	85.49	24.24	75.76	0	

TABLE A_I (CONTINUED)

RUN NO.	REACTOR TYPE	CATALYST PRECURSOR	MASS OF CATALYST (g)	MASS OF SAND (g)	CALC. GAS	CALC. GAS FLOW (STD ml/min)	CALC. TEMP (C)	CALC. TIME (hours)	FEED COMP. nC4/N2/O2	TOTAL FEED FLOW (STD ml/min)	RXN TEMP (C)	TOTAL RXN TIME (hours)	n-C4 CONV. C %	CO SEL. %	CO2 SEL. %	MA SEL. %	MASS BALANCE C %
11	Oven	Deactivated	1	5	-	-	-	-	1.44/78.56/20	50	350	1.18	5.208	50	50	0	98.01
		Industrial							1.44/78.56/20	25	350	0.88	9.375	44.44	55.56	0	
		Catalyst							1.44/78.56/20	25	360	1.41	11.11	37.5	62.5	0	
									1.44/78.56/20	50	360	1.75	5.208	50	50	0	
									1.44/78.56/20	100	360	1	2.387	54.55	45.45	0	
									1.44/78.56/20	200	360	1	0.781	100	0	0	
									1.44/78.56/20	25	380	1	20.43	33.16	55.26	11.57	
									1.44/78.56/20	50	380	0.2	12.81	32.15	40.19	27.65	
									1.44/78.56/20	100	380	0.7	9.1	38.63	41.38	19.98	
									1.44/78.56/20	25	400	1.4	29.04	29.76	47.35	22.87	
									1.44/78.56/20	50	400	17.8	18.54	29.62	37.02	33.34	
									1.44/78.56/20	100	400	1.3	9.1	38.63	41.38	19.98	
									1.44/78.56/20	25	420	0.5	32.4	34.88	58.14	6.96	
									1.44/78.56/20	50	420	20.75	29.76	29.29	48.83	21.86	
									1.44/78.56/20	100	420	2.83	16.56	31.64	46.14	22.21	
									1.44/78.56/20	100	440	0.26	16.15	40.86	59.14	0	
									1.44/78.56/20	50	440	0.5	32.29	40.86	59.14	0	
12	Oven	PV1.2	1	5	-	-	-	-	1.44/78.56/20	50	400	20.45	16.12	51.61	48.38	0	97.92
									1.44/78.56/20	25	400	4	26.22	47.36	52.63	0	
									1.44/78.56/20	100	400	2	9.94	48.97	51.02	0	
									1.44/78.56/20	100	380	1.5	4.85	58.33	41.66	0	
									1.44/78.56/20	50	380	0.91	8.288	45.45	54.54	0	
									1.44/78.56/20	25	380	0.8	14.3	52.38	47.62	0	
									1.44/78.56/20	25	430	18.05	58.81	39.75	60.24	0	
									1.44/78.56/20	100	430	0.51	24.72	37.5	62.5	0	
									1.44/78.56/20	200	430	0.6	17.92	36.78	63.21	0	
13	Cartridge	PV1.1	0.25	-	-	-	-	-	1.44/78.56/20	50	400	4.96	45.31	16.67	83.33	0	96.12
									1.44/78.56/20	100	400	5.18	21.27	90	10	0	
14	Cartridge	PV1.1HCl	0.5	-	-	-	-	-	1.44/78.56/20	50	400	6.2	2.604	100	0	0	98.56
15	Cartridge	PV1.5	0.3	-	-	-	-	-	1.44/78.56/20	50	400	7.75	12.59	80	20	0	95.84
16	Cartridge	PV1.15HCl	0.4	-	-	-	-	-	1.44/78.56/20	50	400	6	5.292	100	0	0	97.23
17	Cartridge	PV1.1	0.4	-	N2	30	550	4.18	1.44/78.56/20	50	400	1.33	99.28	82.67	17.33	0	98.12
18	Cartridge	PV1.1	0.3	-	N2	30	400	5	1.44/78.56/20	30	400	7	8.681	100	0	0	96.56
19	Cartridge	PV1.2	0.3	-	-	-	-	-	1.44/78.56/20	50	400	6.8	37.76	33.33	66.67	0	95.35
20	Cartridge	Experimental	0.3	1	-	-	-	-	1.44/78.56/20	30	390		11.72	44.44	55.56	0	97.63
		Commercial							1.44/78.56/20	15	390		22.92	39.39	60.61	0	
		Catalyst							1.44/78.56/20	45	390		8.333	44.44	55.56	0	
									1.44/78.56/20	45	400		10.42	44.44	55.56	0	
									1.44/78.56/20	30	400		15.36	40.68	59.32	0	
									1.44/78.56/10	27	400		10.26	47.37	52.63	0	
									1.44/78.56/20	30	400		12.24	46.81	53.19	0	
									1.44/78.56/30	33	400		11.87	46.81	53.19	0	
									1.44/78.56/20	30	390	190	11.72	44.44	55.56	0	

TABLE A_{II}: SUMMARY OF REACTION RUNS OVER HPA CATALYST

RUN NO.	REACTOR TYPE	CATALYST	MASS OF CATALYST (g)	MASS OF SAND (g)	CALC. GAS	CALC. GAS FLOW (STD ml/min)	CALC. TEMP (C)	CALC. TIME (hours)	FEED COMP iC4/O2/N2	TOTAL FEED FLOW (STD ml/min)	RXN TEMP (C)	i-C4 CONV. C%	CO YIELD %	CO2 YIELD %	MAA YIELD %	MASS BALANCE C %
1	Cartridge	K3PMo12O40	0.3	-	Air	60	300	1	17/30/53	15	330	6.04	1.69	4.07	0	97.21
									17/30/53	15	350	8.97	2.52	6.002	0.02	
									17/30/53	15	380	16.99	5.34	10.88	0.05	
									17/30/53	15	400	6.76	2.09	3.44	0.28	
									17/30/53	15	420	7.29	2.45	3.002	0.37	
									17/30/53	15	450	11.46	4.64	4.69	0.43	
2	Cartridge	K(NH4)2PMo12O40/FeO1.5	0.3	1	O2	20	300	1	17/30/53	9	380	14.5	6.6	7	1.25	96.57
3	Cartridge	K(NH4)2PMo12O40/FeO1.5	0.3	1	O2	20	300	1	17/30/53	11.25	380	12.34	5	5.8	1.19	97.17
4	Cartridge	K(NH4)2PMo12O40/FeO1.5	0.3	1	O2	20	300	1	17/30/53	15	380	9.5	3.7	4.7	1.3	97.83
5	Cartridge	K(NH4)2PMo12O40/FeO1.5	0.3	1	O2	20	300	1	17/30/53	22.5	380	5.8	1.6	2.8	1.35	95.18
6	Cartridge	K(NH4)2PMo12O40/FeO1.5	0.3	1	O2	20	300	1	17/30/53	9	380	5.21	1.68	2.1	1.32	99.12
									17/30/53	15	380	3.68	0.98	1.34	1.28	
									17/30/53	22.5	380	2.5	0.5	0.72	1.22	
									17/30/53	30	380	1.82	0.32	0.48	0.98	
									17/30/53	37.5	380	1.6	0.24	0.3	1.01	
									17/30/53	45	380	1.3	0.18	0.3	0.79	
									17/30/53	60	380	1.02	0.11	0.14	0.73	
									17/30/53	67.5	380	1.02	0.14	0.18	0.66	
									17/30/53	90	380	0.71	0.06	0.16	0.46	
									17/30/53	112.5	380	0.54	0	0.16	0.37	
									17/30/53	180	380	0.23	0	0	0.23	
7	Cartridge	K(NH4)2PMo12O40/FeO1.5	0.3	1	O2	20	300	1	17/30/53	9	400	8.56	3.36	3.85	1.21	97.27
									17/30/53	15	400	5.05	1.8	1.93	1.2	
									17/30/53	30	400	3.06	0.79	1.15	1.06	
									17/30/53	45	400	1.96	0.4	0.58	0.94	
									17/30/53	52.5	400	2.15	0.44	0.55	1.12	
									17/30/53	60	400	1.57	0.31	0.47	0.75	
									17/30/53	66.6	400	1.1	0.2	0.25	0.63	

APPENDIX B: SAMPLE CARBON BALANCE CALCULATION

	GC Integrator Peak Area	GC Integrator Peak Area x GC Response Factor
CH_4 standard	801286	801286
Isobutane feed	4428986	4428986
Methacrolein	21587	35834
Methacrylic acid	32196	58983
Propanal	17819	26728

Volume % CO as measured by CO/CO_2 analyser = 2.44
Volume % CO_2 as measured by CO/CO_2 analyser = 2.75
Flow through CO/CO_2 analyser = 22.9 STP ml/min
Flow of CO = 0.56 STP ml/min
Flow of CO_2 = 0.63 STP ml/min
Flow of CH_4 internal standard added after reactor = 0.57 STP ml/min

Convert flows of CO and CO_2 to relative peak areas based on peak area of CH_4 on GC printout and flows of CH_4 compared to flows of CO and CO_2
Relative peak area of CO = 0.56/0.57 x 801286 = 783539
Relative peak area of CO_2 = 0.63/0.57 x 801286 = 883087

Hence actual relative carbon ratios are:

CH_4	801286
Isobutane	4428986
Methacrolein	35834
Methacrylic Acid	58983
Propanal	26728
CO	783539
CO_2	883087

Conversion of isobutane based on GC carbon ratios

$$= \frac{(Methacrolein + Methacrylic\ Acid + Propanal + CO + CO_2)}{(Methacrolein + Methacrylic\ Acid + Propanal + CO + CO_2 + Isobutane)}$$

$$= \frac{(35834 + 58983 + 26728 + 783539 + 883087)}{(35834 + 58983 + 26728 + 783539 + 883087 + 4428986)}$$

$$= 28.76\%$$

Ratio of isobutane / CH_4 peaks = 5.52
Ratio of isobutane / CH_4 peaks on bypass sample = 8.11
Hence conversion calculated from bypass = 32%

From bypass:
Total relative number of carbons entering reactor

= 4428986 / (1 - 0.32)
= 6513214

Carbons accounted for

= isobutane + Methacrolein + Methacrylic Acid + Propanal + CO + CO_2
= 6217157

Number of carbons unaccounted for

= 296057
= 4.5% of original number of carbons entering

Hence Carbon balance = 95.49%

APPENDIX C: MASS SPECTRA

Below are given mass spectra for all the compounds identified, as well as the mass ion breakdown and relative intensities from more than one source, as reported in the Eight Peak Index of mass spectra [1991]. Peaks at 18, 28, 32 and 44 on the spectrum for methacrolein are on account of H_2O and air and should be ignored. It should be noted that the incidence and relative intensities of mass ions will not agree exactly with the references, as they are dependent on the experimental setup. Because peaks were close together, small amounts of ions from adjacent compounds may occur on the mass spectra. These peaks are however easily distinguished by considering adjacent spectra.

ETHYL METHYL ETHER (Molecular weight 60, boiling point 10.8°C, retention time 23 min)

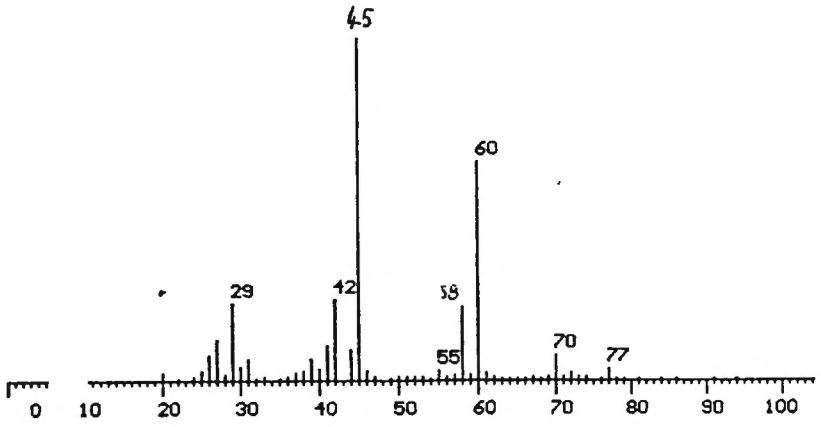

Ion	45	60	29	31	59	27	28	43
Intensity	100	33	19	18	12	11	6	4

Ion	45	60	29	31	59	43	27
Intensity	100	34	31	18	17	17	14

PROPANAL (Molecular weight 58, boiling point 48-49°C, retention time 24 min)
Peaks around 28 are more clearly seen on the adjacent spectrum assigned to methacrylic acid.

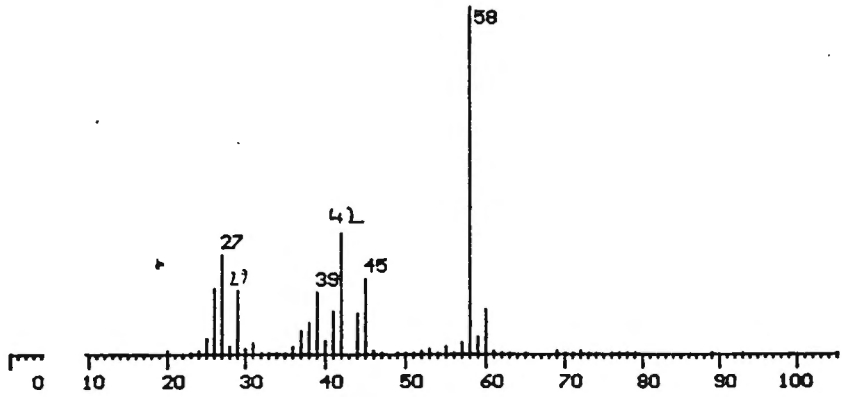

Ion	29	28	27	58	26	57	30	25
Intensity	100	69	55	39	19	11	6	4
Ion	29	28	27	58	26	57	43	30
Intensity	100	69	58	37	21	11	11	6
Ion	29	58	28	27	57	26	30	59
Intensity	100	90	74	49	24	13	6	5

METHACROLEIN (Molecular weight 70, boiling point 69°C, retention time 24 min)

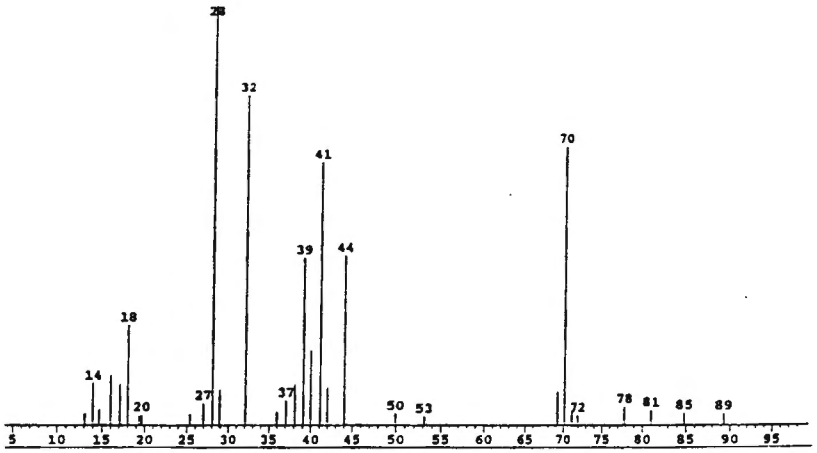

Ion	41	70	39	43	40	42	29	27
Intensity	100	70	70	25	21	17	17	16
Ion	41	70	39	42	40	38	29	27
Intensity	100	82	67	15	13	13	13	9

METHACRYLIC ACID (Molecular weight 86, boiling point 163°C, retention time 25 min)

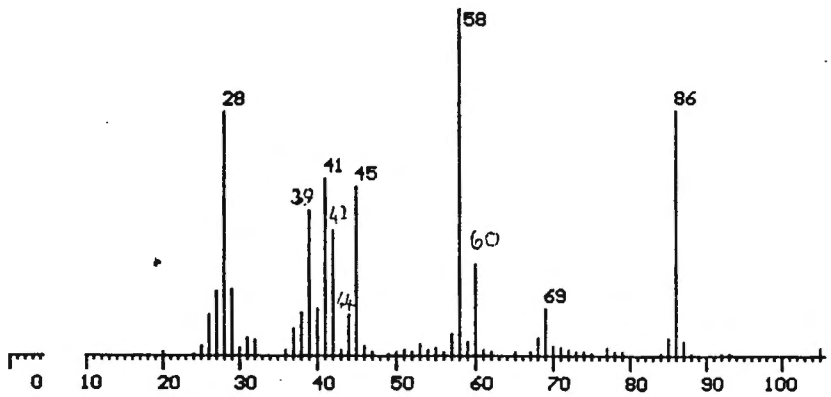

Ion	41	86	40	69	45	42	68	43
Intensity	100	67	16	15	13	9	6	6
Ion	41	86	39	40	28	69	45	38
Intensity	100	71	65	21	17	14	14	14
Ion	41	39	86	40	38	28	68	44
Intensity	100	88	49	26	19	17	13	13

The spectrum given below (retention time 29 min) correlates well with any of the species given below.

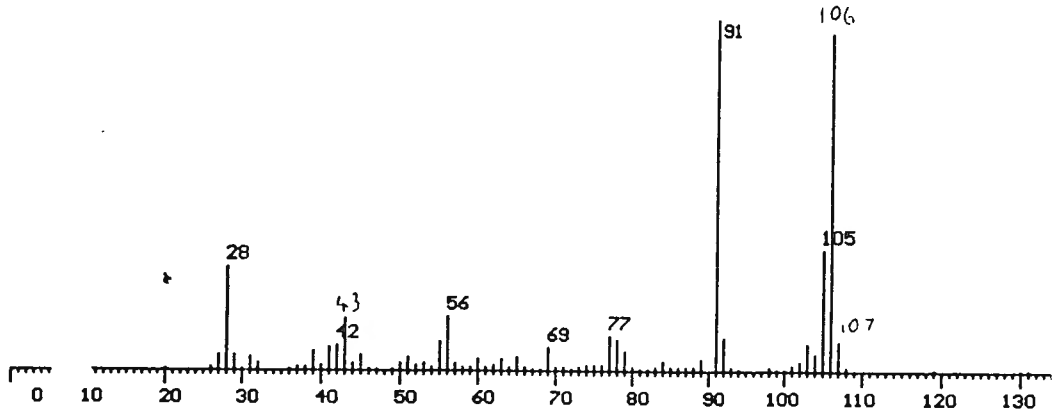

1,2-DIMETHYL BENZENE

Ion	91	106	105	77	57	39	92	59
Intensity	100	90	33	13	12	9	8	7
Ion	91	106	105	39	51	77	27	50
Intensity	100	58	24	17	16	13	11	8
Ion	91	106	105	92	107	79	28	77
Intensity	100	98	45	17	13	11	11	9

1,3-DIMETHYL BENZENE

Ion	91	106	105	39	51	77	27	65
Intensity	100	64	28	19	15	13	11	8
Ion	91	106	105	77	57	107	59	39
Intensity	100	98	36	12	11	9	8	8
Ion	91	106	105	77	51	39	92	79
Intensity	100	59	28	12	11	10	8	7

1,4-DIMETHYL BENZENE

Ion	91	106	105	77	51	92	39	107
Intensity	100	75	35	13	12	8	8	7
Ion	91	106	105	51	39	77	27	50
Intensity	100	62	30	16	16	14	12	8
Ion	91	106	105	28	107	92	79	77
Intensity	100	89	28	13	8	8	6	4

5-ISOPROPYLIDENE-1,3-CYCLOPENTADIENE

Ion	91	106	105	39	65	51	77	63
Intensity	100	71	33	31	23	18	16	12

3-METHYLENE-1-VINYL-CYCLOPENTENE

Ion	91	106	105	78	79	77	51	39
Intensity	100	81	33	27	25	22	18	18

APPENDIX D: PARTICLE SIZE DISTRIBUTION OF THE VPO CATALYST

The Malvern size distribution of VPO catalyst PV1.1 is given below.
(5 μm < Particle size < 20 μm; mean dp = 10.18 μm)

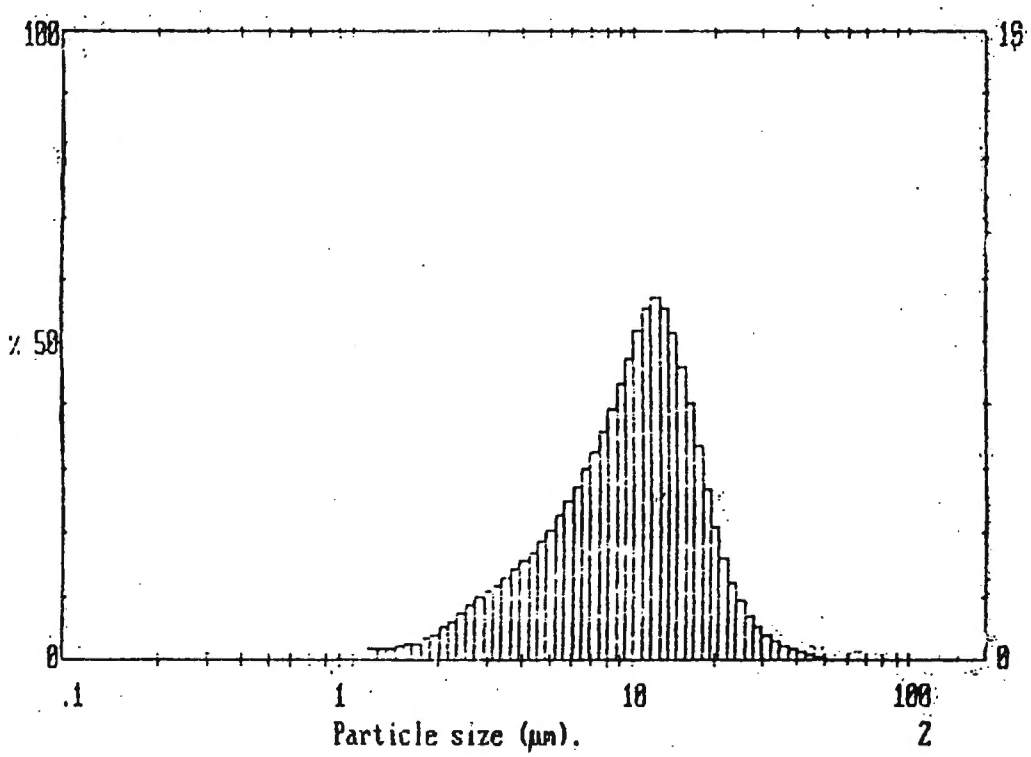

APPENDIX E: THE AMPOULE SAMPLING METHOD

The ampoule sampling technique of Schulz et al [1984c] was employed for the taking of gas product samples. A sealed, evacuated glass ampoule (5 mm diameter) is made with a 10 cm capillary on one end. The glass ampoule is inserted into a sampling hole (with a septum to prevent gas leakage) on the outlet gas line. Inside the outlet line is a switch with which the tip of the capillary inside the line is broken off, thereby sucking in a sample of the product gas into the ampoule. The ampoule is immediately sealed by melting shut the end of the capillary with a butane flame. The glass ampoule now contains a product sample which can be analysed at any future date.

Analysis of the ampoule takes place on a gas chromatograph. A metal ampoule breaker is built and connected to the gas chromatograph valve. The ampoule breaker consists of a tubular metal chamber, wide enough for the ampoule to fit inside, i.e. approximately 10 mm i.d. The ampoule is placed inside the chamber which is then closed off with a copper nut. Metal tubes connect the ampoule chamber with the gas chromatograph so as to form a sampling loop of which the chamber is a part. A metal rod fits inside the nut and can be pushed down to crush the glass ampoule inside the chamber. The rod is sealed with a viton o-ring where it fits inside the nut, making the chamber leak-free. The gas chromatograph carrier-gas then carries the gas sample out of the loop into the column of the gas chromatograph and the contents of the ampoule are separated and analysed on the GC FID.